

APPENDICES

Seismic behaviour of a LNG tank foundation

MSc Thesis Jesper van Es

27 March 2014

Final Report

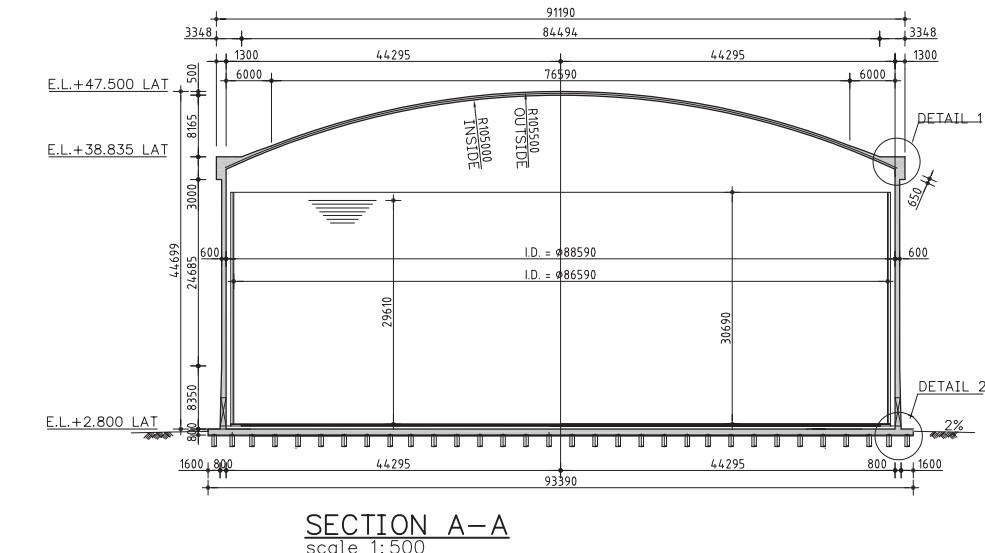
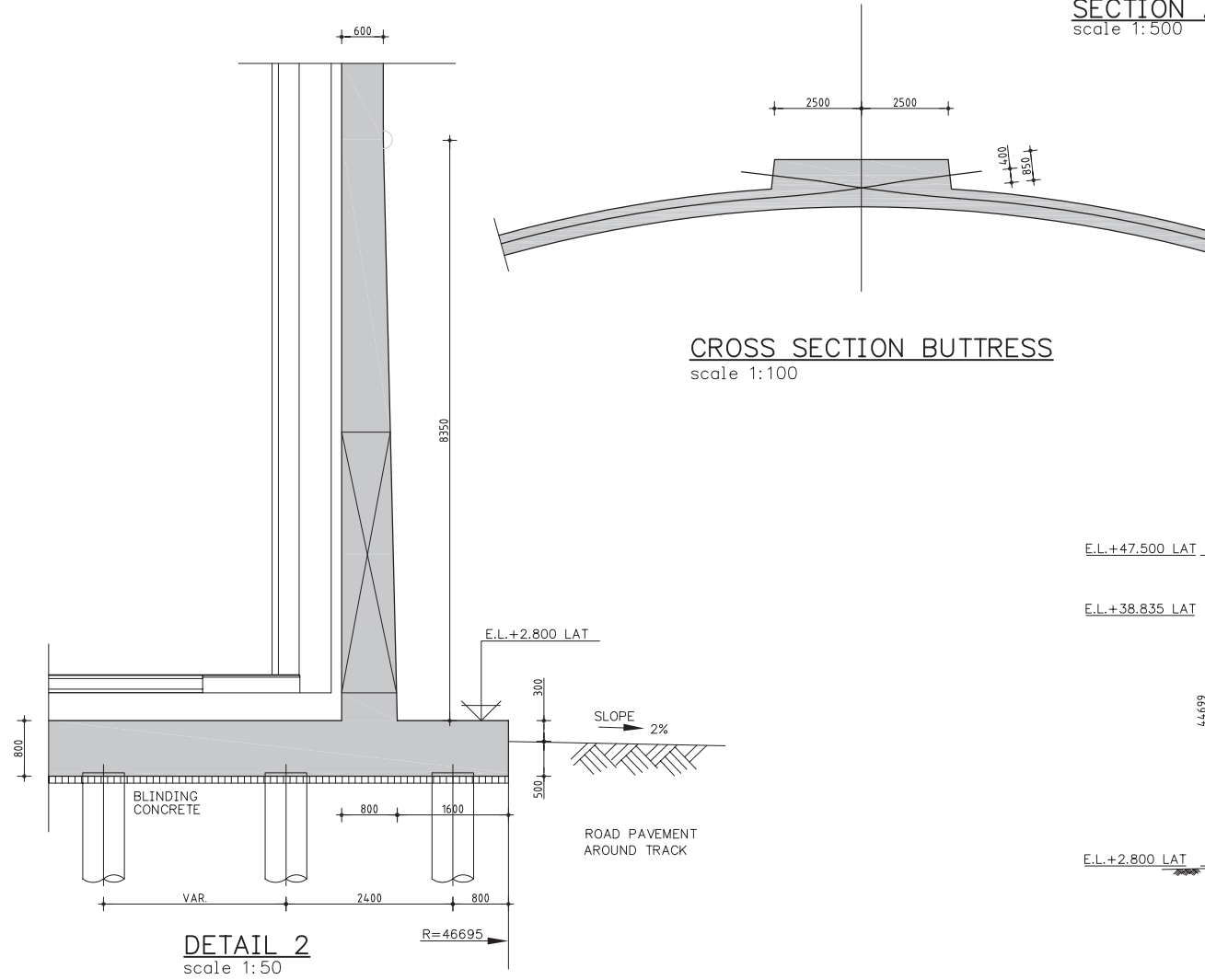
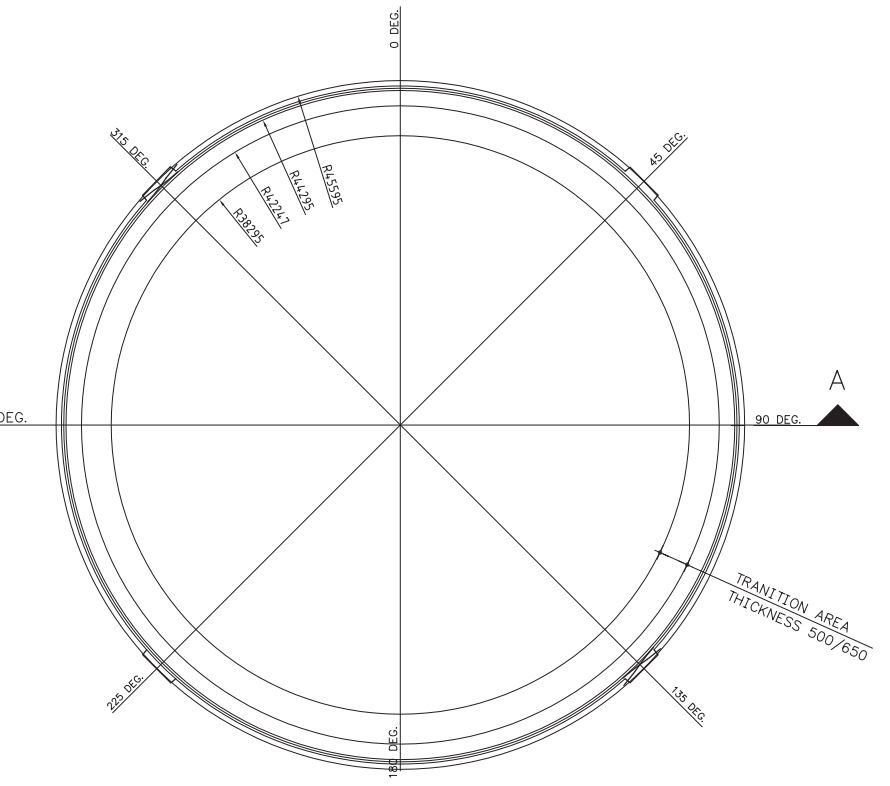
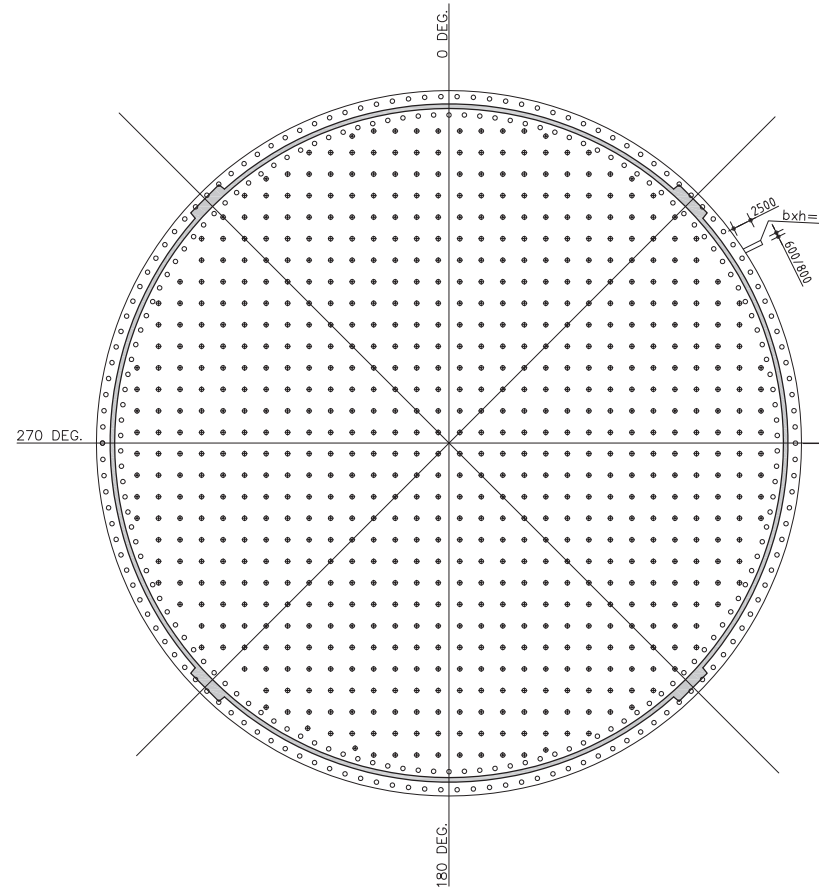
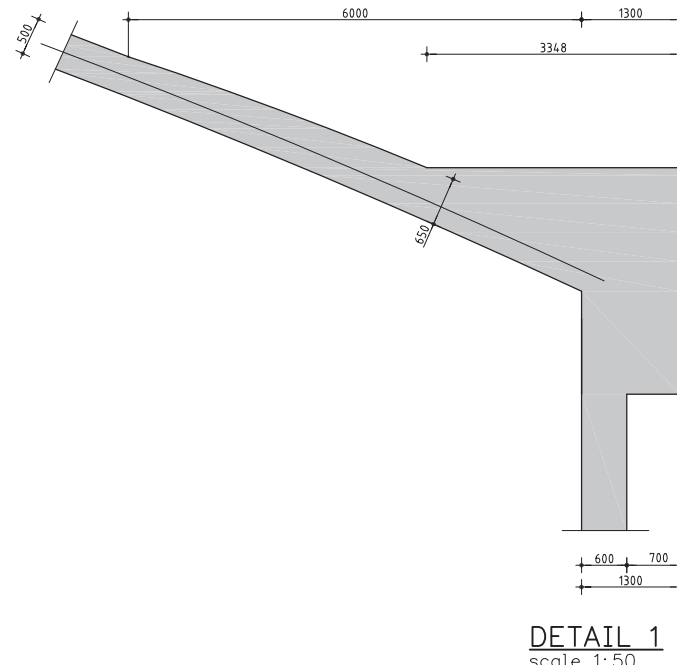
CONTENTS

	Page
A. DRAWINGS LNG STORAGE TANK	3
A.1 LNG storage tank - Geometry	3
A.2 LNG storage tank - Pile geometry	3
A.3 LNG storage tank - Pile (connection) details	3
B. SELECTION PROCEDURE FOR TIME HISTORIES	5
B.1 Site location	5
B.2 Design response spectra	6
B.3 Selection representative time histories	10
B.4 Demands on time histories according to Eurocode 8	13
B.5 OBE 1% damping	14
B.6 OBE 2% damping	15
B.7 OBE 10% damping	16
B.8 SSE 2% damping	18
B.9 SSE 5% damping	19
B.10 SSE 10% damping	20
B.11 OBE bedrock	21
B.12 SSE bedrock	22
C. MATLAB CODE FOR FAST FOURIER TRANSFORMATION OF EARTHQUAKE SIGNAL	23
D. CACULATION OF MESH ELEMENT SIZE AND CRITICAL TIME STEP	25
E. RESULTS SITE RESPONSE ANALYSES	27
E.1 Check of input signal	27
E.2 Check horizontal accelerations at ground level	35
E.3 Horizontal displacement at ground level	43
E.4 Vertical acceleration at ground level	45
F. CALCULATION INPUT PARAMETERS FOR IMPULSIVE LIQUID MASS	53
G. VERIFICATION OF FLUID BEHAVIOUR (BEAM ON AUXILIARY STRUCTURE)	57
G.1 Considered models	57
G.2 Static behaviour after building phase	59
G.3 Static behaviour after loading phase	61
G.4 Dynamic behaviour after	67
H. RESULTS EARTHQUAKE CALCULATIONS	73
H.1 Horizontal displacements	74
H.2 Axial forces in vertical supports of auxiliary structure during SSE earthquake	76
H.3 Shear forces in vertical supports of auxiliary structure during SSE earthquake	77
H.4 Axial forces in vertical supports of auxiliary structure during normative time steps	78

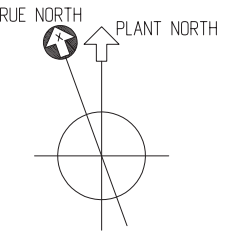
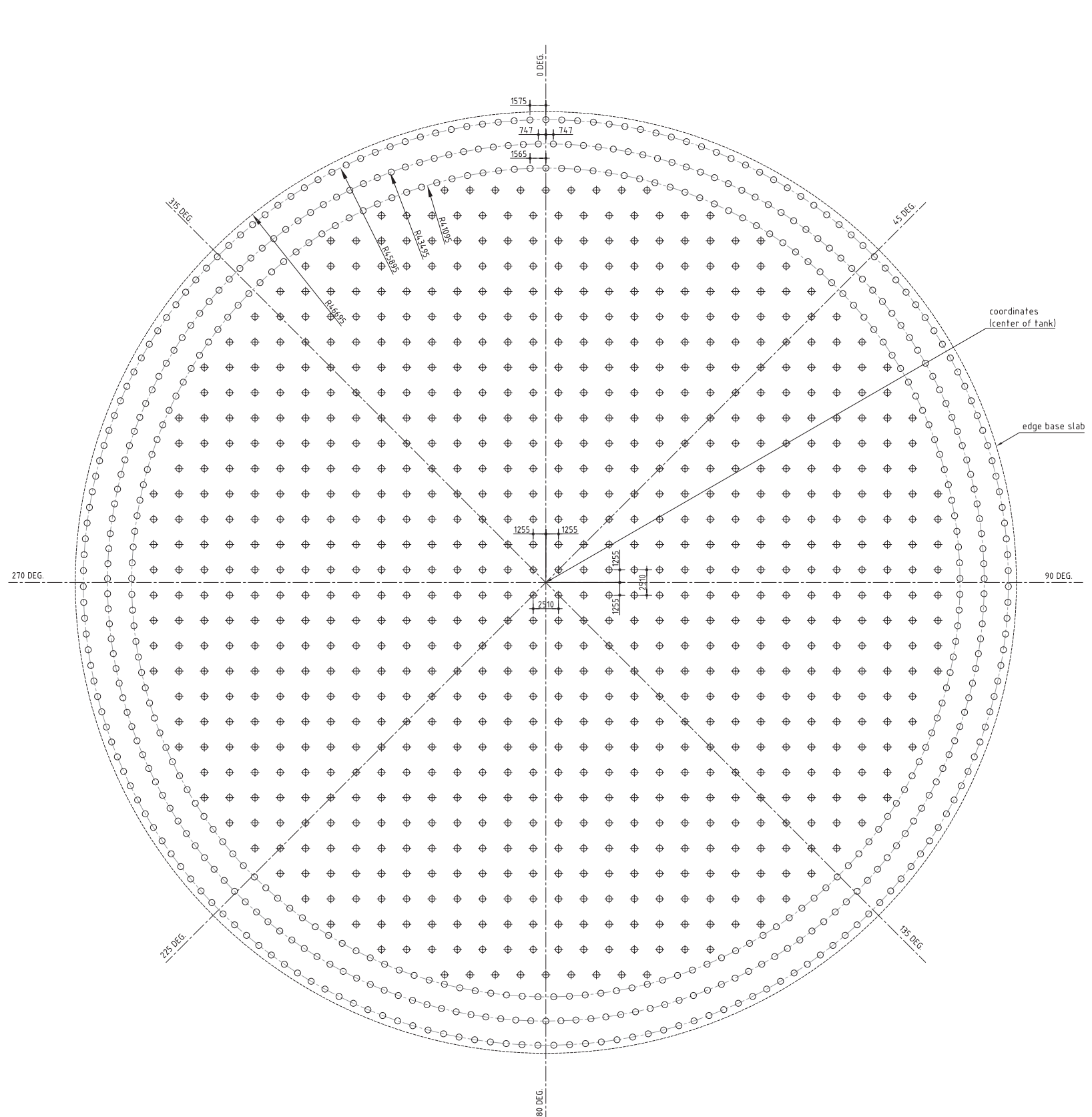
H.5	Shear forces in vertical supports of auxiliary structure during normative time steps	79
H.6	Dynamic and Pseudo static pile forces	80

Appendix A

- A. DRAWINGS LNG STORAGE TANK
 - A.1 LNG storage tank - Geometry
 - A.2 LNG storage tank - Pile geometry
 - A.3 LNG storage tank - Pile (connection) details



-All sizes in mm	
-All levels in m	
0	1000
1000	2000
2000	3000
3000	4000
4000	5000
5000	6000
6000	7000
7000	8000
8000	9000
9000	10000
10000	
A 13.APR.2007 Modification	S.M. A.H. A.R. R.V. -
0 11.APR.2007 First issue	S.M. A.H. A.R. R.V. -
REV DATE	DESCRIPTION DESIGN DRAWN CHECK'D APPR'D APPR'D
ANGOLA LNG PROJECT	
ANGOLA, WEST AFRICA	
Plant:	ONSHORE FACILITIES
159,000m ³	LNG STORAGE TANK T-2401A & T-2401B 2 NOS
DWG.TITLE:	GENERAL Arrangement tank
DRAWING No.	REV.
002	0



COORDINATES (CENTER OF THE TANK)

TANK	Northing (m)	Easting (m)
T-2401-A (West LNG)	9322835	204663
T-2401-B (East LNG)	9322787	204838

FOR MATERIAL SPECIFICATIONS SEE DOCUMENT N3870A-M-308
"MATERIAL SPECIFICATION FOR PILE FOUNDATION"

○ and ⊕ STEEL PILE O.D. = 0.61m; TH = 20MM
PILE TIP LEVEL -33.500 LAT
PILE TOP LEVEL +3.350 LAT
NUMBER OF PILES (1345)

JOB & V.P. NO.	EQUIP. NO. T-2401A/T-2401B
<input type="checkbox"/> (1) Work May Proceed	DATE RECEIVED _____
<input type="checkbox"/> (2) Revise & Resubmit Work May Proceed Subject to incorporation of changes indicated.	SIGNED _____ DATE _____
<input type="checkbox"/> (2a) Revise Incorporate Changes as Indicated. Resubmit Not Required. Work May Proceed.	BECHTEL
<input type="checkbox"/> (3) Revise & Resubmit Work May Not Proceed. Revise & Resubmit Work May Proceed.	
<input type="checkbox"/> (4) Revise Not Required. Work May Proceed.	

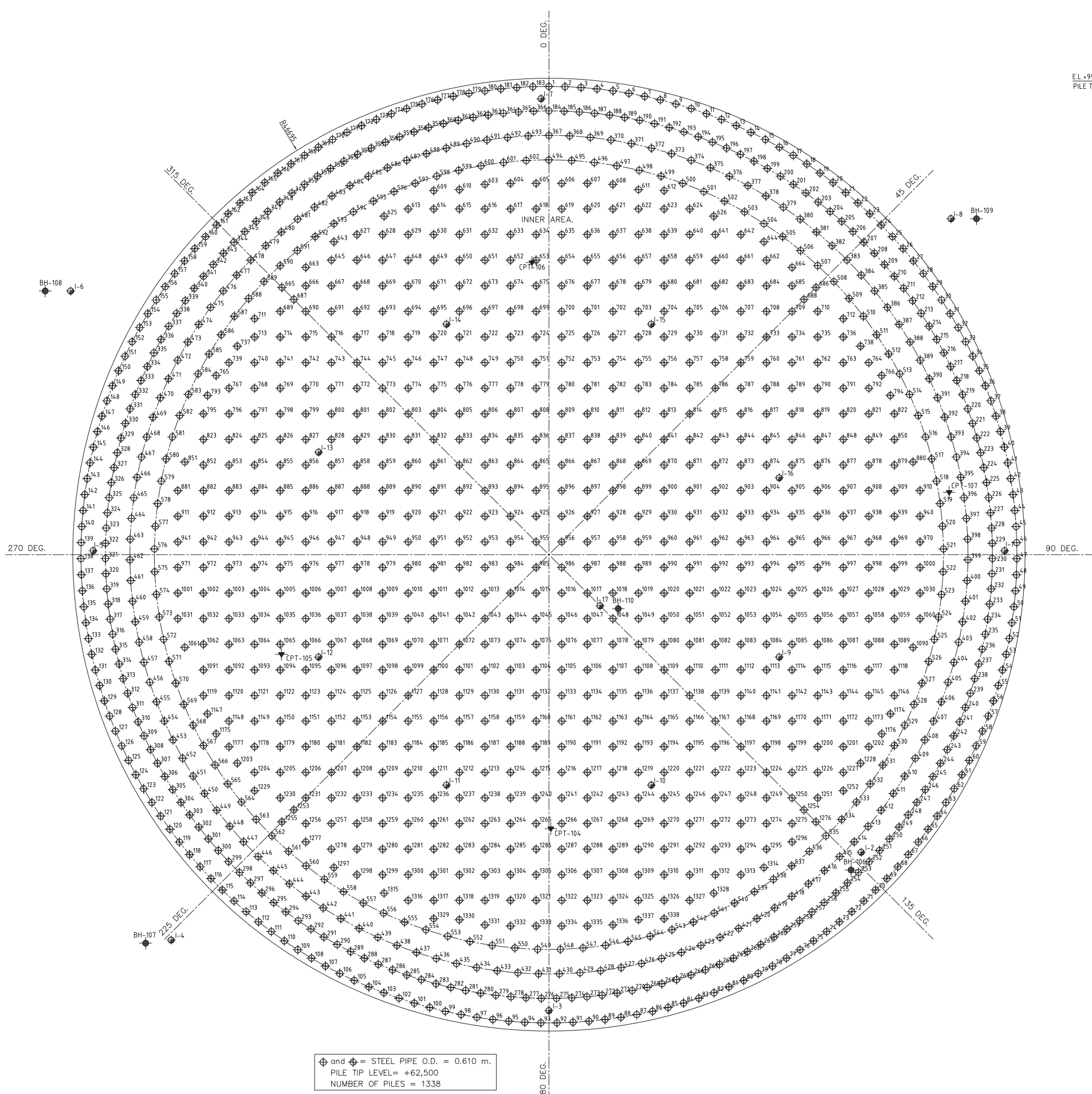
Job No.	Sub.No.	Doc.Type	Locator Code	Seq.No.	Rev.No.
TKK	TOYO KANETSU K.K.	SUB CONTRACT No.	25317-301-HC1-MTDO-00003		

FOR ANGOLA LNG PROJECT/BECHTEL
159,000 m³LNG TANK
EQUIPMENT TAG NO.:T-2401A/T-2401B

DRAWING TYPE: PILE FOUNDATION					
DRAWING NO. DST04-3870A-303 REVISION 0					
△					
△					
△					
NO.	DESCRIPTION	DATE	BY	CHKD APPD	PROJECT (EM)
NAME S.Negi D.Badal A.Rijswijk R.Vonk K.Matsuo					
REVISIONS DATE 13-12-2007 13-12-2007 13-12-2007 13-12-2007					
DST04-3870A-303.dwg M C B R5R4R3R2R1R0					

LAYOUT PILE FOUNDATION

Scale 1:250

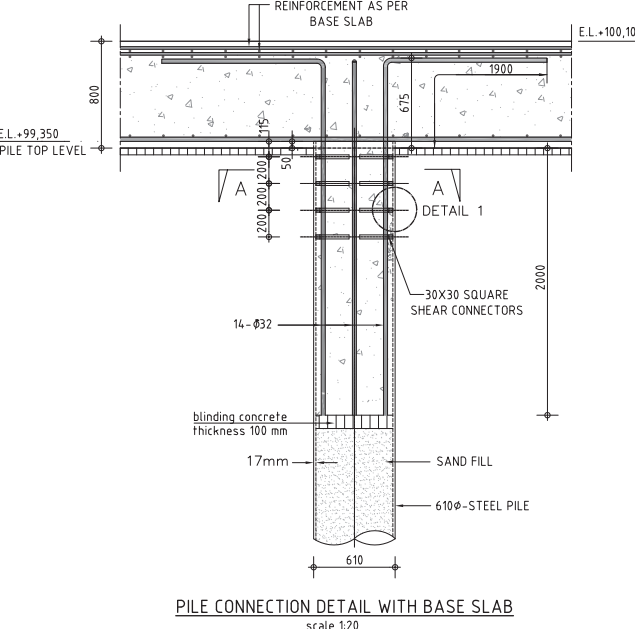


⊕ and ⊕ = STEEL PIPE O.D. = 0.610 m
 PILE TIP LEVEL= +62,500
 NUMBER OF PILES = 1338

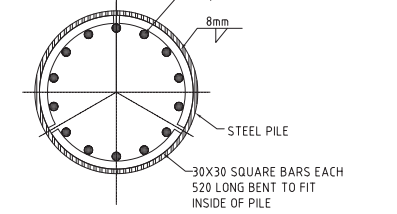
LAYOUT PILE PLAN
scale 1:150

PILE MATERIAL SPECIFICATION

S.NO		GRADE	DIMENSION	NUMBER
1.	PIPE	ASTM 252 Gr.3	O.D. 610 mm, THICKNESS 17 mm, LENGTH=36.85 m	1338
2.	SQUARE BAR	ASTM 252 Gr.3	30X30 BARS, LENGTH=520 cm	16056



PILE CONNECTION DETAIL WITH BASE SLAB



SECTION A-A
scale 1:10

DETAIL OF NOS. OF PILES		
SL. NO.	PILE AT LOCATION	NOS.
1.	FIRST ROW	183
2.	SECOND ROW	183
3.	THIRD ROW	127
4.	FOURTH ROW	109
5.	INNER AREA	736
	TOTAL	1338

LEGEND:

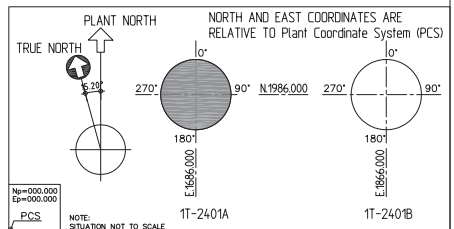
- LEGEND:**
ALL DIMENSIONS IN MM.
ALL LEVELS IN M.
LEVEL EL. +100,00 = LAT. +4,40 M.

REFERENCE DRAWING:

- FOR COORDINATES SEE DRAWING DST04-3870A-303-03.

CONSTRUCTION SEQUENCE:

- DRIVE PILES TO ACHIEVE REQUIRED CAPACITY.
CUT PILES AT THE REQUIRED HEAD LEVEL.
LEVEL SAND INSIDE PILE AND POUR BLINDING CONCRETE
(TO SEAL THE JOINT).
WELD SHEAR CONNECTORS TO THE INSIDE OF PILE.
LOWER THE REBARS IN POSITION.
CAST PILE PLUG TOGETHER WITH BASE SLAB CONCRETE
AS SPECIFIED IN DOCUMENT N3870A_C-024



Contractor Name	OVERSEAS BECHTEL INC.			Project Location	SOYO ANGOLA	
Bechtel Client Name	ANGOLA LNG			TKK Job No.	DST04-3870	
Job No.	Sub.No.	Doc.Type	Locator Code	Seq.No.	Line No.	
2 5 3 1 7	3 0 1	V 3 1	M T D 0	0 0 1 4 9		
TKK TOYO KANETSU K.K.			BECHTEL SUB CONTRACT NO.			

TOKYO JAPAN 25317-301-HC1-MTDO-00003
FOR ANGOLA LNG PROJECT/BECHTEL
159,000 m³ LNG TANK

EQUIPMENT TAG NO. :1T-2401A/1T-2401B
DRAWING TITLE

Pile Plan 1T-2401A

DST04-3870A-303-01 4

	DSGN'D	DRAWN	CHECKED	APPROVED	PROJECT (EM)

PROJECT NAME A.Rijswijk D.Badal D.Kukrety R.Vonk K.Matsuo
(EM)

DATE 2008-03-07 2008-03-07 2008-03-07 2008-03-07
DST04-3870A-303-01-04.dwg M C B R5R4R3R2R1R0

DRAWING/Teq001

Appendix B

B. SELECTION PROCEDURE FOR TIME HISTORIES

Site response analyses may be carried out using artificial generated time histories (or seismic motions) showing peak ground acceleration as function of time, or by selecting representative ‘real’ seismic motions during an earthquake, as recorded by the various monitoring stations that have been installed throughout the world. The latter is to be preferred in this case. The time histories are used in a plaxis to analyze the behavior of a piled LNG tank foundation subjected to an earthquake.

This document describes the selection procedure for the time histories that are needed in the plaxis analysis. The following subjects are covered:

- Site location
- Origin design response spectrum
- Selection representative time histories
- Control time histories according to eurocode 8

B.1 Site location

The site is located along the west Coast of Africa in the mouth of the Congo River near the town of Soyo (Angola). The general location of the site is shown in Figure 1. Further information about the site can be found in chapter 4 of the report.

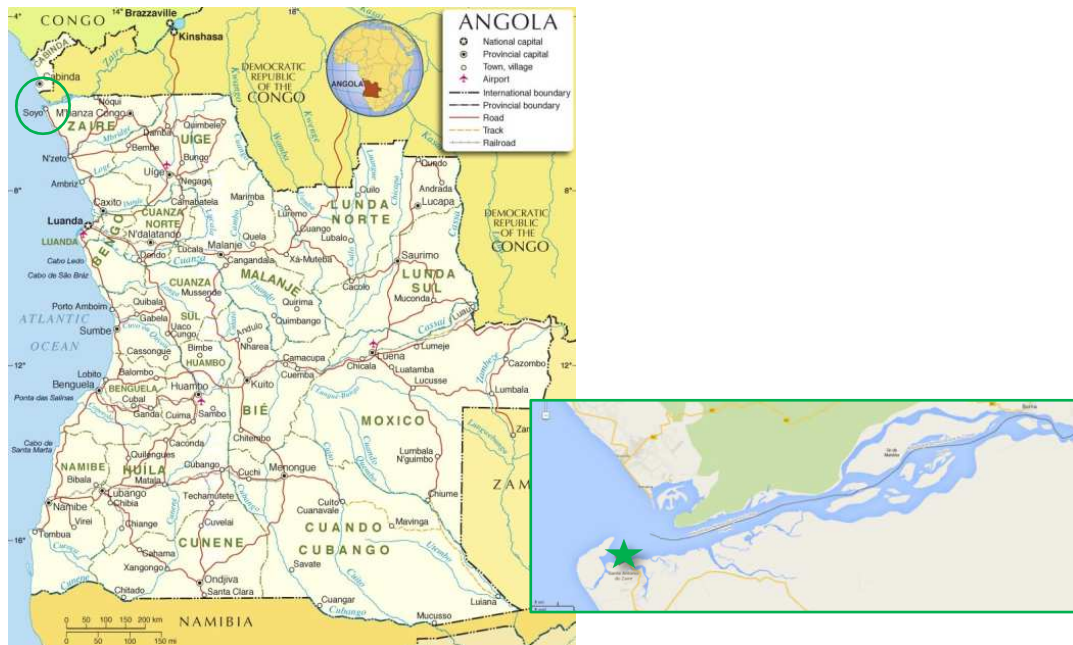


Figure 1 Site location

B.1.1 Subsurface conditions

The subsurface conditions of the site are described with the use of NEHRP, 1996. Preliminary geotechnical borings performed as part of initial siting studies show that the site is underlain by mostly soft clayey and low compressibility silty soils with interbedded layers of high compressibility organic and clayey soils. Based on this information, soil profile D is assigned to the site:

Soil Profile Type D

Stiff soil with $180 < v_s \leq 360$ m/s or with $15 \leq N \leq 50$ or $50 \leq S_u \leq 100$ kPa.

This soil type classification is different than the types used in Eurocode 8!

B.2 Design response spectra

The design response spectrums are delivered by MMI engineers and are based on a seismic hazard analysis. Real events from the past, area sources and fault sources are combined in a probabilistic analysis that have led to the design response spectra for an operating basis earthquake (OBE) and a safe shutdown earthquake (SSE).

B.2.1 Operating basis earthquake (OBE)

The LNG facility is expected to remain operational post OBE event without causing any damage. The OBE is defined by the 2001 NFPA 59A as 2/3rds of the maximum considered earthquake (MCE). The code defines the MCE as a probabilistically derived ground motion with a 2% probability of exceedance in 50 years, unless they exceed a deterministic limit specified in the code. The MCE for this project is derived by the probabilistic analysis and is plotted in Figure 2.

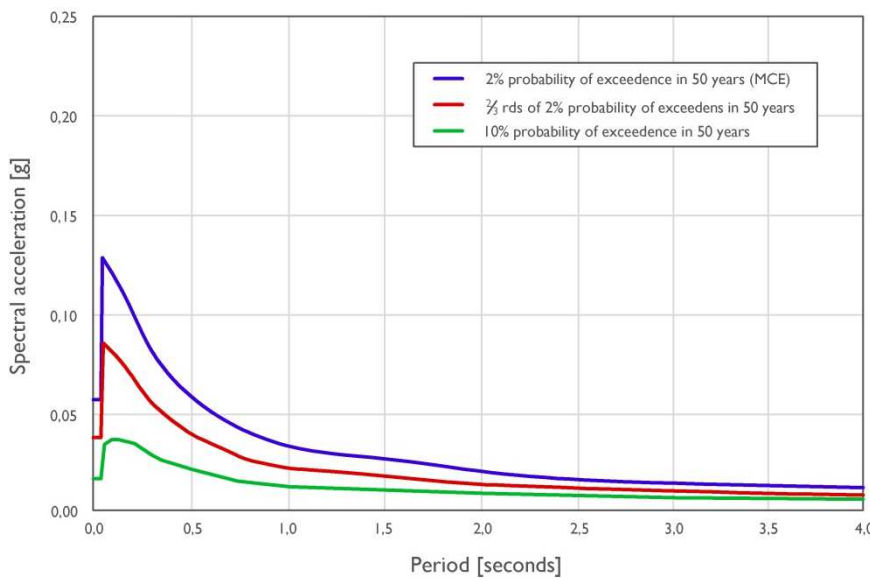


Figure 2 MCE and OBE based on 10% in 50 year

The OBE is defined as 2/3rds of the MCE ground motion, but the code allows the OBE to be no more than a ground motion with 10% probability of exceedance within a 50 year period (also shown in Figure 2).

Figure 2 shows that the 2/3rds MCE spectrum is significantly greater than the 10% in 50 year spectrum. Such a difference is observed in regions of low seismic activity. The 10% in 50 year ground motions is generally considered to provide an adequate level of safety and it is therefore recommended to use this as OBE.

B.2.2 Safe Shutdown Earthquake (SSE)

It is not required that the LNG facility remains operational during and after an SSE event, the facility is designed to contain the LNG and prevent catastrophic failure. The NFPA 59A recommends using 1% in 50 year ground motion for the SSE, with the limitation that the SSE motion may not be greater than two times OBE. In Figure 3 the two motions are compared and it shows that 1% in 50 year spectrum is significantly larger than two times OBE spectrum.

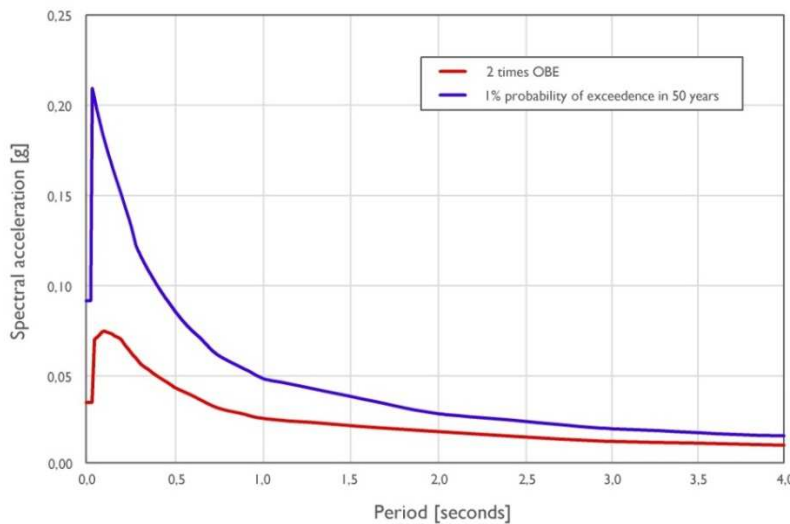


Figure 3 Two times OBE compared to 1% in 50 year

To evaluate whether the NFPA 59A factoring of twice the OBE is reasonable in Angola, area with low seismicity, the annual probability is approximated. The results are shown in Figure 4. Because of the critical nature of the facility it is recommended to use an SSE ground motion with lower annual probability than approximately 1.000 year return period (associated with minimum requirements of NFPA 59A). The petroleum industry typically uses earthquake motions associated with 2.500 to 5.000 year return period for ductility checks on critical structures. It is therefore recommended to use at least the 2% in 50 year probability level (equivalent return period of 2.500 year) as SSE ground motion.

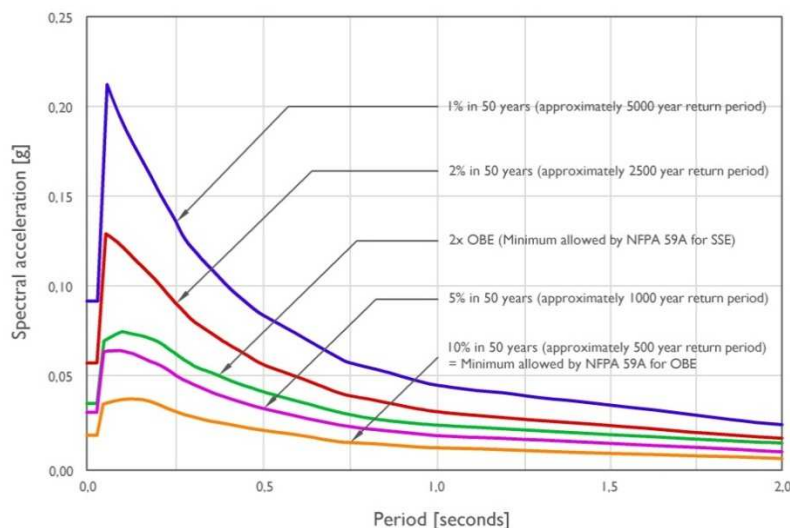


Figure 4 Comparison of NFPA 59A based OBE & SSE spectra with probability spectra

B.2.3 Recommended design spectra for rock

As described in the previous paragraphs, it is recommended to use 10% in 50 year and the 2% in 50 year response spectra for respectively the OBE and SSE. The spectra show a sharp peak at short periods of vibration. For design purposes, it is preferred to use smoothed response spectra, which take account for uncertainties in the calculation of structural period and add an appropriate level of conservatism. Figure 5 shows the recommended smooth spectra for OBE and SSE

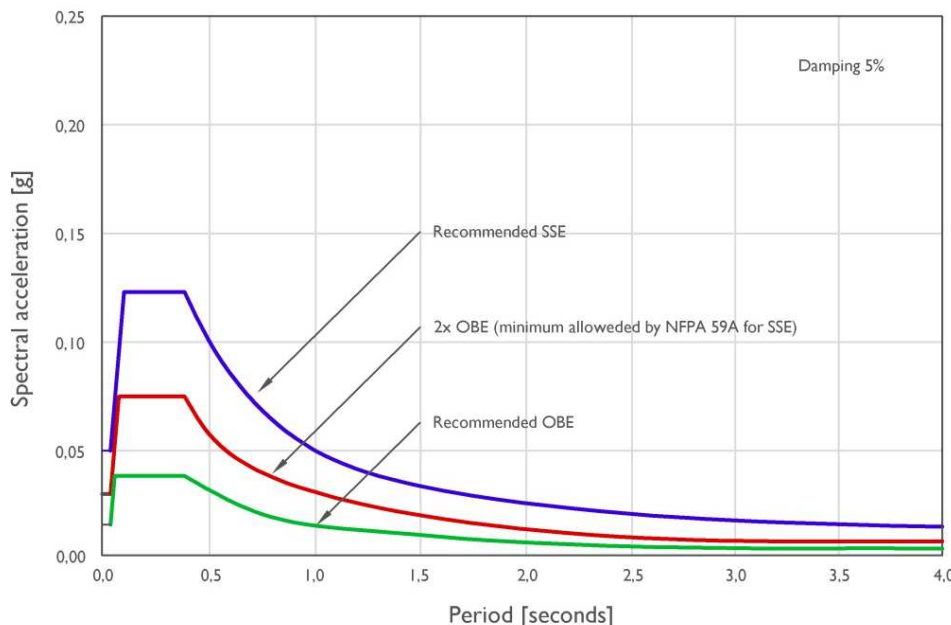


Figure 5 Recommended smoothed OBE and SSE spectra for rock (soil type A)

B.2.4 Recommended design spectra for soil type D

The recommended design response spectra presented in Figure 4 are representative for bedrock conditions classified as soil type A:

Soil Profile Type A

Hard rock with measure shear wave velocity $v_s > 1,500 \text{ m/s}$; where v_s is the average shear wave velocity.

The Angola LNG site is classified as soil profile type D (see section B1.1). The recommended OBE and SSE design response spectra for soil type D can be computed by using F_a and F_v site amplification factors provided in NEHRP, 2000 (also used in eurocode 8), see Figure 6

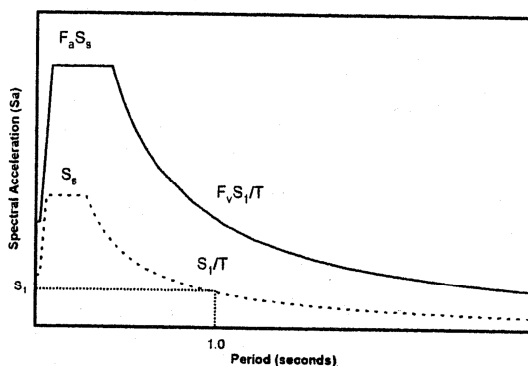


Figure 6 Two factor approach for local site response (NEHRP, 2000)

The F_a value, as given in NEHRP, 2000 for soil type A is 0.8 and that for soil type D is 1.6. Similarly, the F_v value for soil types A and D are respectively 0.8 and 2.4. Therefore, F_a and F_v values of 2.0 and 3.0 are used to scale the smoothed OBE and SSE rock spectra shown in Figure 6 to compute the soil type D recommended design response spectra which are shown in Figure 7 for different damping ratios.

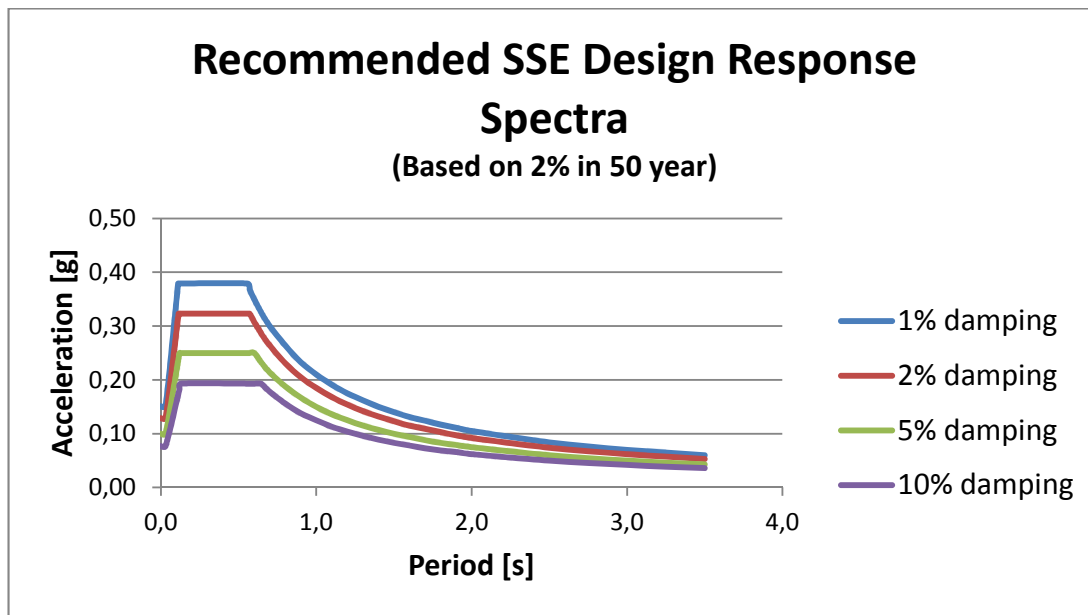
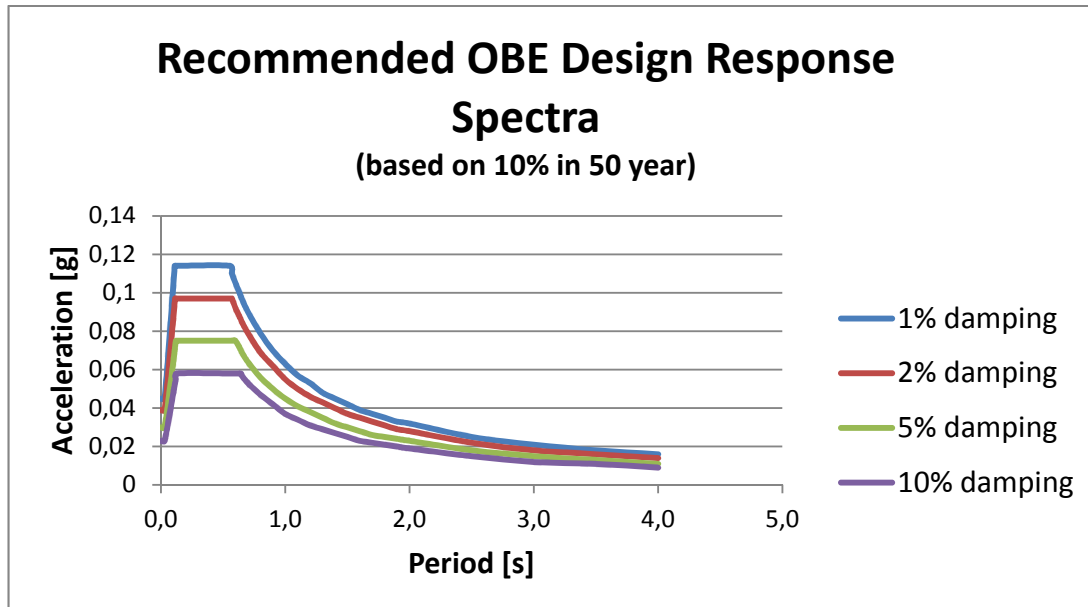


Figure 7 Recommended smoothed OBE & SSE spectra for different damping ratio (soil type D)

B.3

Selection representative time histories

Site response analyses may be carried out using artificial generated time histories (or seismic motions) showing peak ground acceleration as function of time, or by selecting representative ‘real’ seismic motions during an earthquake, as recorded by the various monitoring stations that have been installed throughout the world. The latter is to be preferred in this case. In this case the site response analyses are performed in Plaxis and include the seismic behavior of a piled LNG tank foundation. The time histories that will be used should comply with the design response spectra, as defined in section B2.4 (Figure 7)

B.3.1

Time histories PEER/NGA 2010 Strong Motion Database

From the PEER/NGA database appropriate time record are selected for use in design calculations. The PEER/NGA data base is an update and extension to the PEER Strong Motion Database. For this project the 2010 beta version of the database is used, it contains 3182 three-component recordings of 104 shallow crustal earthquakes compiled from over 1000 stations.

From the PEER/NGA database a selection is made, aiming at obtaining time records matching as good as possible to the conditions and response spectra from the site in Angola:

- Earthquake magnitude;
- Peak ground acceleration (PGA);
- Preferred NEHRP soil type classification based on $V_{s;30}$

For the selection of seismic motions (time histories), approximation the design response spectrum of 5% damped OBE ground motion, following selection options have been used:

- Magnitude : 6.2 – 7.2 (all situations)
- Preferred NEHRP based on $V_{s;30}$: D (all situations)

OBE				
	1% damping	2% damping	5% damping	10% damping
PGA [g]	0.045-0.055	0.029-0.049	0.020-0.040	0.013-0.033
SSE				
	1% damping	2% damping	5% damping	10% damping
PGA [g]	0.136-0.166	0.114-0.143	0.085-0.115	0.062-0.092

Table 1 peak ground acceleration for different earthquakes

The PGA is integrated in the design response spectrum that can be uploaded to the PEER/NGA 2010 database. By uploading a site specific design response spectrum and defining the other criteria (magnitude and preferred NEHRP soil type classification), the database will find a list of time histories whose response spectra approach the one that is uploaded. From this list it will make a set of ± 7 time histories whose average approaches the uploaded response spectrum even better. All data (horizontal motions, vertical motion and recording properties) from the time histories of this set can be downloaded.

B.3.2 Representative time histories

For the case of OBE 5% damping the following list of 20 earthquake records is provided by the PEER/NGA 2010 database after comparison with the uploaded design response spectrum from Figure 7.

Number on list	Record number in database	Earthquake	Year	Magnitude	Peak acceleration
1	3224	Chi-Chi- Taiwan-05	1999	6.20	0.034
2	933	Big Bear-01	1992	6.46	0.038
3	1799	Hector Mine	1999	7.13	0.0301
4	1830	Hector Mine	1999	7.13	0.0391
5	3448	Chi-Chi- Taiwan-06	1999	6.30	0.0299
6	51	San Fernando	1971	6.61	0.0292
7	2757	Chi-Chi- Taiwan-04	1999	6.20	0.0359
8	2971	Chi-Chi- Taiwan-05	1999	6.20	0.0283
9	1824	Hector Mine	1999	7.13	0.0291
10	2605	Chi-Chi- Taiwan-03	1999	6.20	0.0266
11	2992	Chi-Chi- Taiwan-05	1999	6.20	0.0283
12	40	Borrego Mtn	1968	6.63	0.0424
13	2785	Chi-Chi- Taiwan-04	1999	6.20	0.0290
14	2976	Chi-Chi- Taiwan-05	1999	6.20	0.0333
15	2611	Chi-Chi- Taiwan-03	1999	6.20	0.0356
16	2499	Chi-Chi- Taiwan-03	1999	6.20	0.0375
17	2730	Chi-Chi- Taiwan-04	1999	6.20	0.0253
18	2756	Chi-Chi- Taiwan-04	1999	6.20	0.0361
19	2970	Chi-Chi- Taiwan-05	1999	6.20	0.0339
20	3456	Chi-Chi- Taiwan-06	1999	6.30	0.0413

Table 2 Provided earthquake records for OBE 5% response spectrum

The first seven records (highlighted in grey) are selected as best suitable set for the uploaded design response spectrum of the 5% damped OBE ground motion. The database provides three time series per record (two in horizontal and one in vertical direction). The comparison between the uploaded design response spectrum (5% OBE) and the returned set of time histories is based on the average values of the two horizontal motions (see Figure 8, example for record 3224). This comparison is shown in Figure 9. Also the average of the seven records is given (red line). This line shows that the selected 7 time histories are a pretty good approximation of the design response spectrum for OBE 5% damped ground motion.

Spectra provided by PEER/NGA database

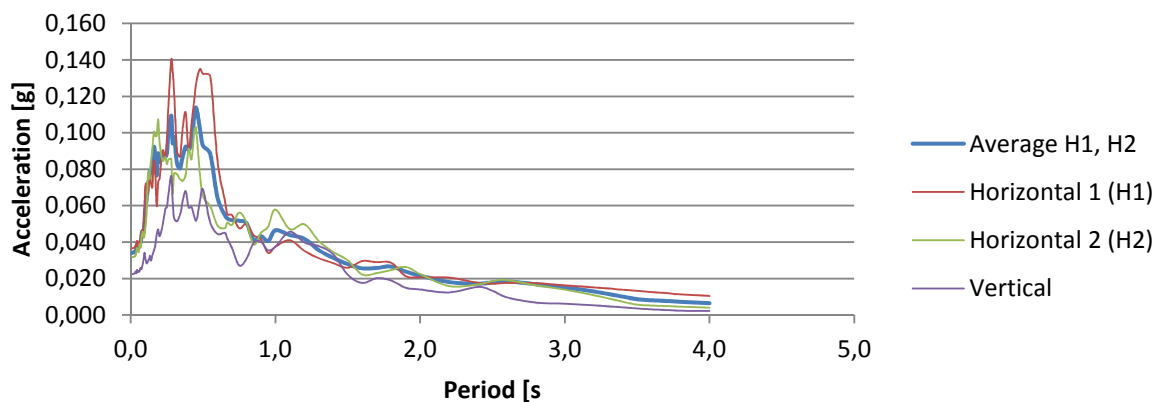


Figure 8 acceleration spectra provided by PEER/NGA for record 3224

OBE 5% - Pseudo spectral acceleration

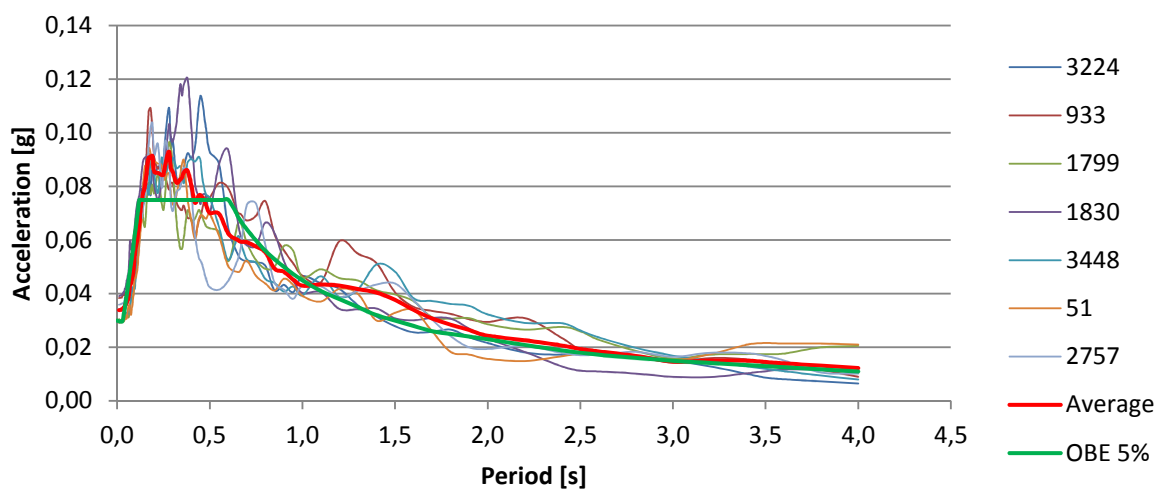


Figure 9 comparison of average spectra of selected records with input spectra

The same analysis procedure is followed to find appropriate time histories for OBE 1%, OBE 2%, OBE 10%, SSE 1%, SSE 2%, SSE 5%, SSE 10%, OBE bedrock and SSE bedrock. The results can be found in paragraphs B5 till B10 for all surface spectra, the bedrock spectra are discussed in paragraph B11 and B12.

For all situations the input values, except design response spectra, for the PEER/NGA database are equal. For the selection of the bedrock signals input values are slightly different. In this case the preferred Vs;30 is based on NEHRP soil type A instead of soil type D.

B.4 Demands on time histories according to Eurocode 8

B.4.1 Recorded or simulated accelerograms

Recorded accelerograms, or accelerograms generated through a numerical simulation of source and travel path mechanisms, may be used, provided that the samples used are adequately qualified with regard to the seismogenetic features of the sources and to the soil conditions appropriate to the site and their values are scaled to the value of $a_g S$ for the zone under consideration.

The suite of recorded or simulated accelerograms to be used should satisfy the following rules:

- a) A minimum of three accelerograms should be used;
- b) The mean of the zero period spectral response acceleration values (calculated from the individual time histories) should not be smaller than the value of $a_g S$ for the site in question
- c) In the range of periods between $0,2T_1$ and $2T_1$, where T_1 is the fundamental period of the structure (eigen frequentie) in the direction where the accelerograms will be applied; no value of the mean 5% damping elastic spectrum, calculated from all time histories, should be less than 90% of the corresponding value of the 5% damping elastic response spectrum.

B.4.2 Check according to Eurocode 8

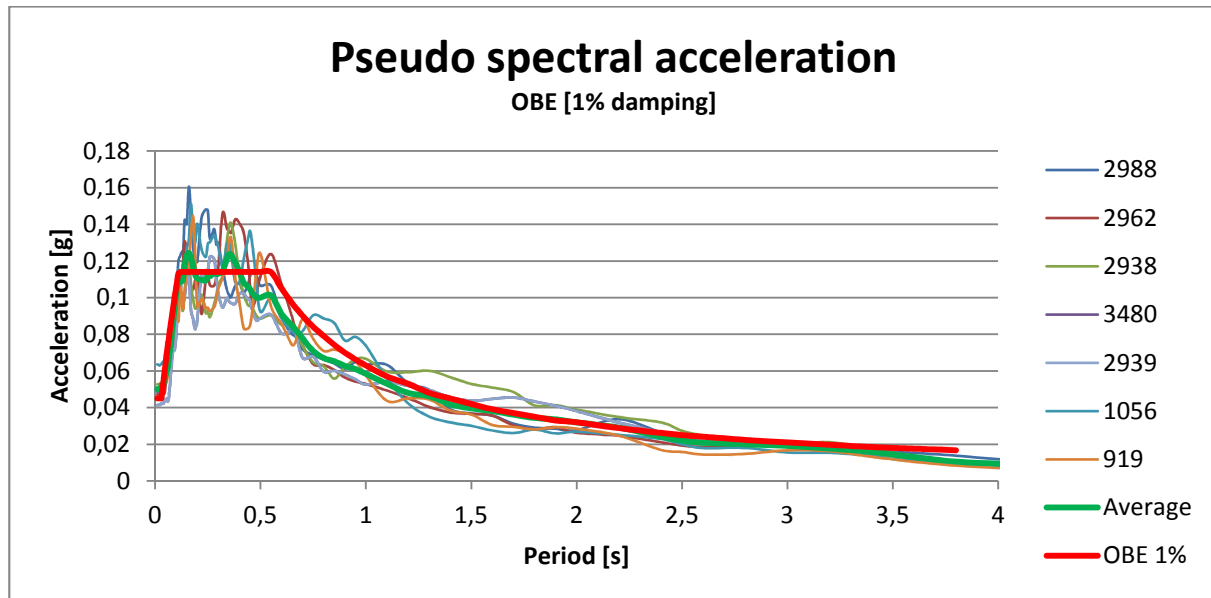
In this thesis the check according to eurocode 8 is not performed because the focus of this thesis is on a few aspects inside a numerical dynamic analysis instead of the complete response. For real designs the check must be performed based on eigen frequency of the outer tank, fluid (impulsive+innertank and convective) and other construction parts.

Also the demand of a minimum number of three different acceleration diagrams is not met in this thesis. Due to time limitations there is chosen to use only one signal for OBE and SSE

B.5

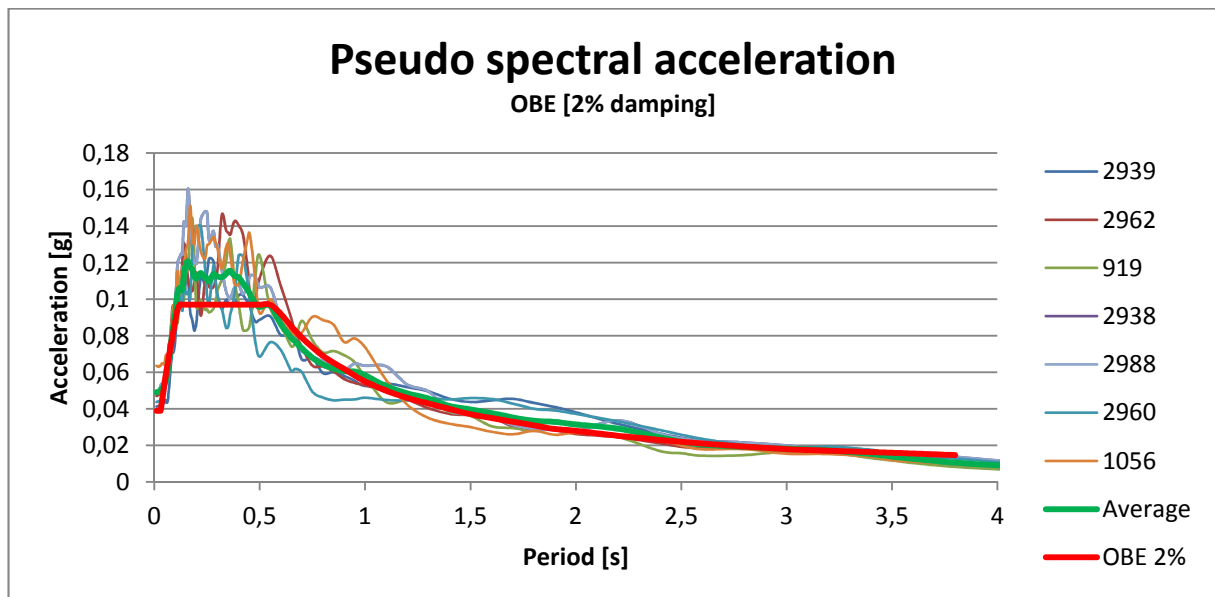
OBE 1% damping

Number on list	Record number in database	Earthquake	Year	Magnitude	Peak acceleration
1	2988	Chi-Chi- Taiwan-05	1999	6.20	0.0484
2	2962	Chi-Chi- Taiwan-05	1999	6.20	0.0471
3	2938	Chi-Chi- Taiwan-05	1999	6.20	0.0526
4	3480	Chi-Chi- Taiwan-06	1999	6.30	0.0502
5	2939	Chi-Chi- Taiwan-05	1999	6.20	0.0412
6	1056	Northridge-01	1992	6.69	0.0627
7	919	Big Bear-01	1994	6.46	0.0493



B.6 OBE 2% damping

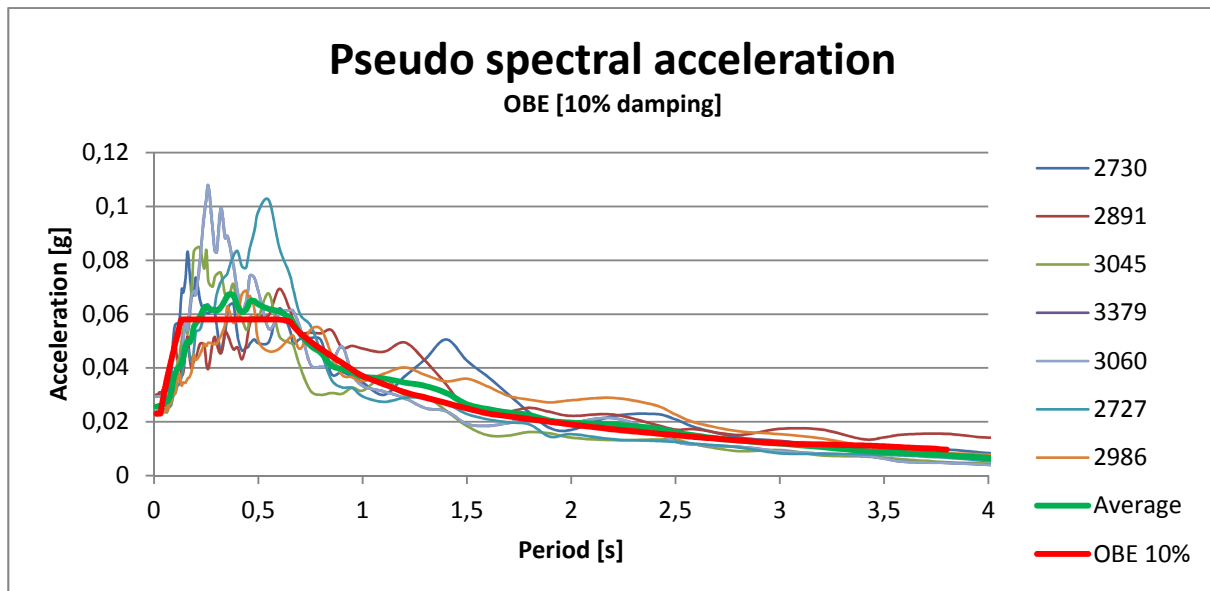
Number on list	Record number in database	Earthquake	Year	Magnitude	Peak acceleration
1	2939	Chi-Chi- Taiwan-05	1999	6.20	0.0412
2	2962	Chi-Chi- Taiwan-05	1999	6.20	0.0471
3	919	Big Bear-01	1992	6.46	0.0493
4	2938	Chi-Chi- Taiwan-05	1999	6.20	0.0526
5	2988	Chi-Chi- Taiwan-05	1999	6.20	0.0484
6	2960	Chi-Chi- Taiwan-05	1999	6.20	0.0438
7	1056	Northridge-01	1994	6.69	0.0627



B.7

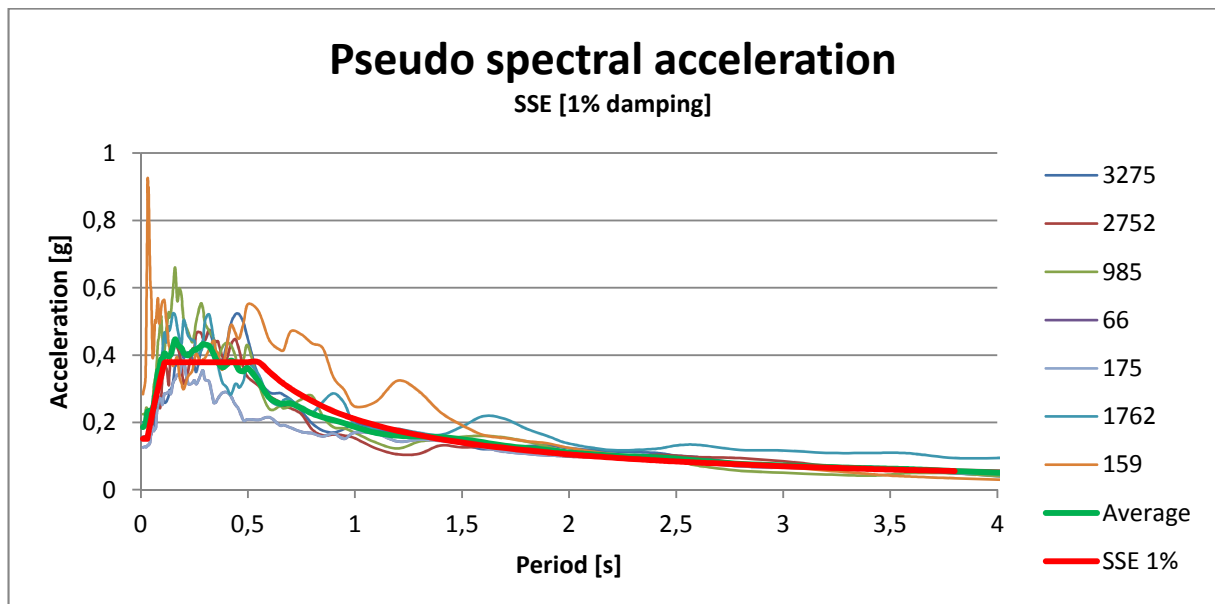
OBE 10% damping

Number on list	Record number in database	Earthquake	Year	Magnitude	Peak acceleration
1	2730	Chi-Chi- Taiwan-04	1999	6.20	0.0253
2	2891	Chi-Chi- Taiwan-04	1999	6.20	0.0301
3	3045	Chi-Chi- Taiwan-05	1999	6.20	0.0227
4	3379	Chi-Chi- Taiwan-06	1999	6.30	0.0264
5	3060	Chi-Chi- Taiwan-05	1999	6.20	0.0293
6	2727	Chi-Chi- Taiwan-04	1999	6.20	0.0283
7	2986	Chi-Chi- Taiwan-05	1999	6.20	0.0224



B.8 SSE 1% damping

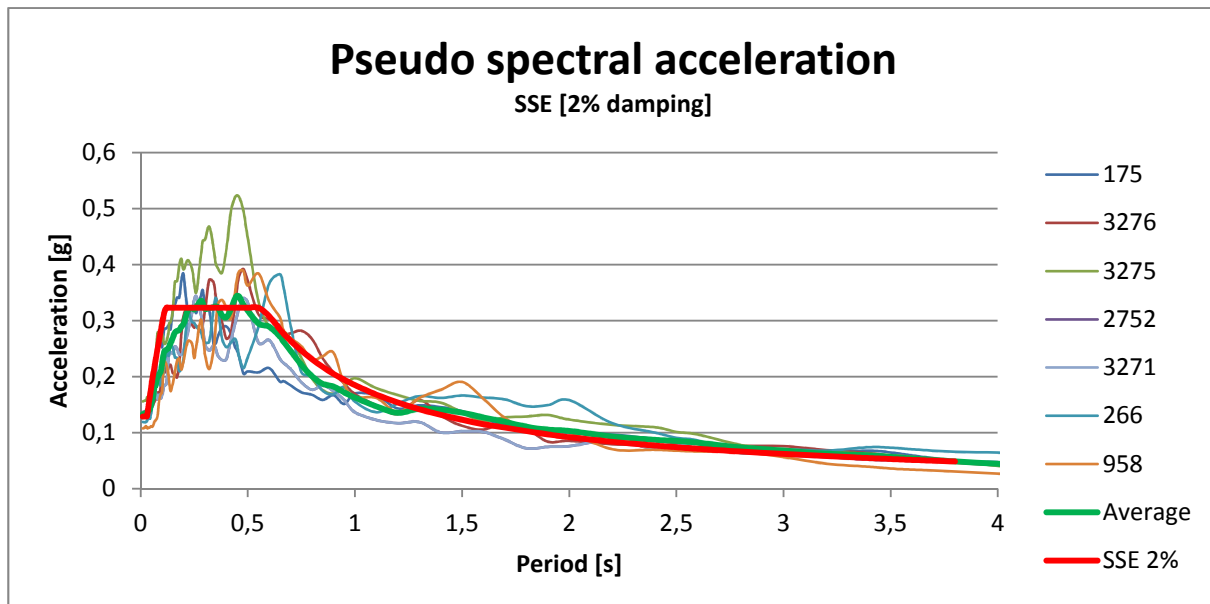
Number on list	Record number in database	Earthquake	Year	Magnitude	Peak acceleration
1	3275	Chi-Chi- Taiwan-06	1999	6.30	0.1557
2	2752	Chi-Chi- Taiwan-04	1999	6.20	0.1574
3	985	Northridge-01	1994	6.69	0.2211
4	66	San Fernando	1971	6.61	0.1887
5	175	Imperial Valley-06	1979	6.53	0.1258
6	1762	Hector Mine	1999	6.13	0.1986
7	159	Imperial Valley-06	1979	9.53	0.2810



B.9

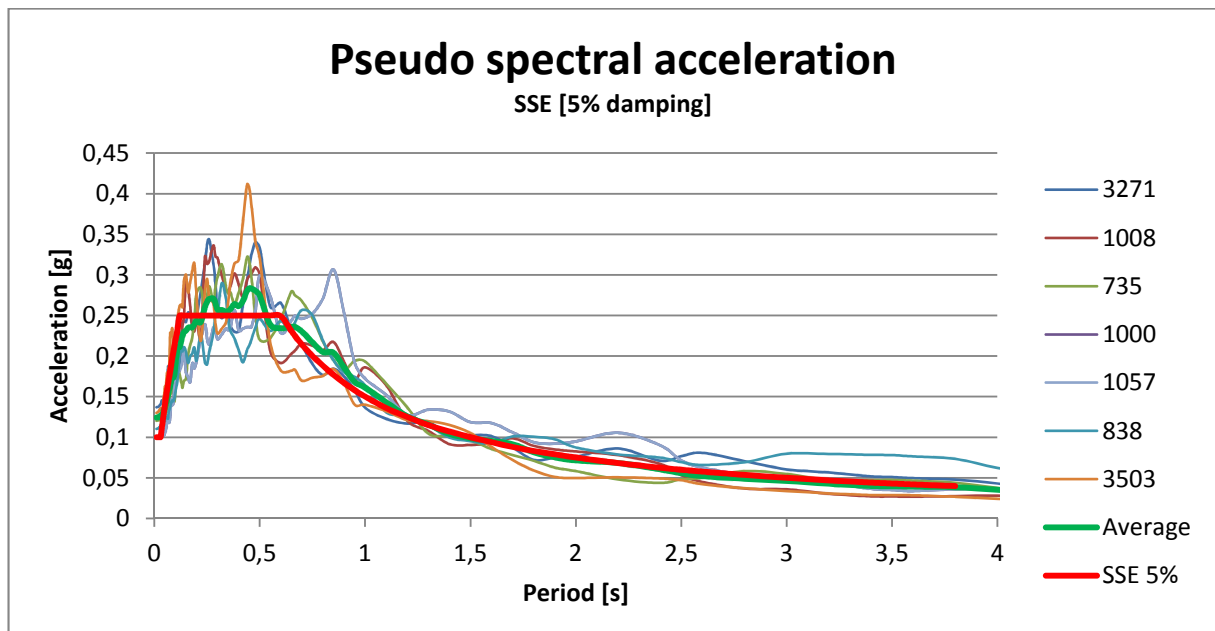
SSE 2% damping

Number on list	Record number in database	Earthquake	Year	Magnitude	Peak acceleration
1	175	Imperial Valley-06	1979	6.53	0.1258
2	3276	Chi-Chi- Taiwan-06	1999	6.30	0.1358
3	3275	Chi-Chi- Taiwan-06	1999	6.30	0.1557
4	2752	Chi-Chi- Taiwan-04	1999	6.20	0.1574
5	3271	Chi-Chi- Taiwan-06	1999	6.30	0.1367
6	266	Victoria-Mexico	1980	6.33	0.1182
7	958	Northridge-01	1994	6.69	0.1068



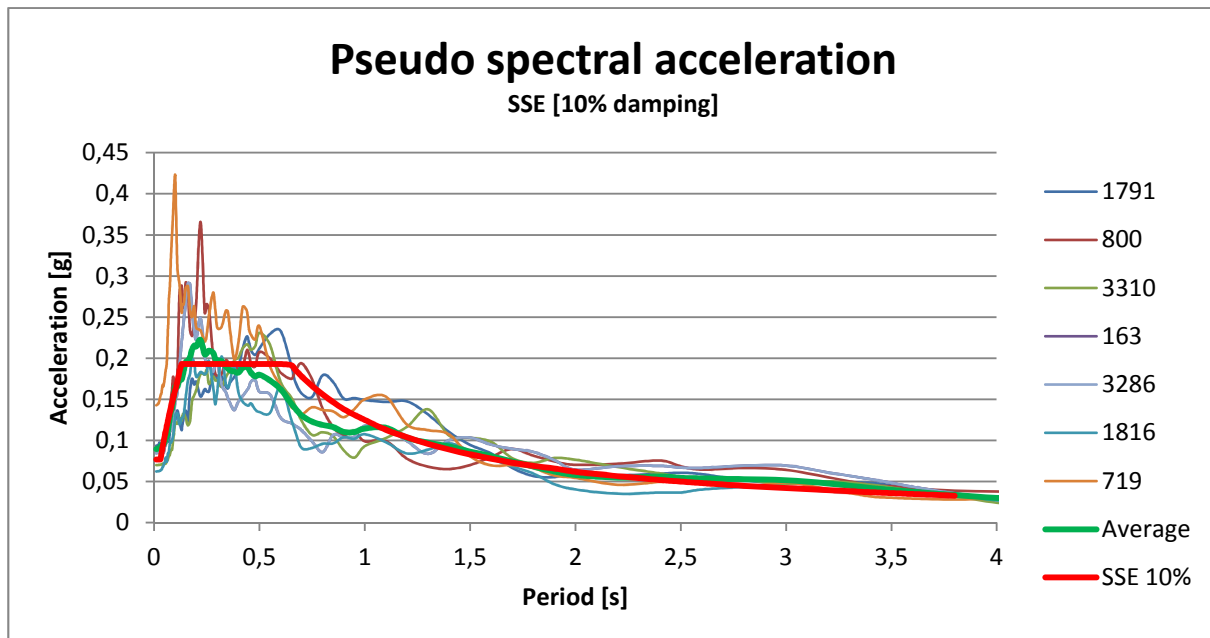
B.10 SSE 5% damping

Number on list	Record number in database	Earthquake	Year	Magnitude	Peak acceleration
1	3271	Chi-Chi- Taiwan-06	1999	6.30	0.1367
2	1008	Northridge-01	1994	6.69	0.1247
3	735	Loma Prieta	1989	6.93	0.1201
4	1000	Northridge-01	1994	6.69	0.1522
5	1057	Northridge-01	1994	6.69	0.0997
6	838	Landers	1992	7.28	0.1092
7	3503	Chi-Chi- Taiwan-06	1999	6.30	0.1299



B.11 SSE 10% damping

Number on list	Record number in database	Earthquake	Year	Magnitude	Peak acceleration
1	1791	Hector Mine	1999	7.13	0.0929
2	800	Loma Prieta	1989	6.93	0.0913
3	3310	Chi-Chi- Taiwan-06	1999	6.30	0.0701
4	163	Imperial Valley-06	1979	6.53	0.1015
5	3286	Chi-Chi- Taiwan-06	1999	6.30	0.0841
6	1816	Hector Mine	1999	7.13	0.0622
7	719	Superstition Hills-02	1987	6.54	0.1404

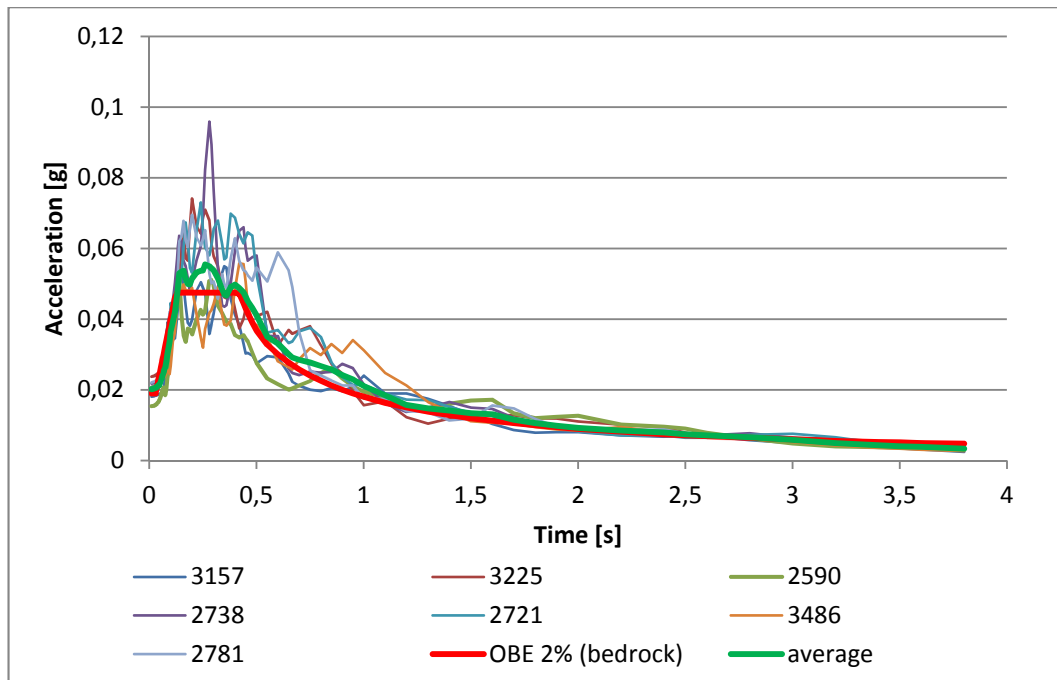


B.12 OBE bedrock

The selection of bedrock signals is a little different than the selection of the OBE and SSE signals for the top soil layers in the previous paragraphs. The OBE bedrock signals are selected from the OBE 2% damping response spectrum according to soil type A. The following selection criteria have been used:

- Magnitude : 6.2 – 7.2
- Preferred NEHRP based on Vs;30 : A
- Peak ground acceleration : 0.02

Number on list	Record number in database	Earthquake	Year	Magnitude	Peak acceleration
1	3157	Chi-Chi- Taiwan-05	1999	6.20	0.0181
2	3225	Chi-Chi- Taiwan-05	1999	6.20	0.0237
3	2590	Chi-Chi- Taiwan-03	1987	6.20	0.0154
4	2738	Chi-Chi- Taiwan-04	1999	6.20	0.0217
5	2721	Chi-Chi- Taiwan-04	1999	6.20	0.0209
6	3486	Chi-Chi- Taiwan-06	1979	6.30	0.0208
7	2781	Chi-Chi- Taiwan-04	1999	6.20	0.0221

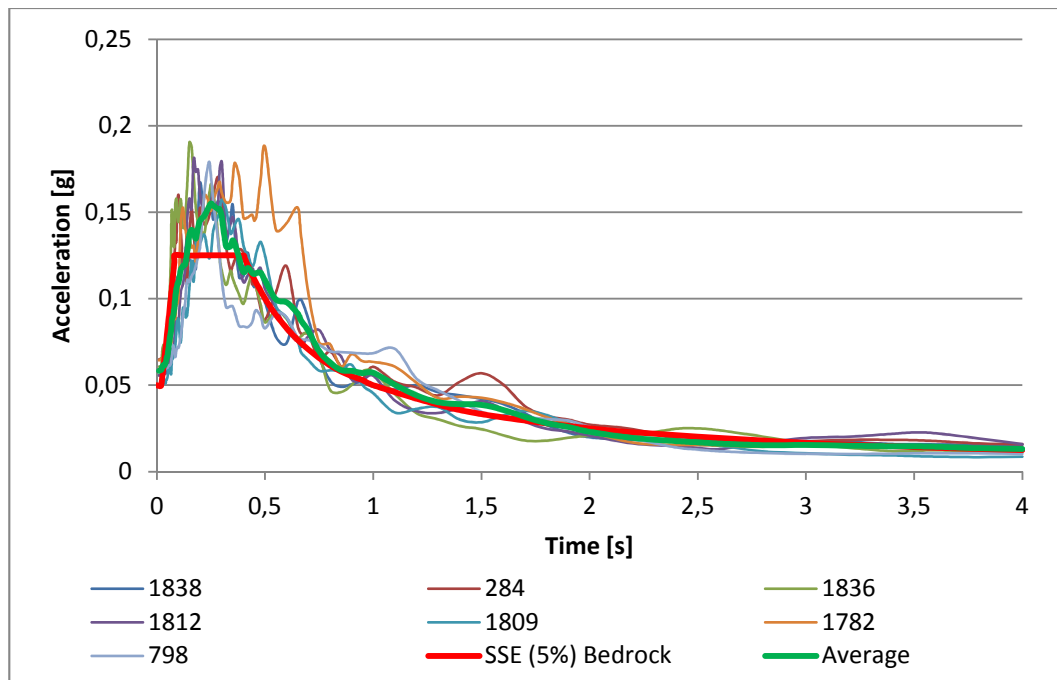


B.13 SSE bedrock

The selection of bedrock signals is a little different than the selection of the OBE and SSE signals for the top soil layers in the previous paragraphs. The SSE bedrock signals are selected from the SSE 5% damping response spectrum according to soil type A. The following selection criteria have been used:

- Magnitude : 6.2 – 7.2
- Preferred NEHRP based on Vs;30 : A
- Peak ground acceleration : 0.05

Number on list	Record number in database	Earthquake	Year	Magnitude	Peak acceleration
1	3157	Hector Mine	1999	7.13	0.0556
2	3225	Irpinia- Italy-01	1980	6.90	0.0647
3	2590	Hector Mine	1999	7.13	0.0601
4	2738	Hector Mine	1999	7.13	0.0557
5	2721	Hector Mine	1999	7.13	0.0486
6	3486	Hector Mine	1999	7.13	0.0643
7	2781	Loma Prieta	1989	6.93	0.0577



Appendix C

C. MATLAB CODE FOR FAST FOURIER TRANSFORMATION OF EARTHQUAKE SIGNAL

```

1 %%%%%%
2 % Fast Fourier Transformation from time to frequency domain %
3 % to analyse dominant frequencies in the signals %
4 %
5 % x = vector of time steps signal 1 %
6 % y = vector of accelerations signal 1 %
7 %
8 % x1 = vector of time steps signal 2 %
9 % y1 = vector of accelerations signal 2 %
10 %
11 %%%%%%
12
13
14 - L=length(x);
15 - L1=length(x1);
16
17 - NFFT=2^nextpow2 (L);
18 - NFFT1=2^nextpow2 (L1);
19
20 - Y=fft(y,NFFT)/L;
21 - Y1=fft(y1,NFFT1)/L1;
22
23 - f=Fs/2*linspace(0,1,NFFT/2+1);
24 - f1=Fs/2*linspace(0,1,NFFT1/2+1);
25
26 - semilogx(f,2*abs(Y(1:NFFT/2+1)), 'k');
27 - xlabel('Frequency [Hz]');
28 - ylabel('Magnitude [-]');
29 - hold on
30
31 - semilogx(f1,2*abs(Y1(1:NFFT1/2+1)), 'b');
32

```


Appendix D

D. CALCULATION OF MESH ELEMENT SIZE AND CRITICAL TIME STEP

Formulas						
Shear wave velocity (PLAXIS 2D manual)			Frequency of soil deposit			
$V_s = \sqrt{\frac{G}{\rho}} = \sqrt{\frac{G}{\gamma}} = \sqrt{\frac{E}{2(1+\nu)}} = \sqrt{\frac{Eg}{2(1+\nu)\gamma}}$			$f_0 = \frac{1}{T_0} = \frac{v_s}{4H}$			
Element size (Lysmer & Kuhlmeier)						
$\text{element size}_{layer} \leq \frac{\lambda_{layer}}{5} = \frac{v_{s,layer}}{5 \cdot f_{max}}$						
Courant's condition						
$\frac{v_{c,layer} \Delta t}{\text{element size}_{layer}} \leq 1 \Rightarrow \Delta t_{max} \leq \frac{\text{element size}_{layer}}{\sqrt{\frac{E(1-\nu)}{\rho(1+\nu)(1-2\nu)}}} = \frac{\text{element size}_{layer}}{v_{s,layer} \sqrt{\frac{2(1-\nu)}{(1-2\nu)}}}$						
General input						
Parameter	Sand Fill Loose - Medium dense	Clay Medium stiff	Sand Medium Dense-Dense	Unit		
E _{ur;ref}	60000	15000	120000	[kN/m ²]		
m	0,5	0,9	0,5	[·]		
g	9,81	9,81	9,81	[m/s ²]		
v _{ur}	0,2	0,2	0,2	[·]		
Y _{sat}	20	15	20	[kn/m ³]		
H	4	29	29	[m]		
f _{impulsive liquid}	2	2	2	[Hz]		
Calculation element size and time step						
Parameter	Sand Fill Loose - Medium dense	Clay Medium stiff	Sand Medium Dense-Dense	Unit		
E _{ur;ref}	60000	15000	300000	[kN/m ²]		
v _{ur}	0,15	0,2	0,15	[·]		
f _{soil deposit}	5,5	0,6	3,0	[Hz]		
f _{signal,max}	20	20	20	[Hz]		
f _{impulsive,max}	2	2	2	[Hz]		
f _{important,max}	12	12	12	[Hz]		
σ _{mid}	36	129	346	[kN/m ²]		
E _{ur,mid}	36000	18798	558032	[kN/m ²]		
v _{s,mid}	88	72	345	[·]		
e size _{soil deposit}	3,20	23,20	23,20	[m]		
e size _{signal max}	0,88	0,72	3,45	[m]		
e size _{impulsive max}	8,76	7,16	34,50	[m]		
e size _{important max}	1,46	1,19	5,75	[m]		
Δt _{max}	0,0064	0,0061	0,0064	[s]		
σ ^t _{top}	9	56	201	[kN/m ²]		
E _{ur,top}	18000	8901	425323	[kN/m ²]		
v _{s,top}	62	49	301	[·]		
e size _{soil deposit}	2,26	15,96	20,25	[m]		
e size _{signal max}	0,62	0,49	3,01	[m]		
e size _{impulsive max}	6,20	4,93	30,12	[m]		
e size _{important max}	1,03	0,82	5,02	[m]		
Δt _{max}	0,0064	0,0061	0,0064	[s]		

Appendix E

E. RESULTS SITE RESPONSE ANALYSES

- Input signal
- 1D - Tied Degrees of Freedom
- 2D - Viscous boundaries - 50 meter
- 2D - Viscous boundaries - 100 meter
- 2D - Viscous boundaries - 150 meter
- 2D - Viscous boundaries - 200 meter
- 2D – Free Field boundaries - 50 meter
- 2D – Free Field boundaries - 75 meter
- 2D – Free Field boundaries - 100 meter
- 2D – Free Field boundaries - 125 meter

E.1 Check of input signal

All models are checked on the input signal for both the OBE- and SSE signal. The horizontal accelerations at bedrock level (-60) in the middle of the model are extracted from PLAXIS 2D and compared with the original input signals. In case of proper implementation of the signal only small differences can be found due to different time steps and/or little numerical errors. All models described in the introduction of this appendix are considered below. first the OBE signals followed by all SSE signals. Results are presented in figures 8 Till 17 for OBE and figure 18 to 27 For SSE

E.1.1 OBE signal check

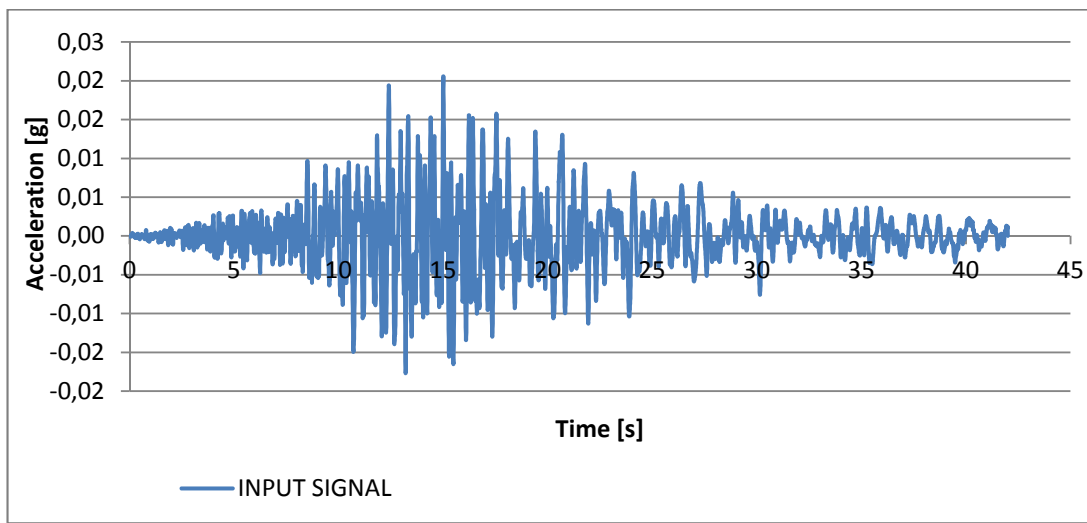


Figure 10 Input signal for all OBE analyses (signal 2781)

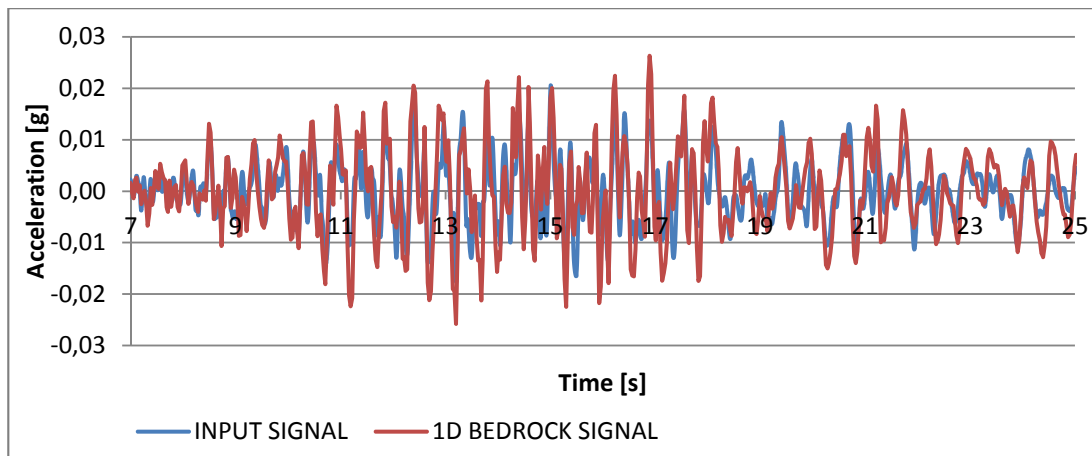


Figure 11 OBE input signal check: 1D - tied degrees of freedom boundaries

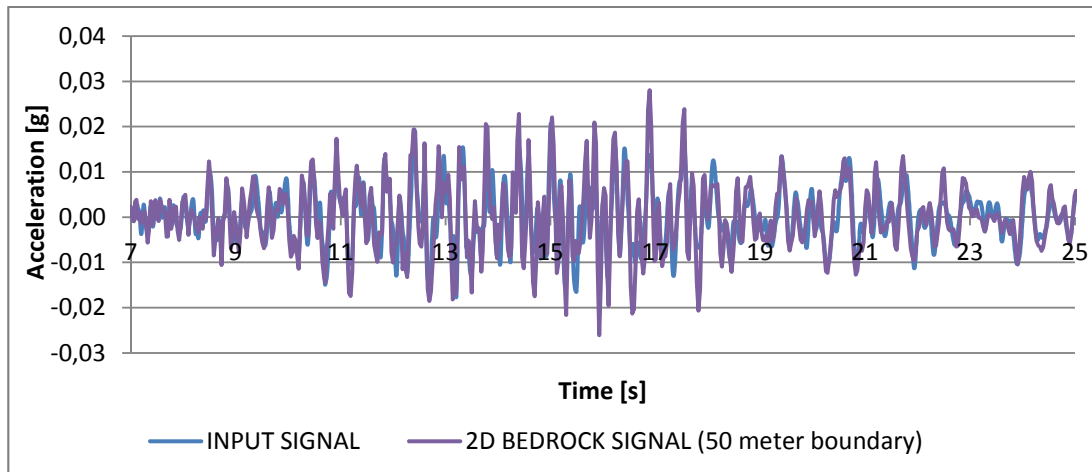


Figure 12 OBE input signal check: 2D - viscous boundaries at a distance of 50 m. (100 m. model width)

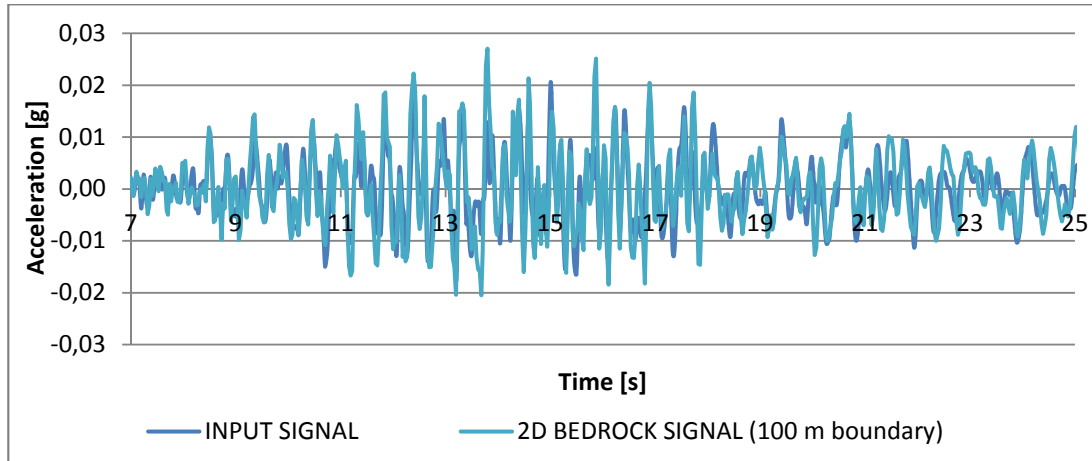


Figure 13 OBE input signal check: 2D - viscous boundaries at a distance of 100 m. (200 m. model width)

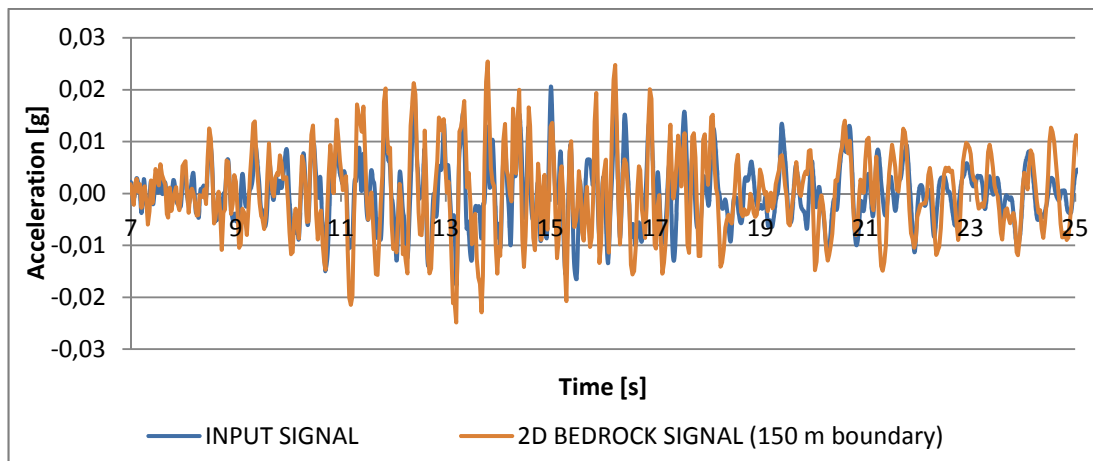


Figure 14 OBE input signal check: 2D - viscous boundaries at a distance of 150 m. (300 m. model width)

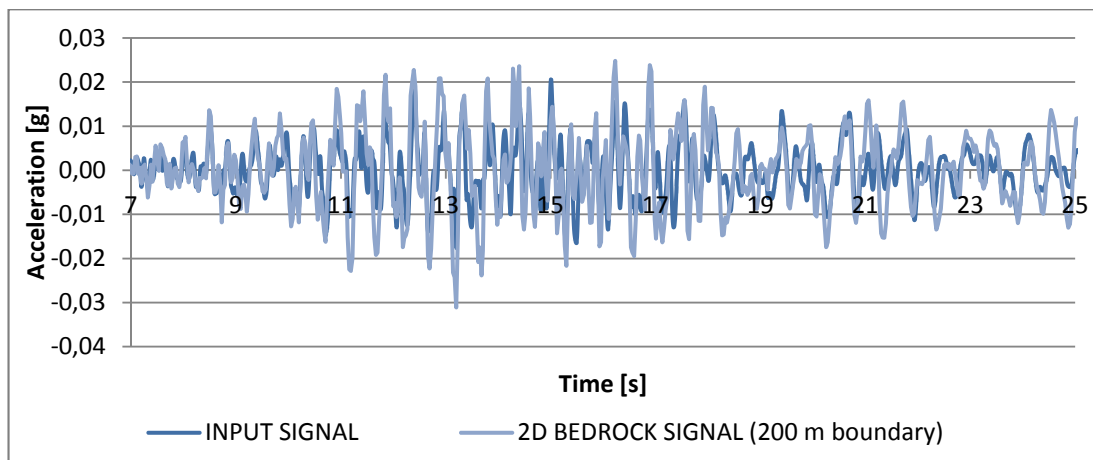


Figure 15 OBE input signal check: 2D - viscous boundaries at a distance of 200 m. (400 m. model width)

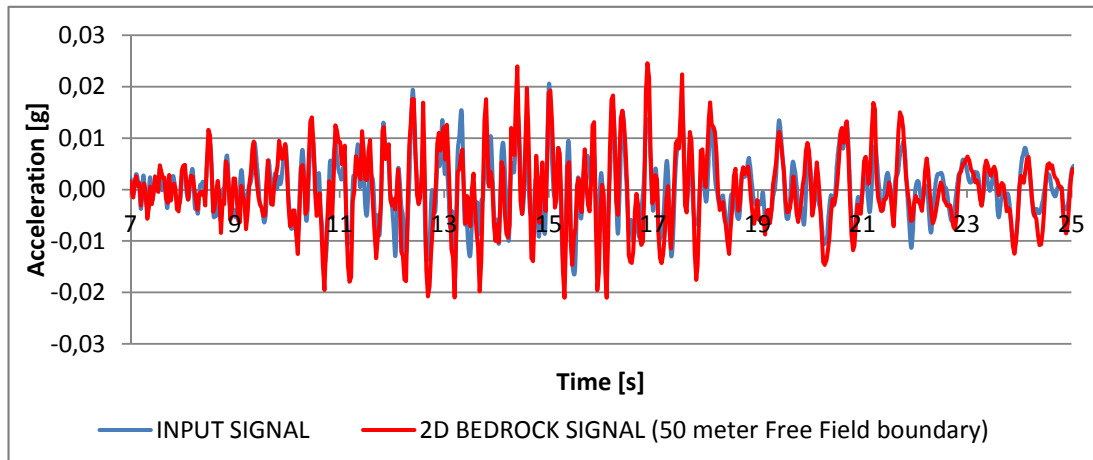


Figure 16 OBE input signal check: 2D - Free Field boundaries at a distance of 50 m. (100 m. model width)

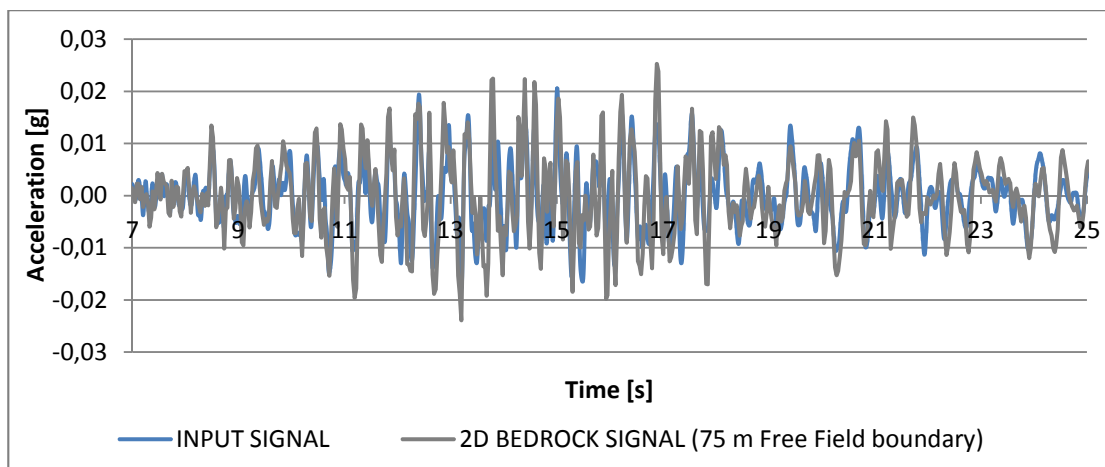


Figure 17 OBE input signal check: 2D - Free Field boundaries at a distance of 75 m. (150 m. model width)

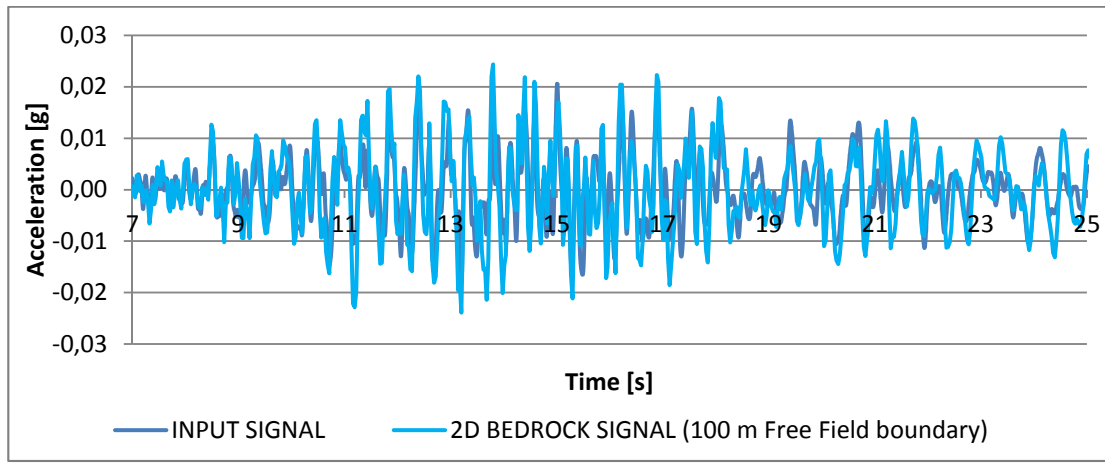


Figure 18 OBE input signal check: 2D - Free Field boundaries at a distance of 100 m. (200 m. model width)

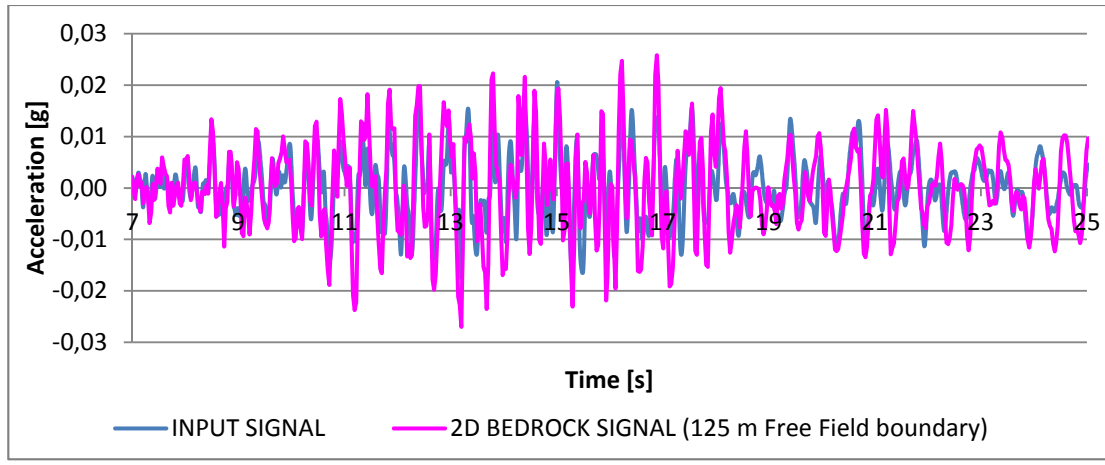


Figure 19 OBE input signal check: 2D - Free Field boundaries at a distance of 125 m. (250 m. model width)

E.1.2 SSE signal check

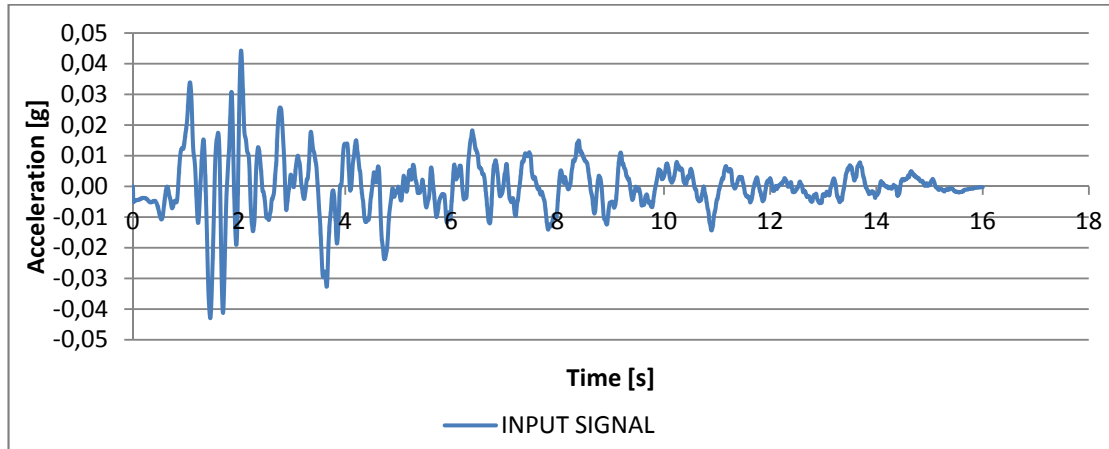


Figure 20 SSE input signal

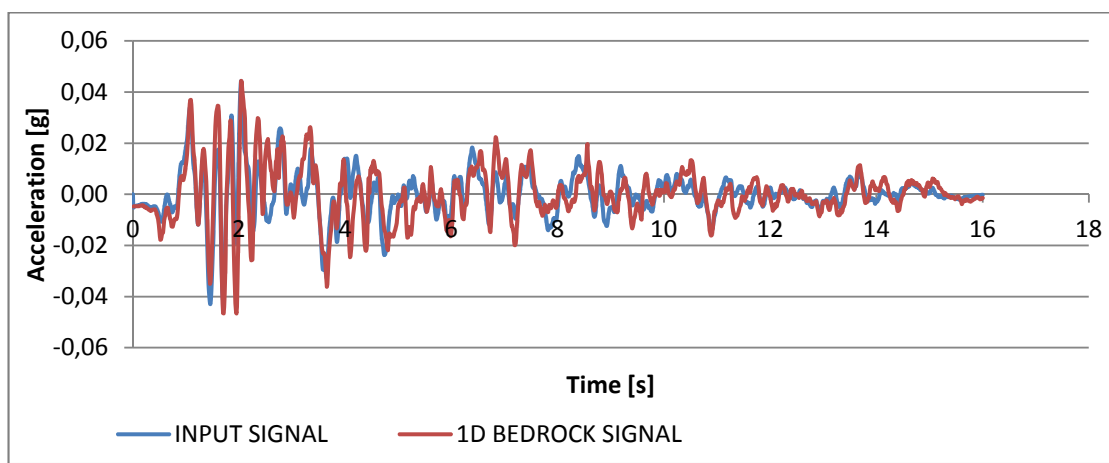


Figure 21 SSE signal check for 1D tied degrees of freedom

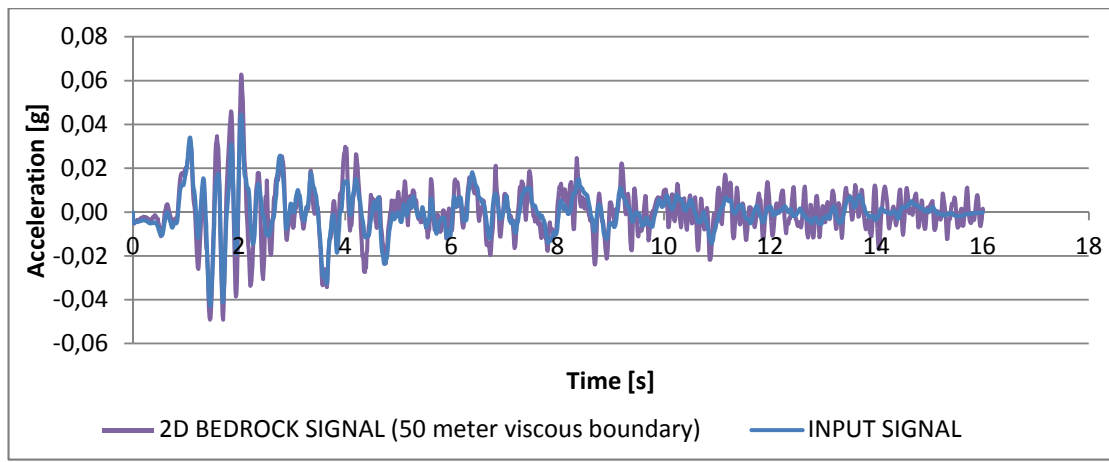


Figure 22 SSE signal check for 2D viscous boundaries at 50 m. (100m. model width)

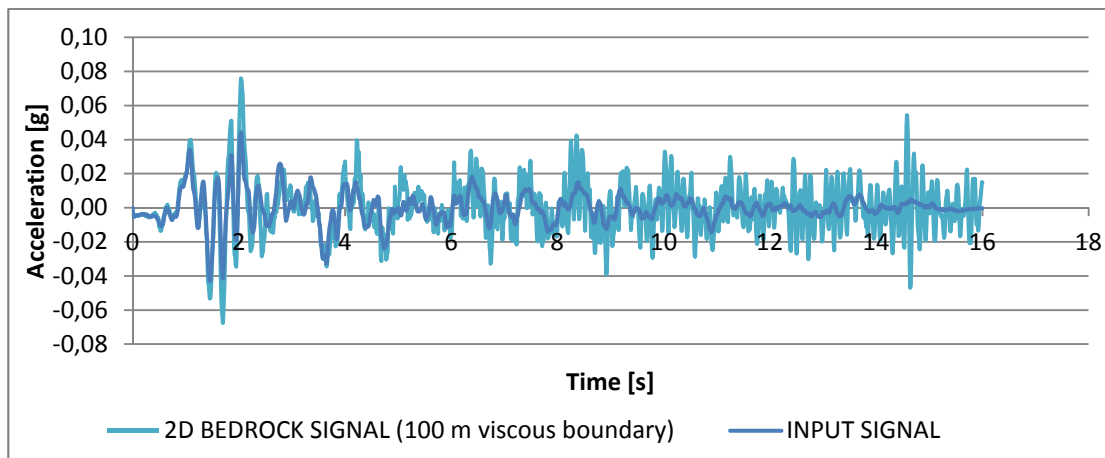


Figure 23 SSE signal check for 2D viscous boundaries at 100 m. (200m. model width)

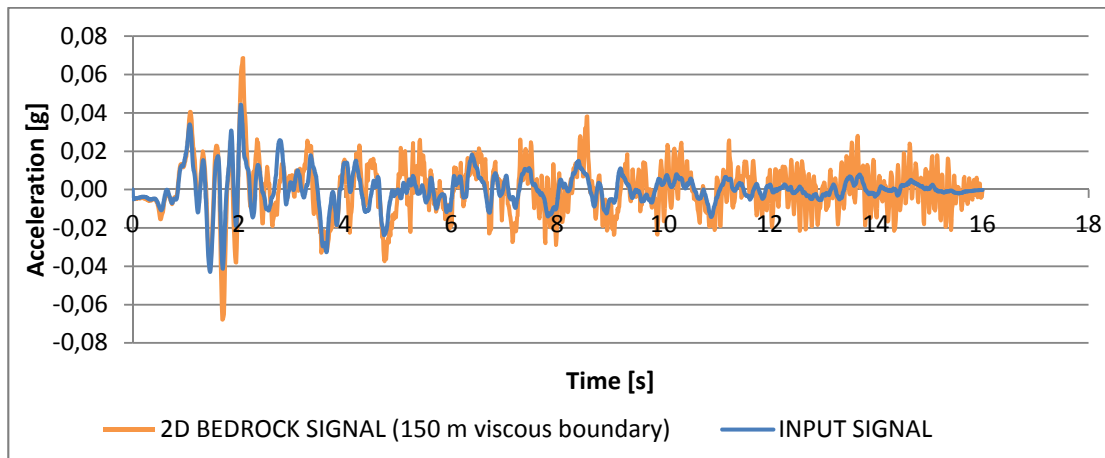


Figure 24 SSE signal check for 2D viscous boundaries at 150 m. (300m. model width)

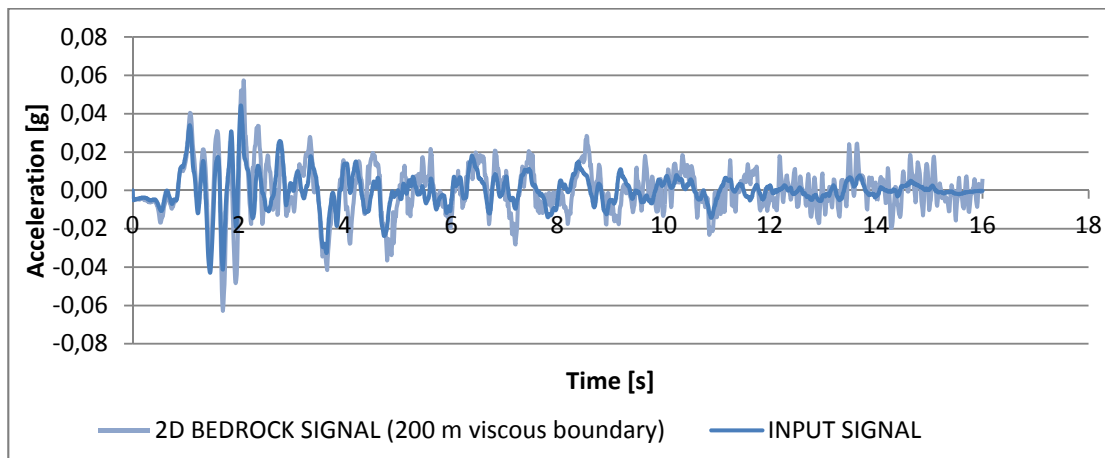


Figure 25 SSE signal check for 2D viscous boundaries at 200 m. (400m. model width)

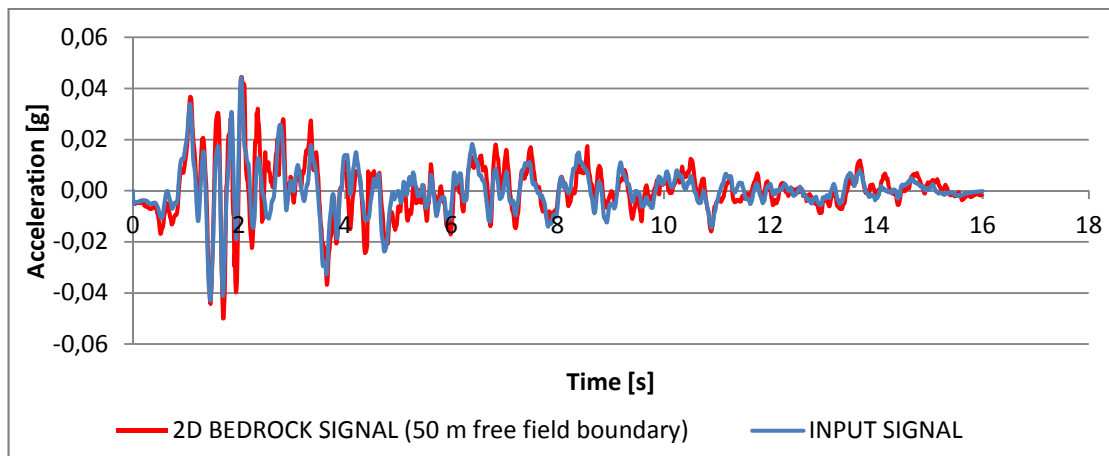


Figure 26 SSE signal check for 2D Free Field boundaries at 50 m. (100m. model width)

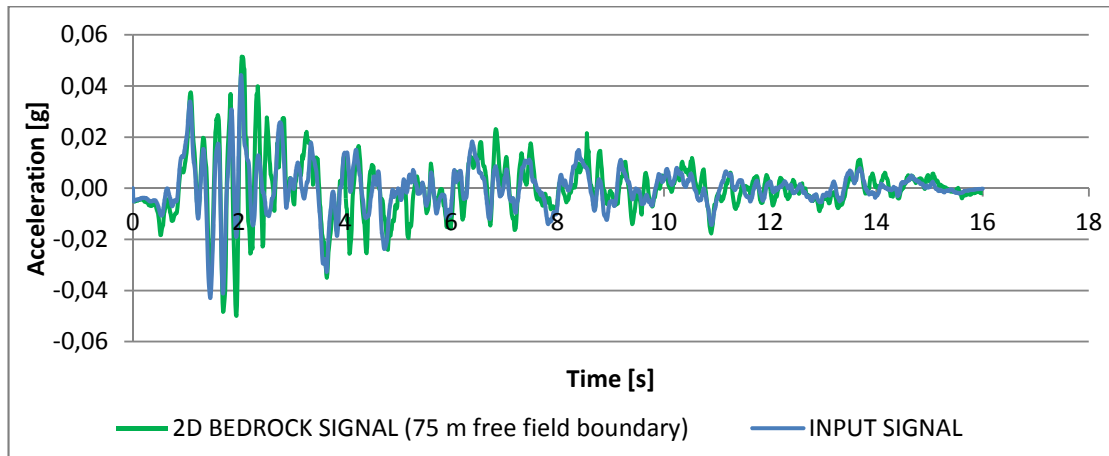


Figure 27 SSE signal check for 2D Free Field boundaries at 75 m. (150m. model width)

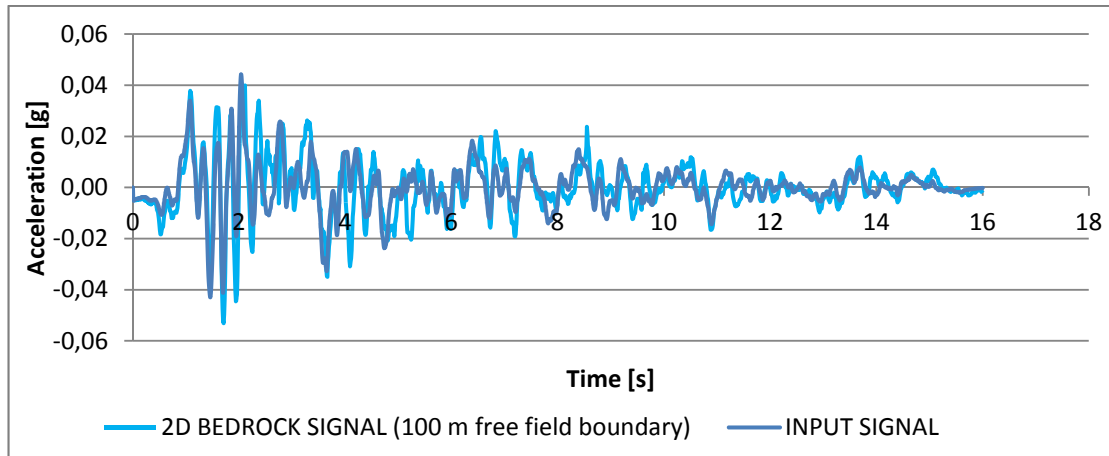


Figure 28 SSE signal check for 2D Free Field boundaries at 100 m. (200m. model width)

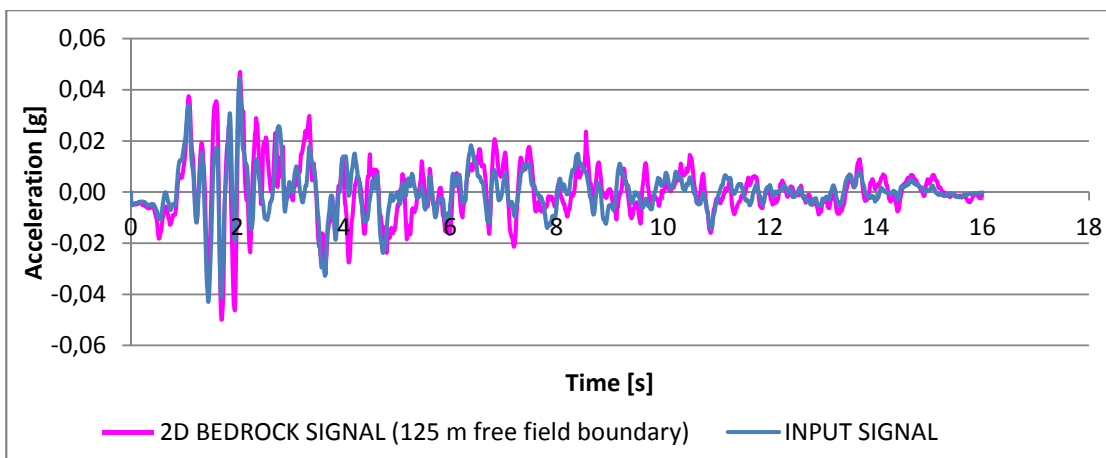


Figure 29 SSE signal check for 2D Free Field boundaries at 125 m. (250m. model width)

E.2 Check horizontal accelerations at ground level

All models are checked on horizontal accelerations at ground level.

E.2.1 OBE horizontal acceleration

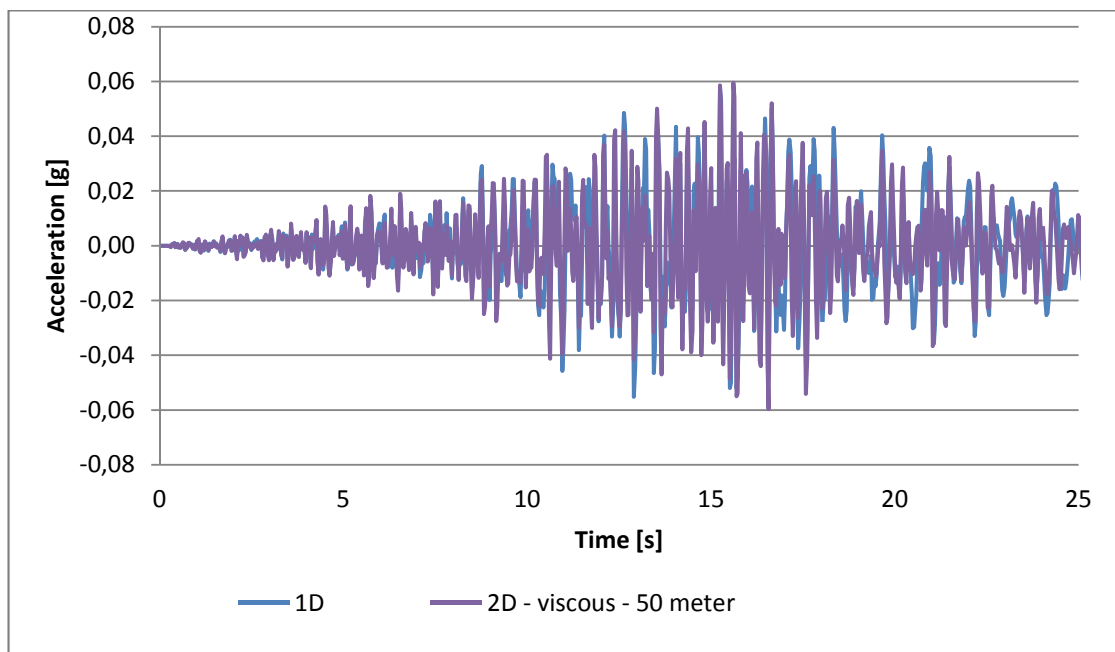


Figure 30 OBE horizontal acceleration (ax): 1D - viscous boundaries 50 meter (100 meter model width)

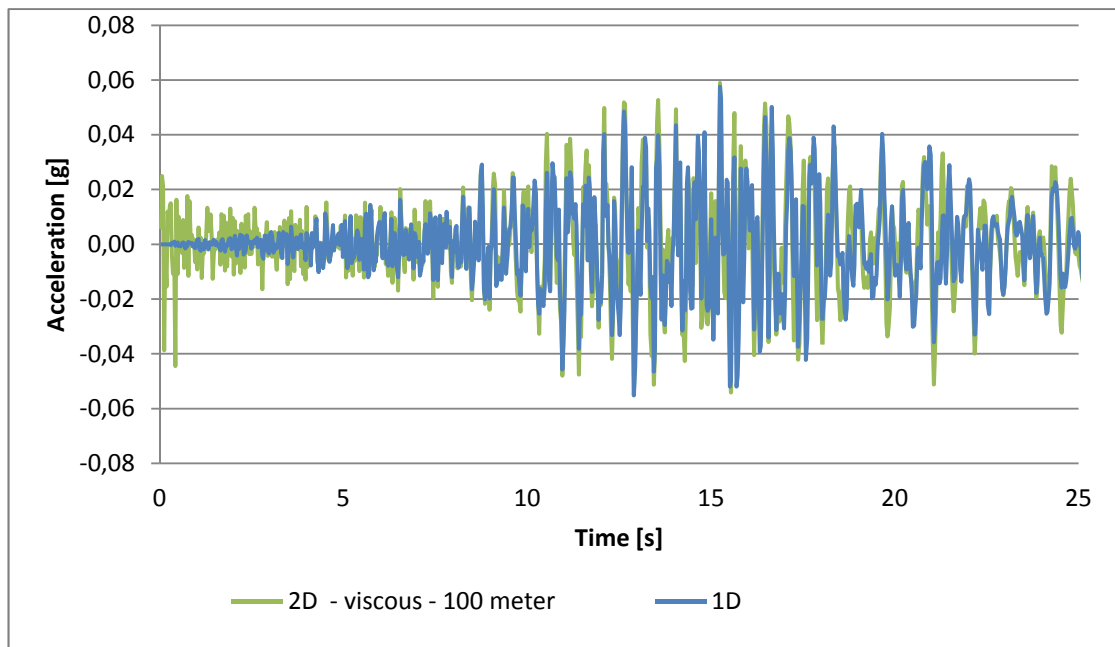


Figure 31 OBE horizontal acceleration (ax): 1D - viscous boundaries 100 meter (200 meter model width)

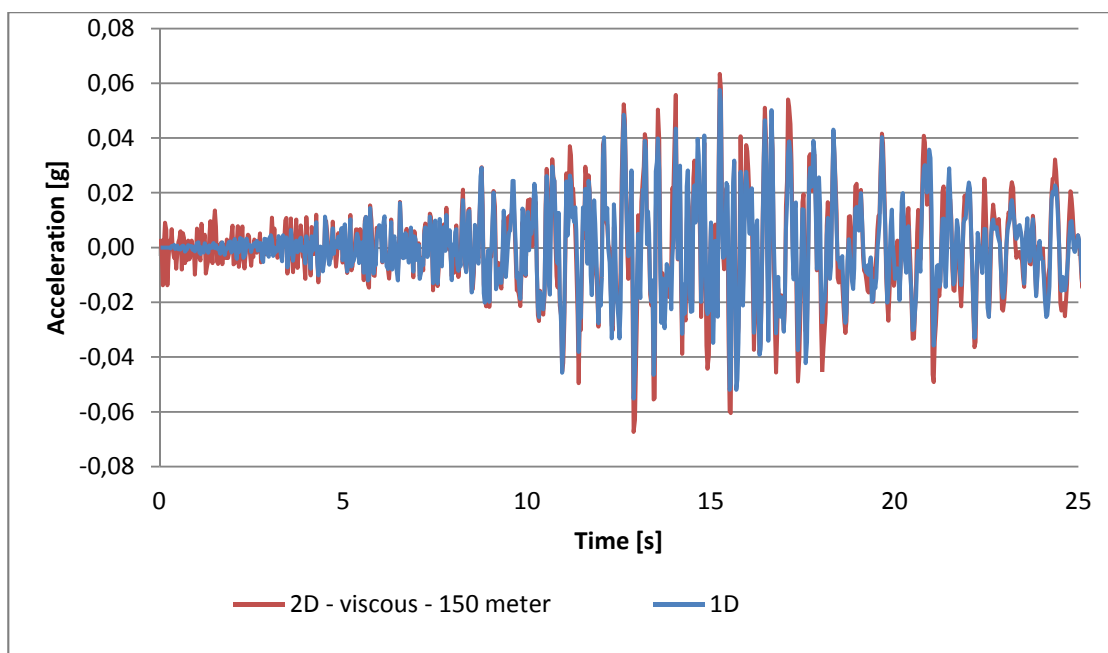


Figure 32 OBE horizontal acceleration (ax): 1D - viscous boundaries 150 meter (300 meter model width)

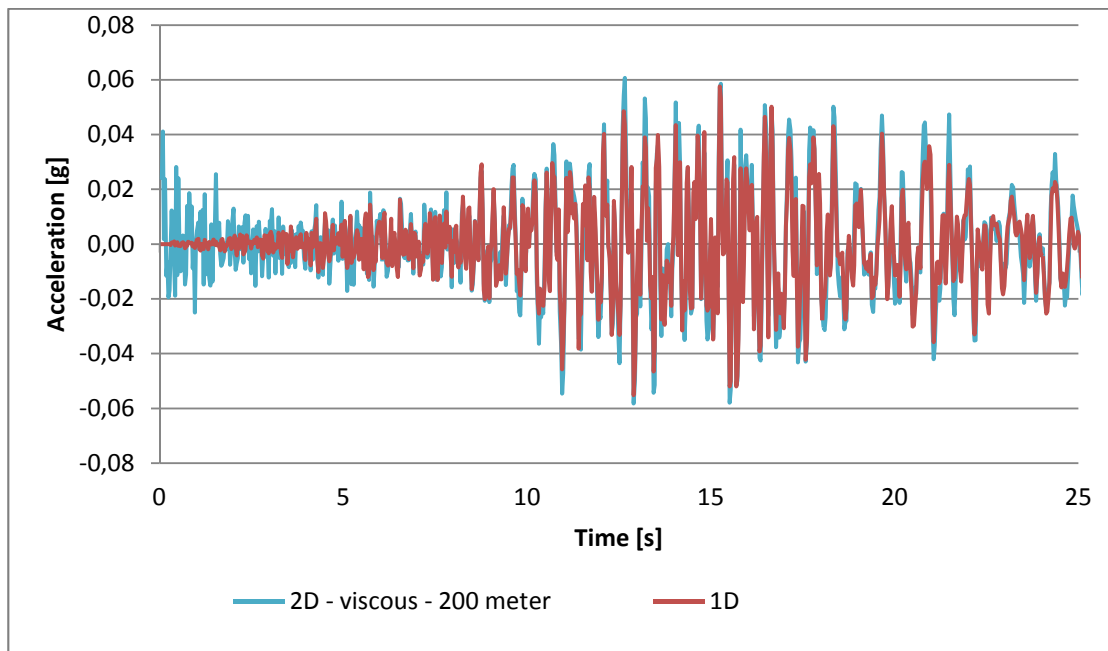


Figure 33 OBE horizontal acceleration (ax): 1D - viscous boundaries 200 meter (400 meter model width)

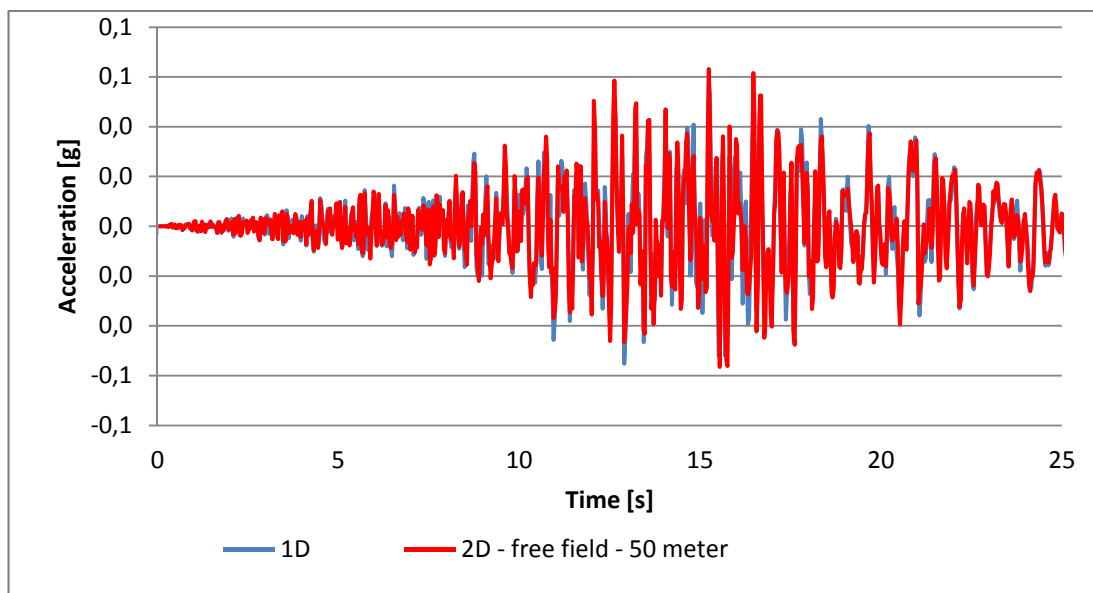


Figure 34 OBE horizontal acceleration (ax): 1D - free field boundaries 50 meter (100 meter model width)

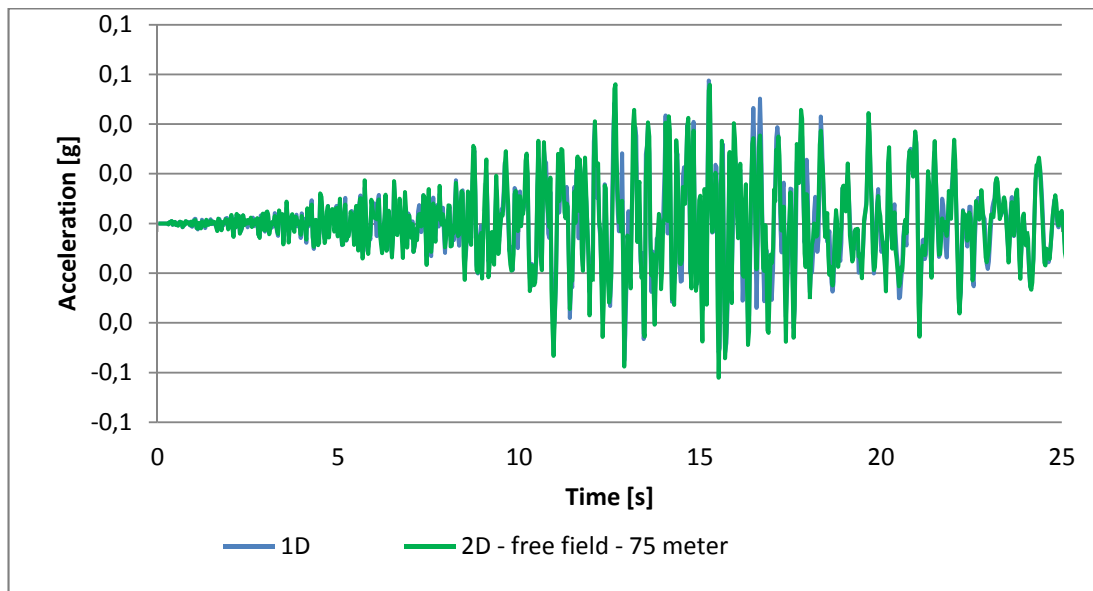


Figure 35 OBE horizontal acceleration (ax): 1D - free field boundaries 75 meter (150 meter model width)

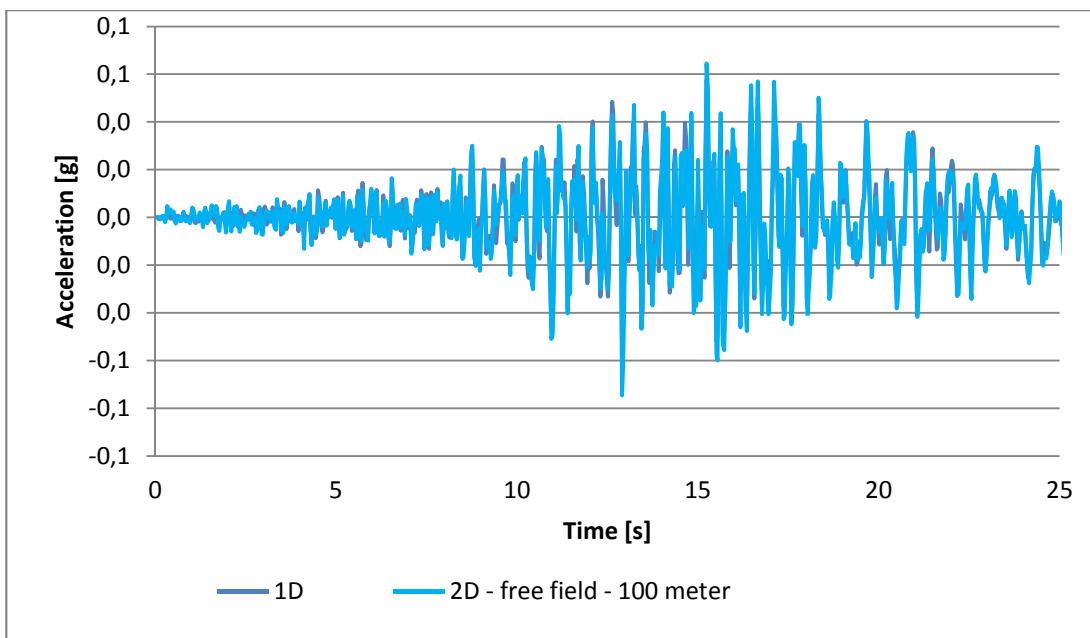


Figure 36 OBE horizontal acceleration (ax): 1D - free field boundaries 100 meter (200 meter model width)

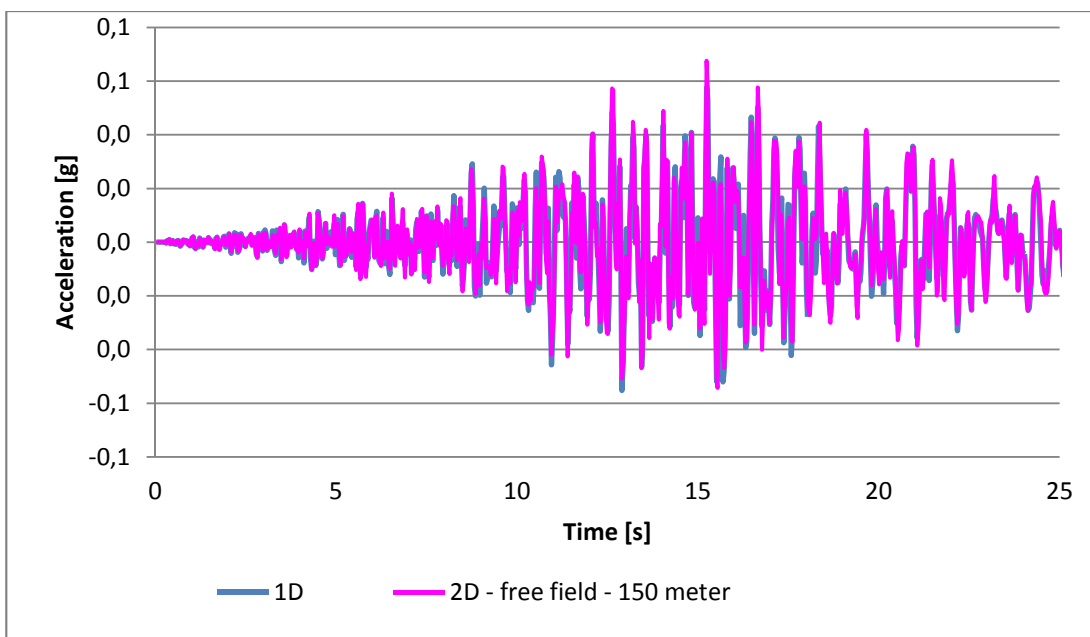


Figure 37 OBE horizontal acceleration (ax): 1D - free field boundaries 125 meter (250 meter model width)

E.2.2 SSE horizontal acceleration

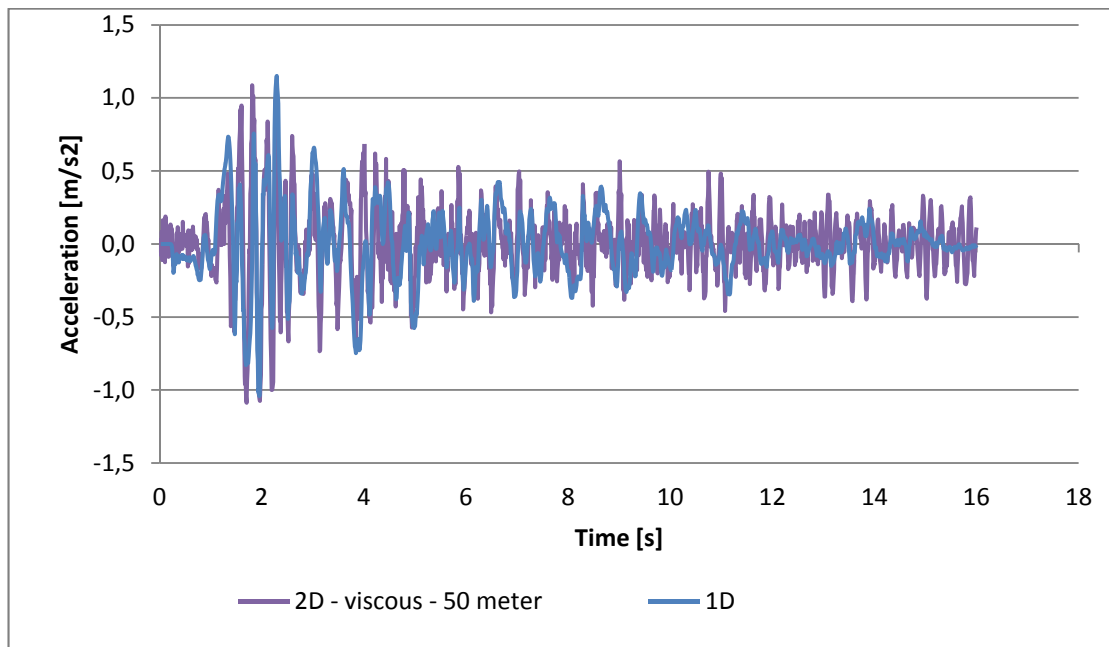


Figure 38 SSE horizontal acceleration (ax): 1D - viscous boundaries 50 meter (100 meter model width)

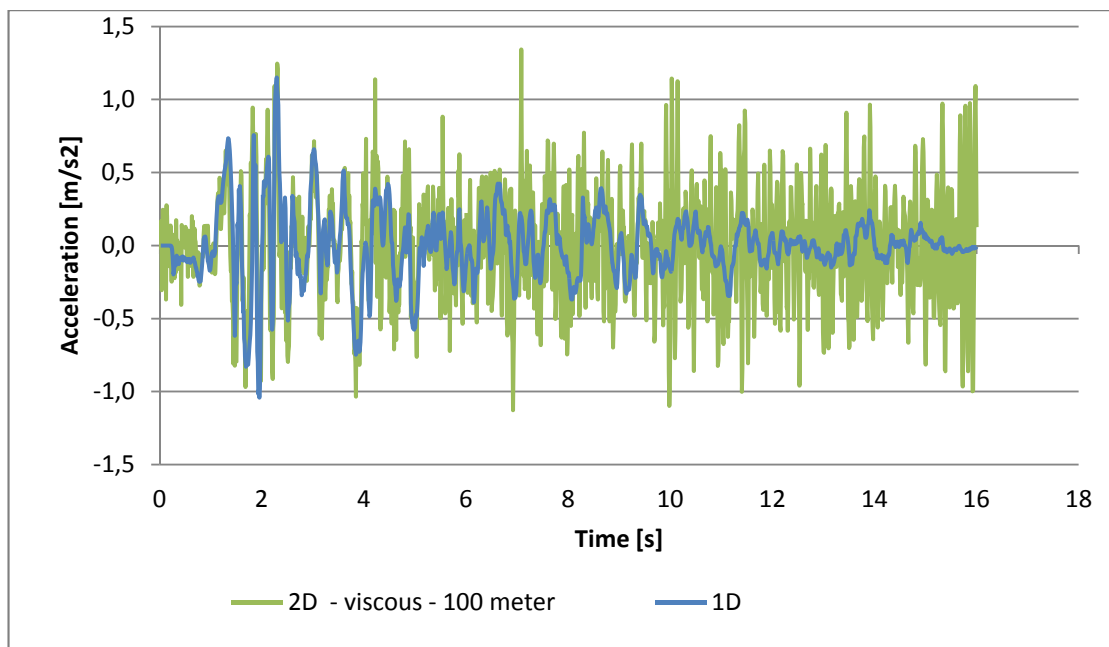


Figure 39 SSE horizontal acceleration (ax): 1D - viscous boundaries 100 meter (200 meter model width)

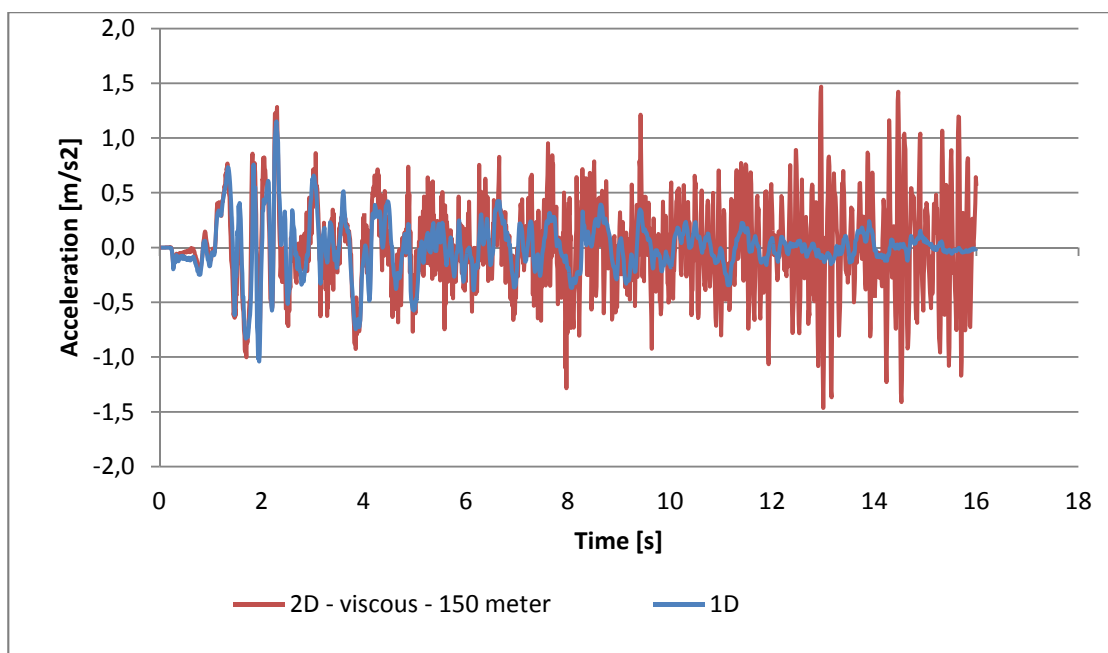


Figure 40 SSE horizontal acceleration (ax): 1D - viscous boundaries 150 meter (300 meter model width)

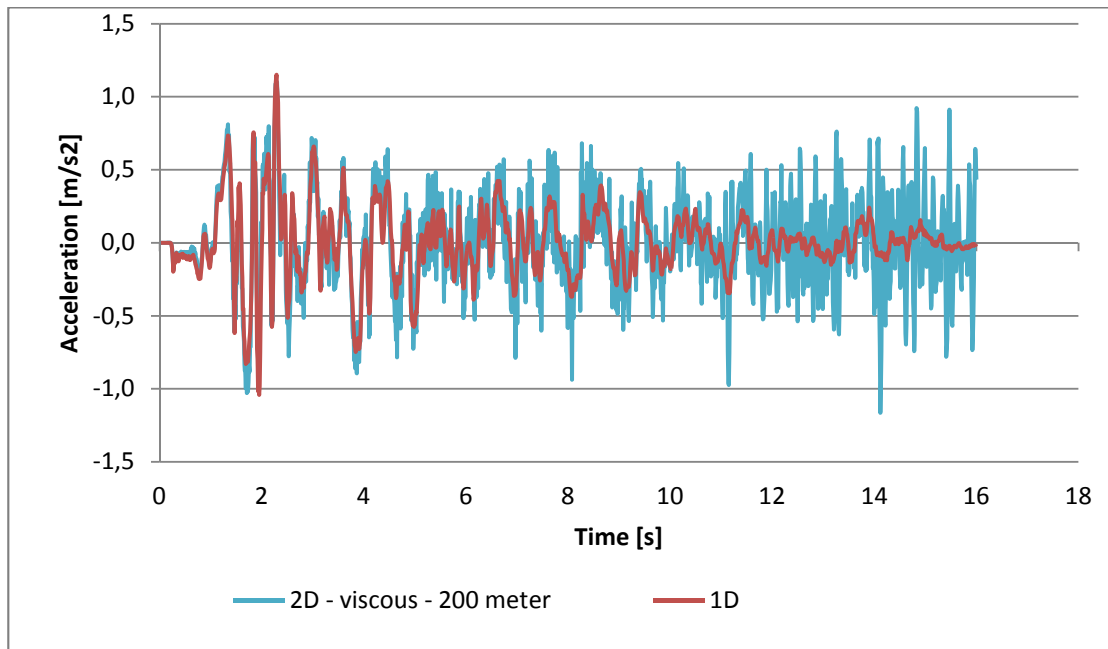


Figure 41 SSE horizontal acceleration (ax): 1D - viscous boundaries 200 meter (400 meter model width)

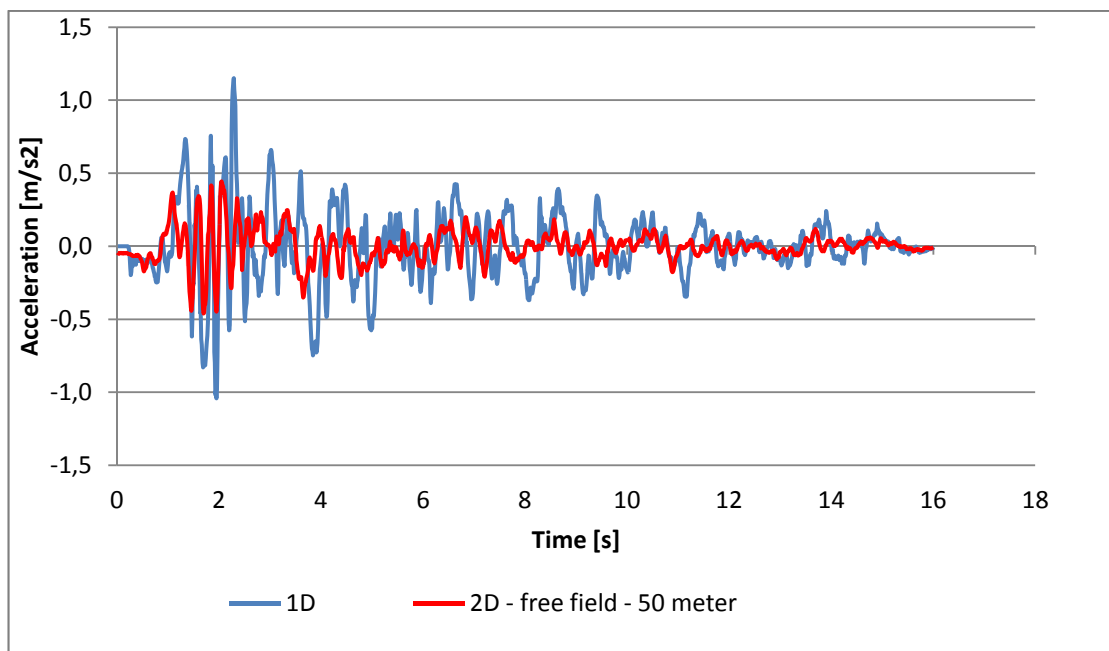


Figure 42 SSE horizontal acceleration (ax): 1D - free field boundaries 50 meter (100 meter model width)

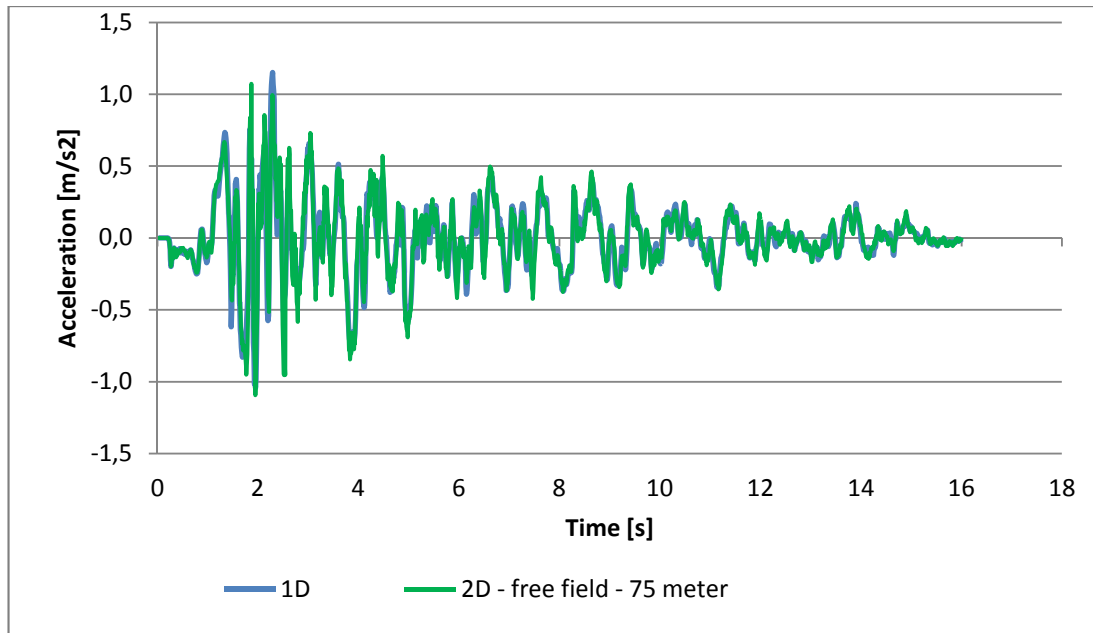


Figure 43 SSE horizontal acceleration (ax): 1D - free field boundaries 75 meter (150 meter model width)

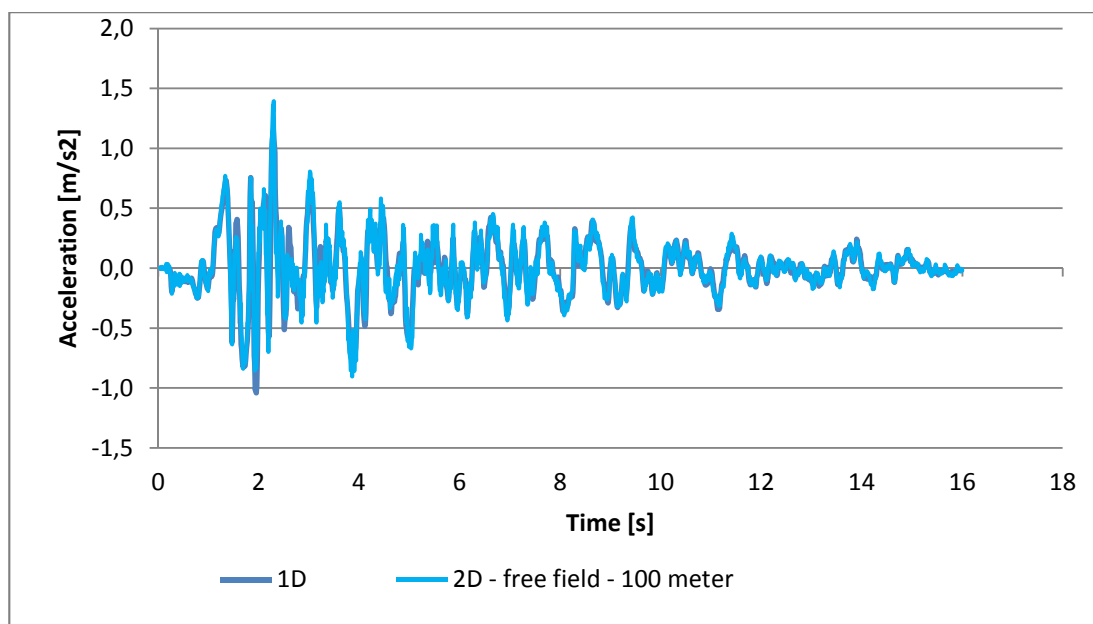


Figure 44 SSE horizontal acceleration (ax): 1D - free field boundaries 100 meter (200 meter model width)

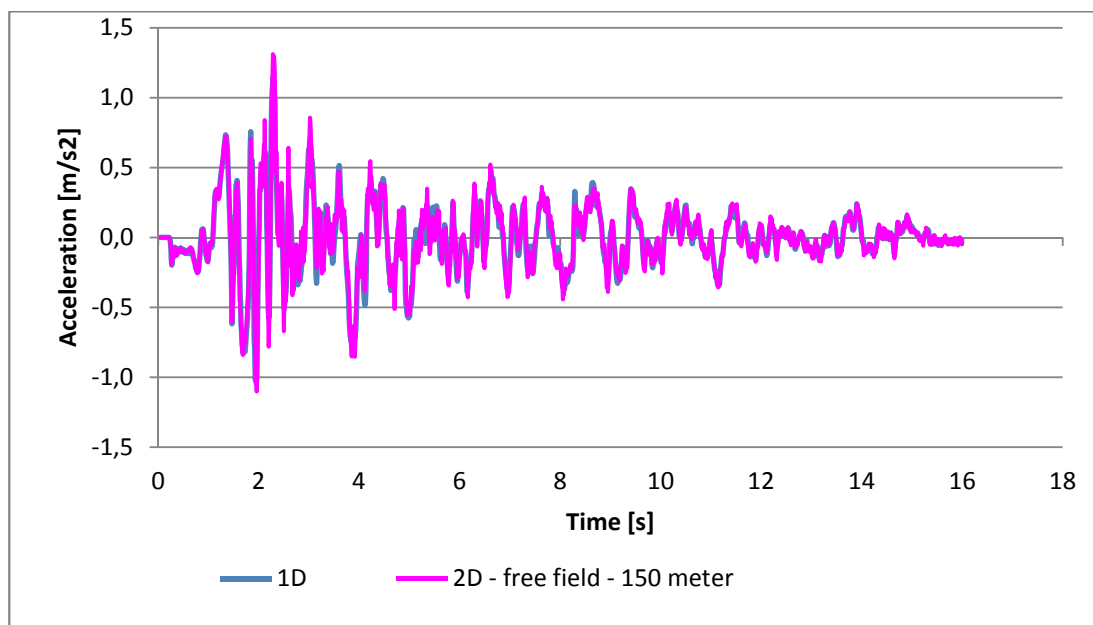


Figure 45 SSE horizontal acceleration (ax): 1D - free field boundaries 150 meter (300 meter model width)

E.3 Horizontal displacement at ground level

E.3.1 OBE horizontal displacement at ground level

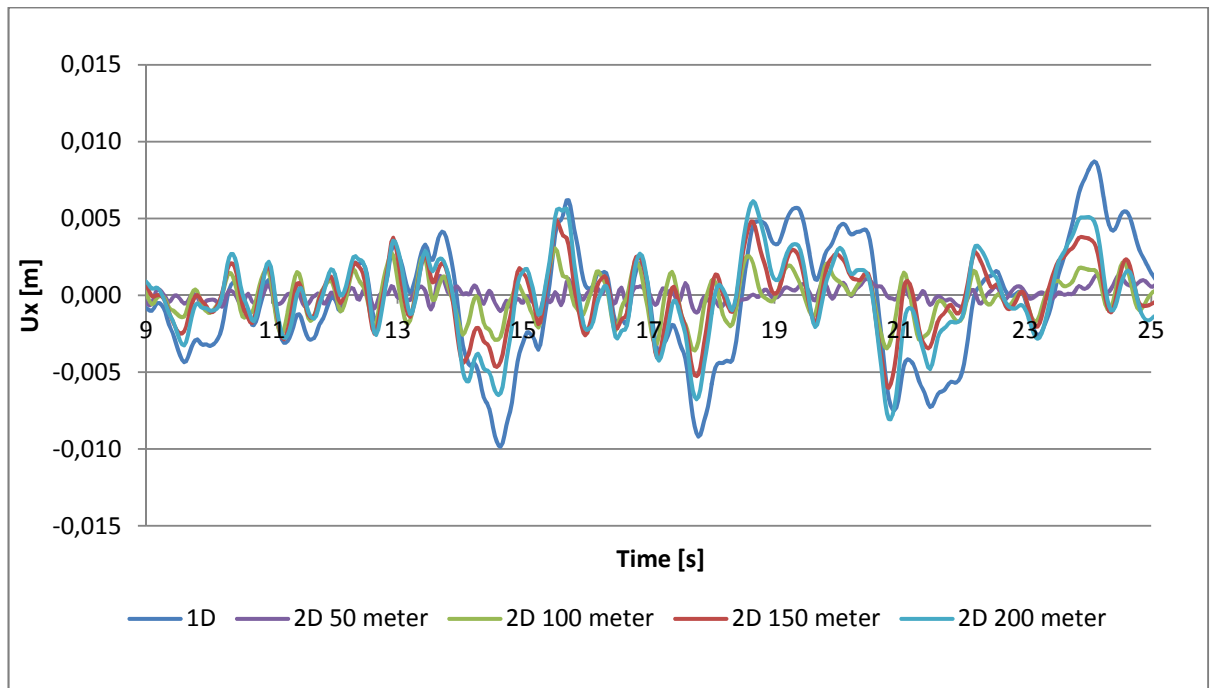


Figure 46 OBE horizontal displacement (u_x) at ground level for models with viscous boundaries

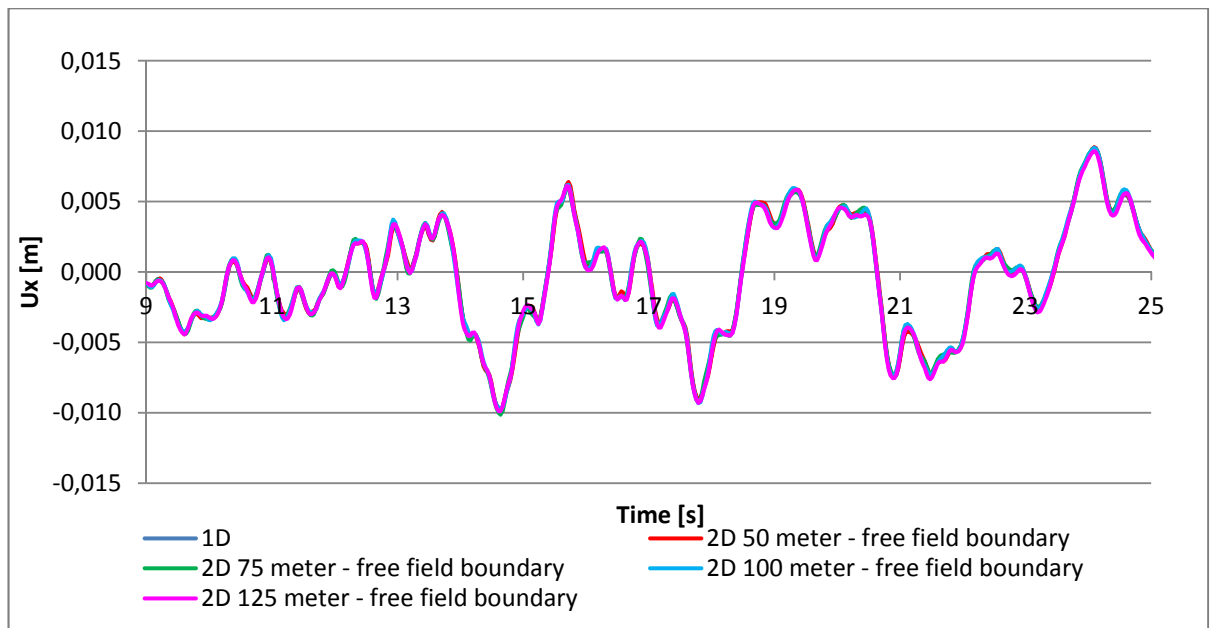


Figure 47 OBE horizontal displacement (u_x) at ground level for models with free field boundaries

E.3.2

SSE horizontal displacement at ground level

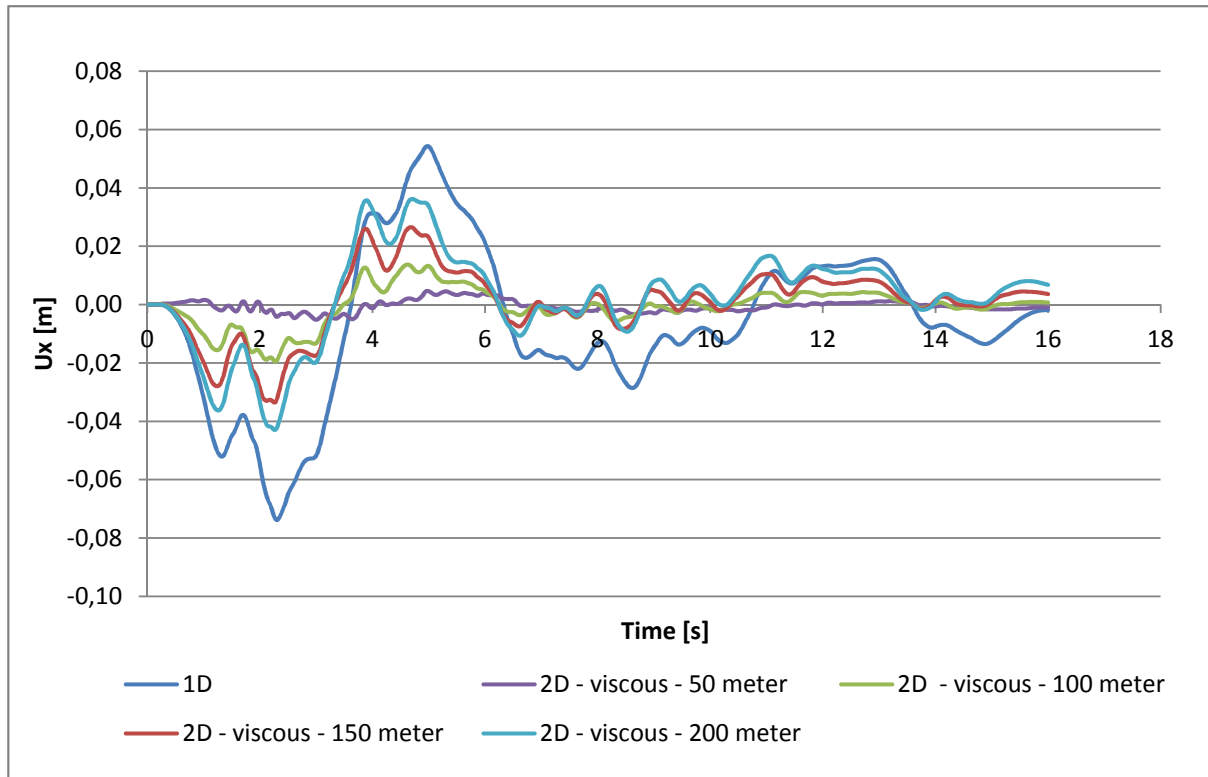


Figure 48 SSE horizontal displacement (u_x) at ground level for models with viscous boundaries

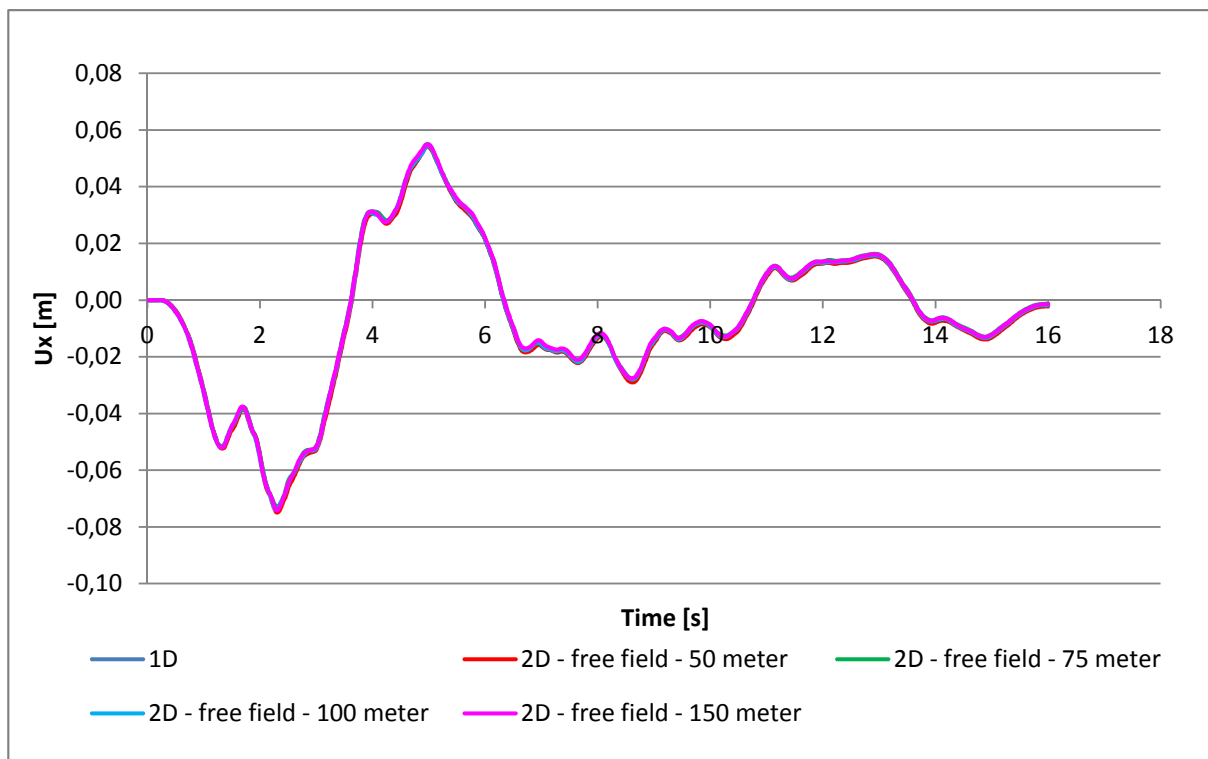


Figure 49 SSE horizontal displacement (u_x) at ground level for models with free field boundaries

E.4 Vertical acceleration at ground level

E.4.1 OBE vertical acceleration at ground level

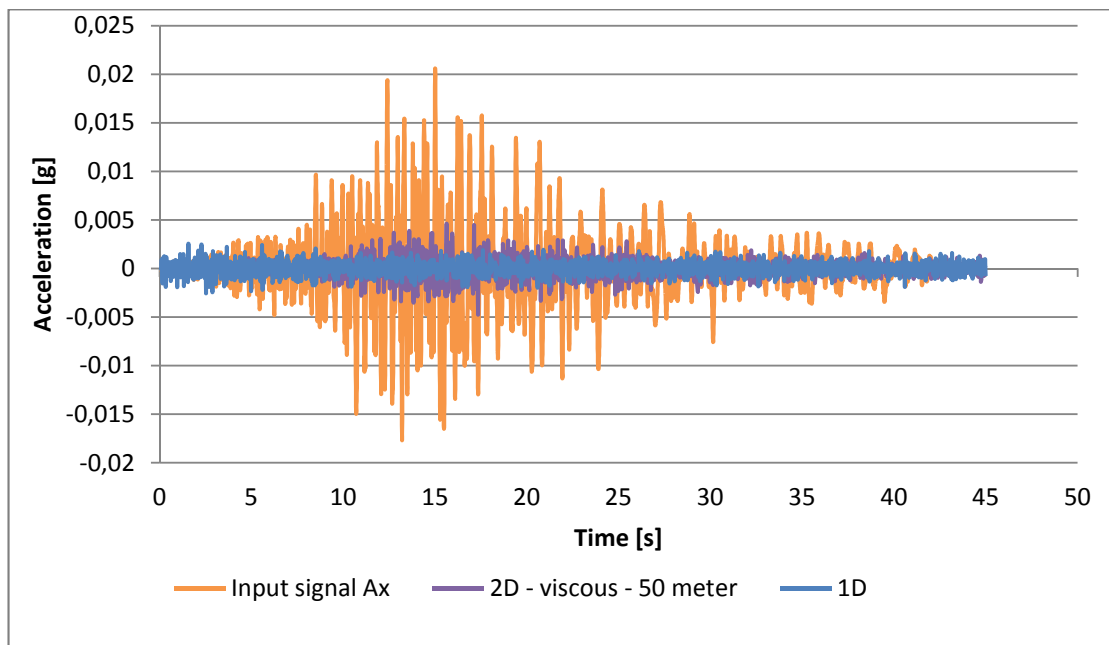


Figure 50 OBE vertical acceleration: 1D - 2D viscous boundaries 50 - input Ax

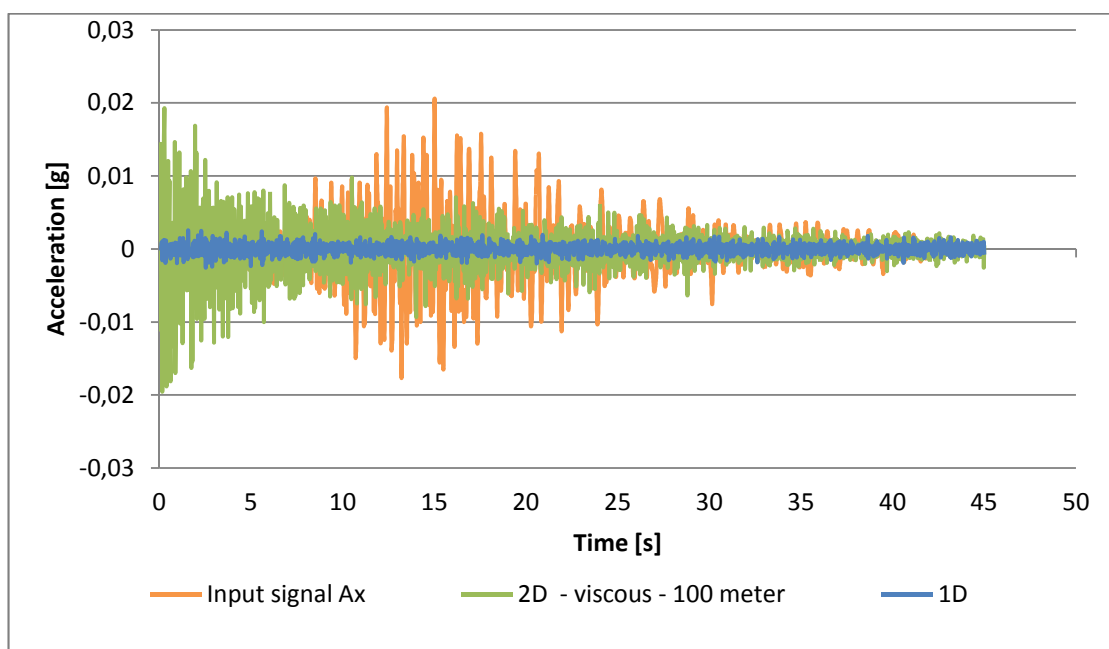


Figure 51 OBE vertical acceleration: 1D - 2D viscous boundaries 100 - input Ax

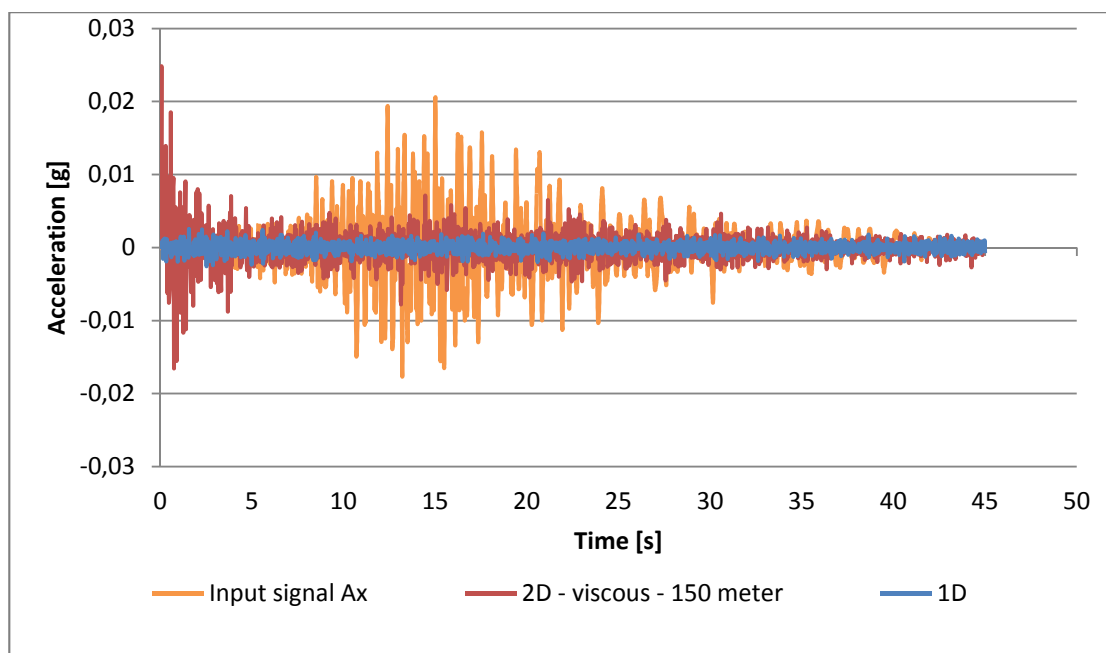


Figure 52 OBE vertical acceleration: 1D - 2D viscous boundaries 150 - input Ax

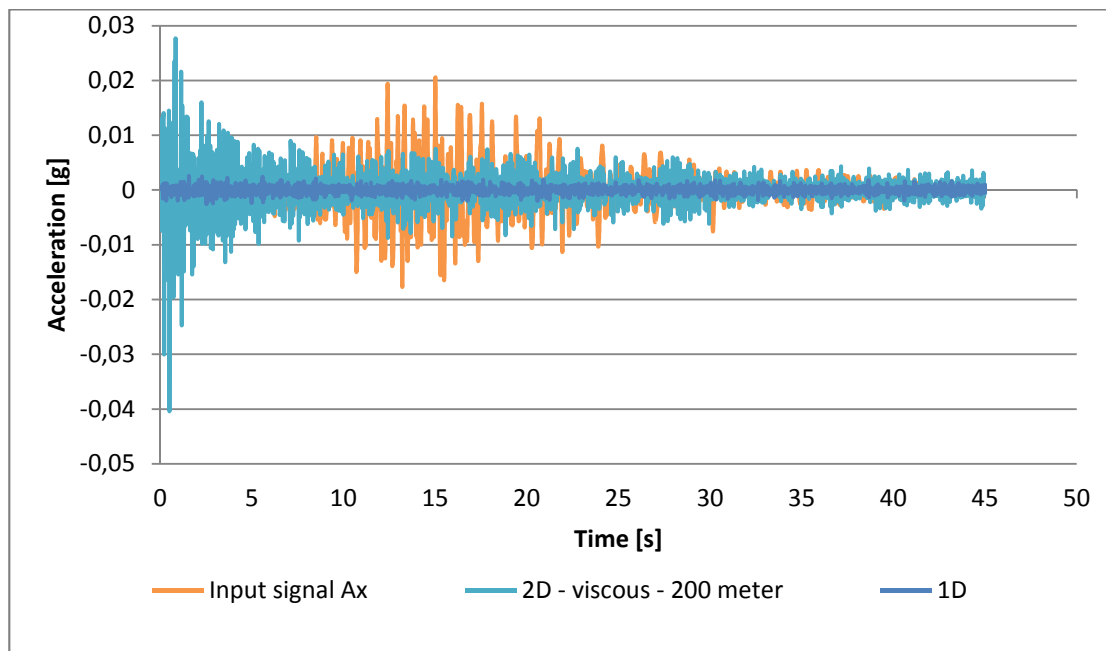


Figure 53 OBE vertical acceleration: 1D - 2D viscous boundaries 200 - input Ax

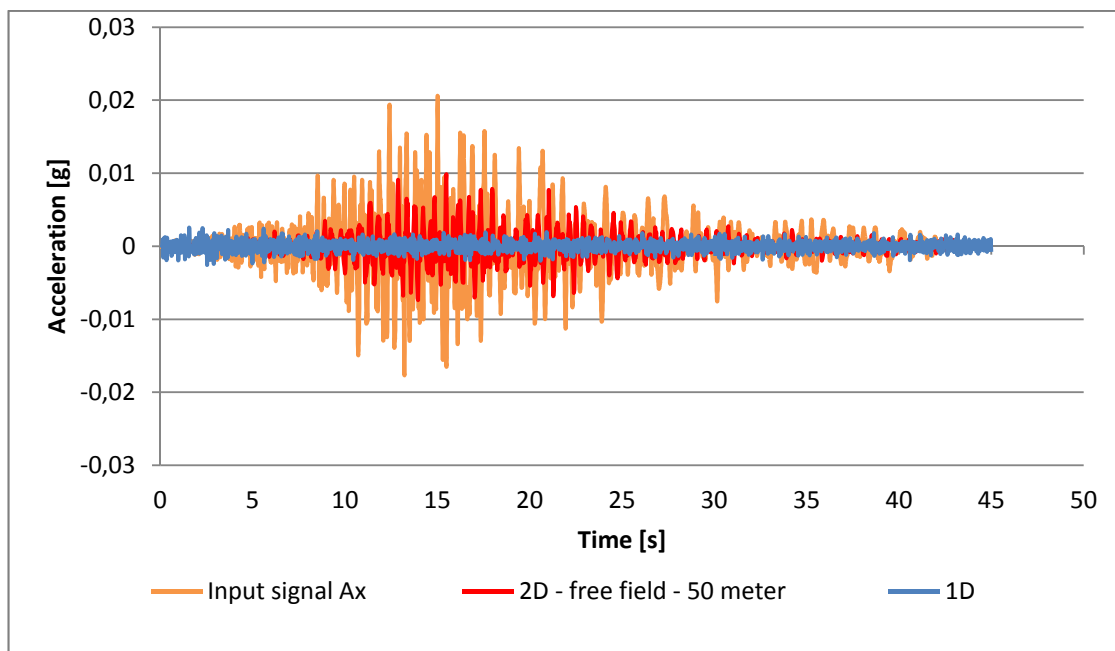


Figure 54 OBE vertical acceleration: 1D - 2D free field boundaries 50 - input Ax

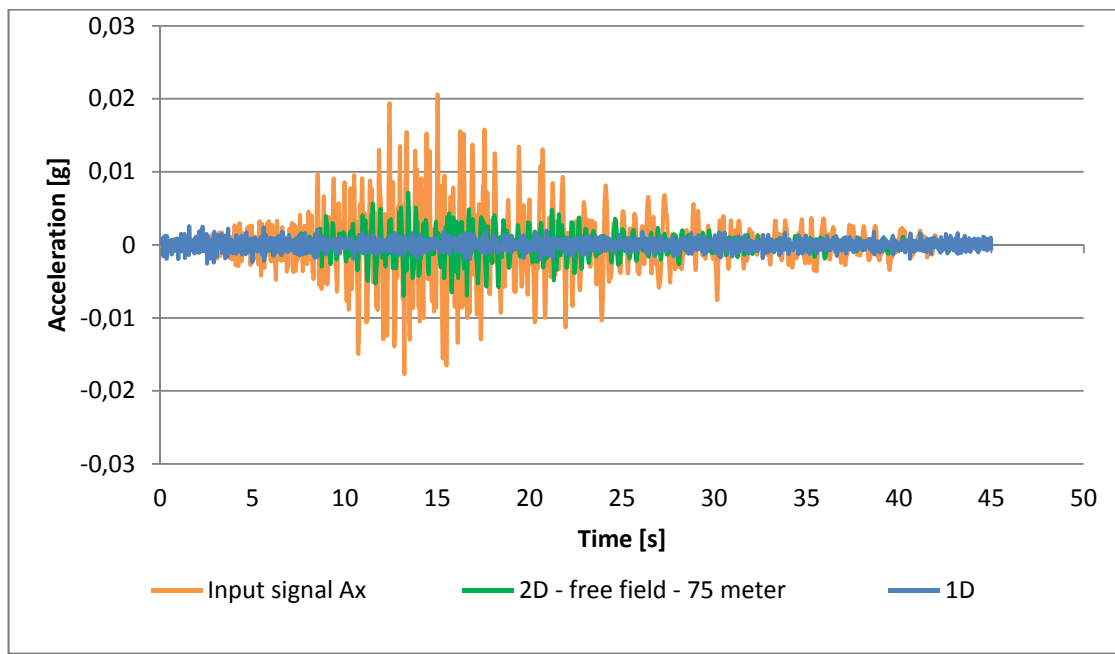


Figure 55 OBE vertical acceleration: 1D - 2D free field boundaries 75 - input Ax

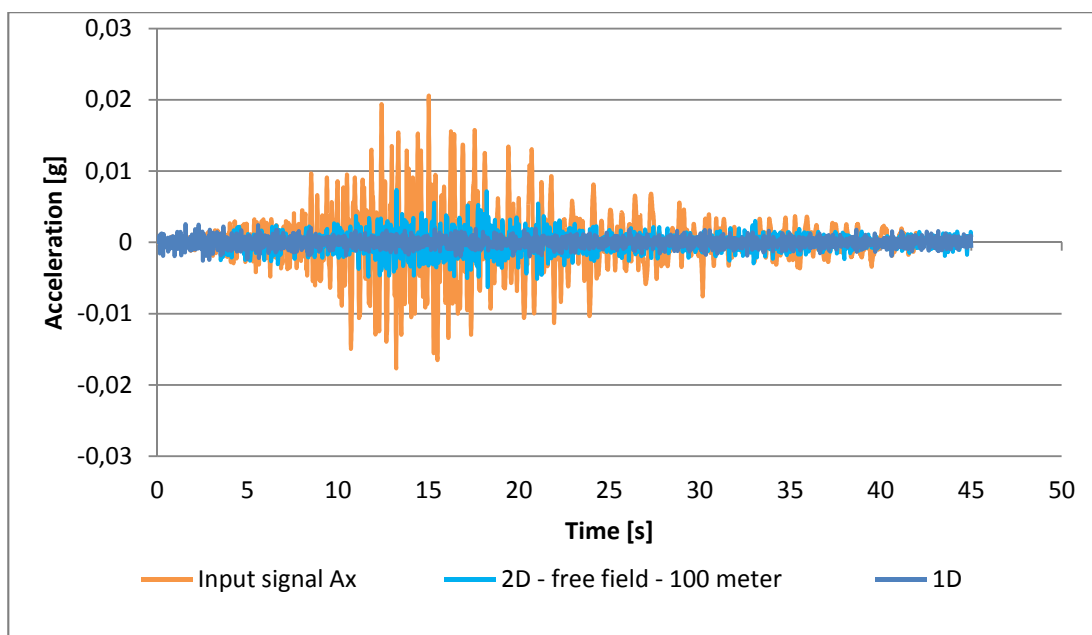


Figure 56 OBE vertical acceleration: 1D - 2D free field boundaries 100 - input Ax

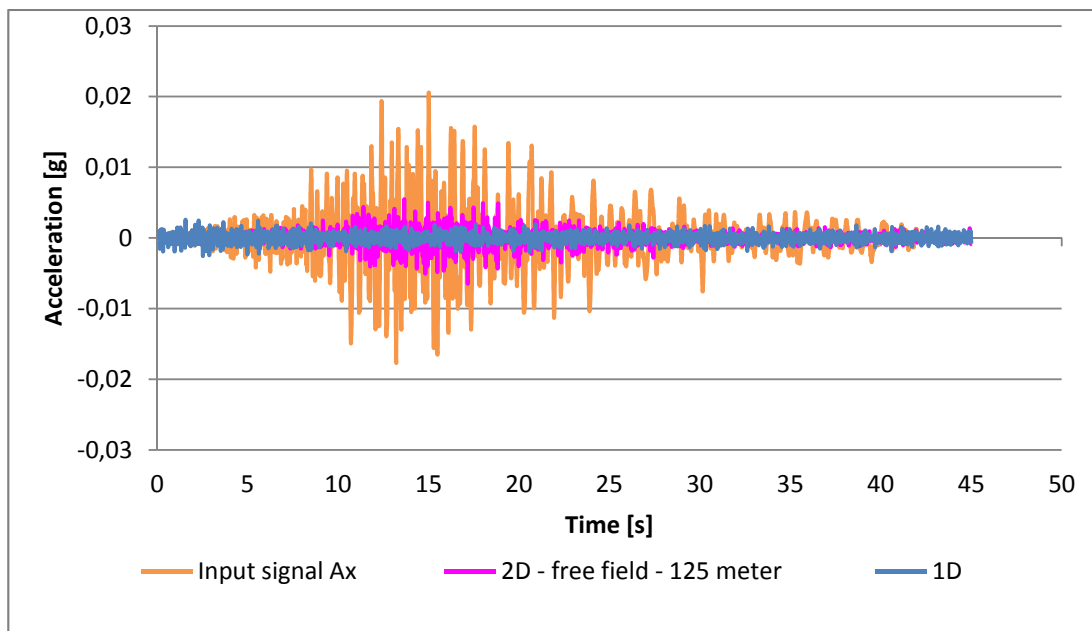


Figure 57 OBE vertical acceleration: 1D - 2D free field boundaries 125 - input Ax

E.4.2 SSE vertical acceleration at ground level

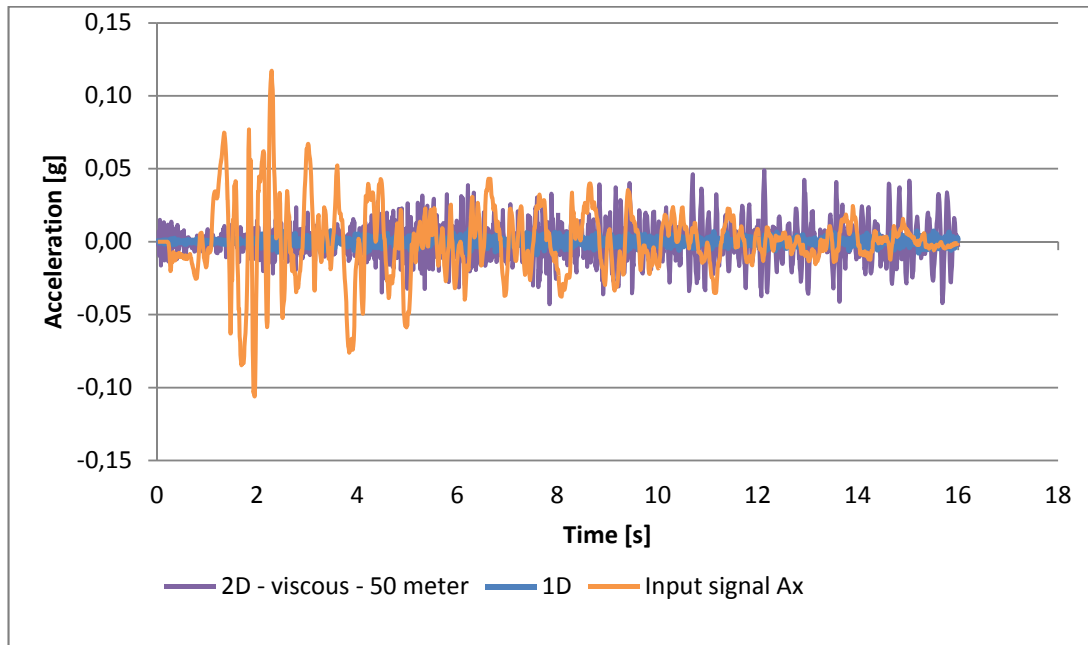


Figure 58 SSE vertical acceleration: 1D - 2D viscous boundaries 50 - input Ax

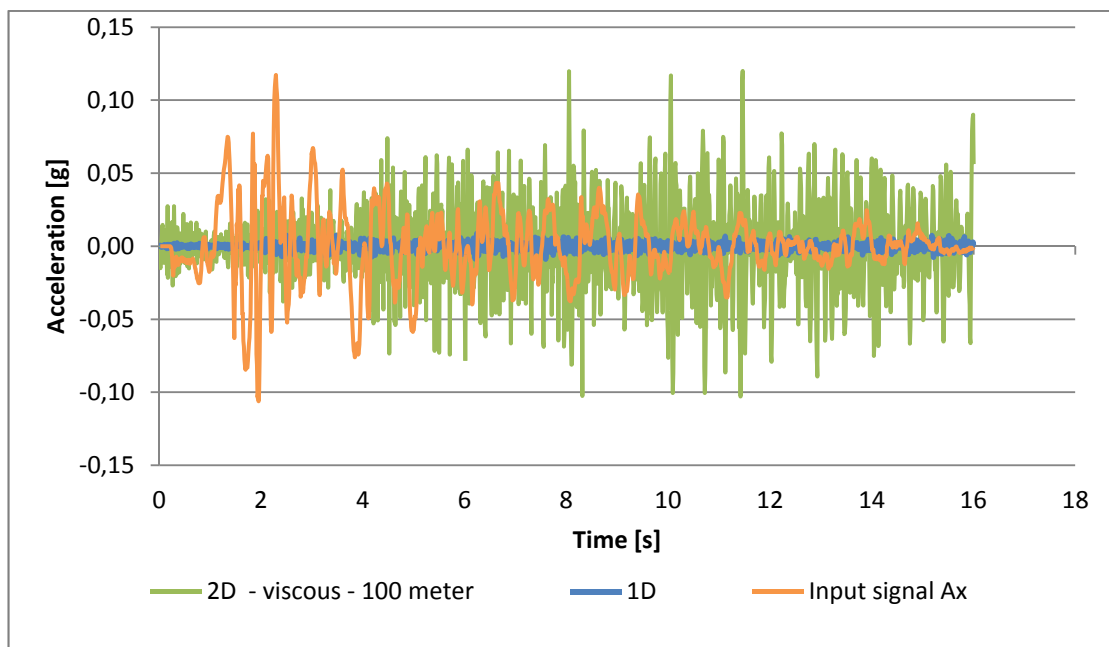


Figure 59 SSE vertical acceleration: 1D - 2D viscous boundaries 100 - input Ax

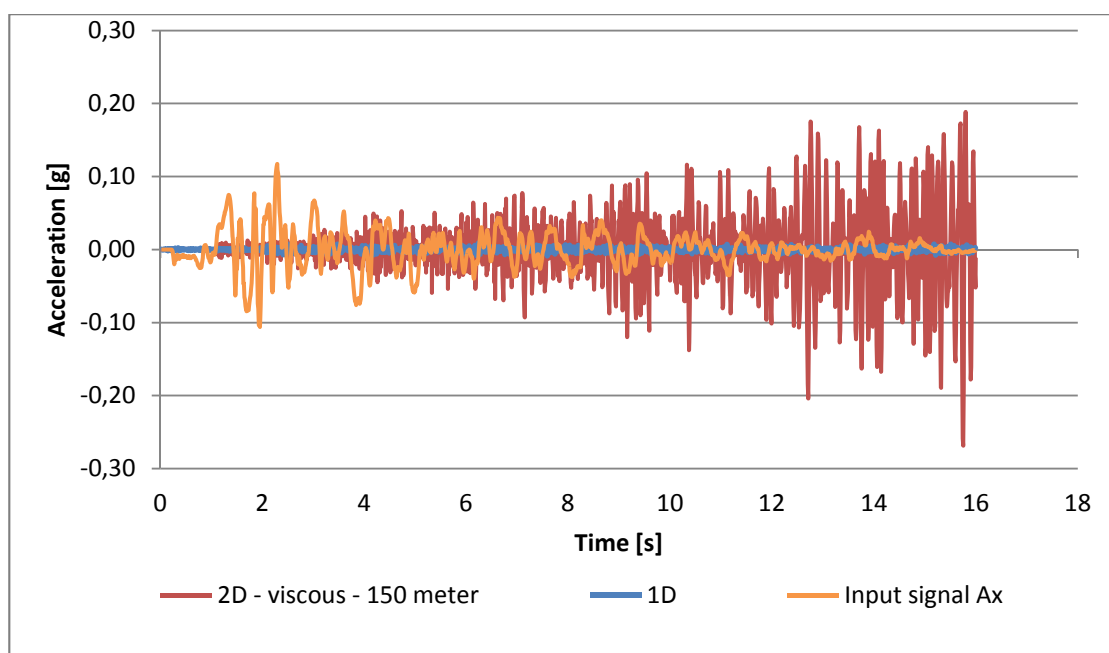


Figure 60 SSE vertical acceleration: 1D - 2D viscous boundaries 150 - input Ax

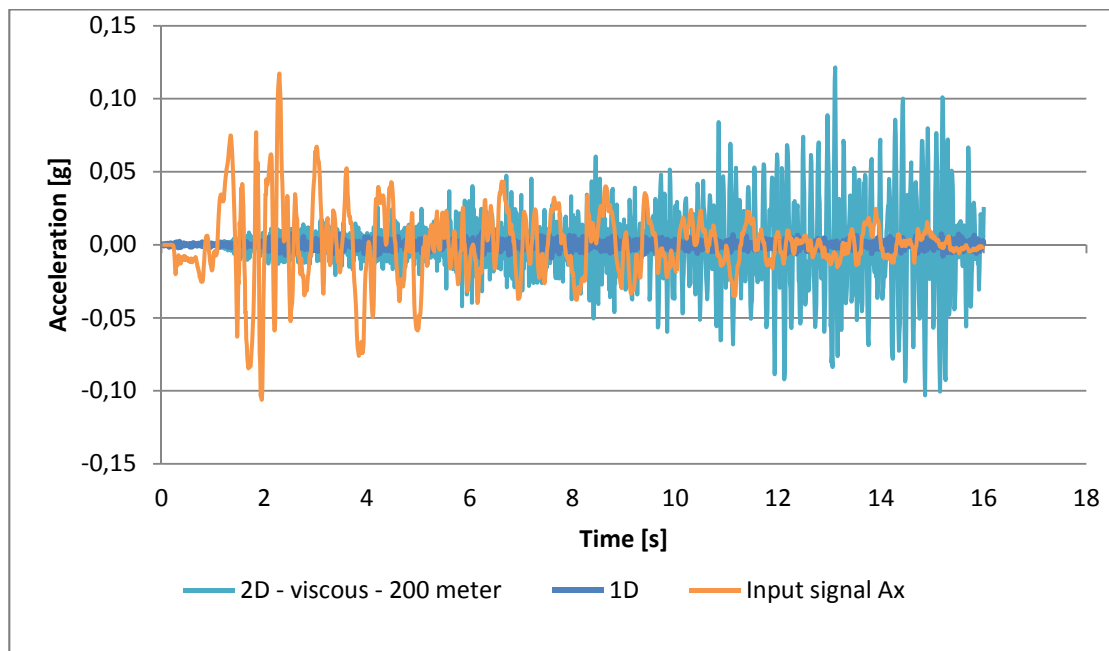


Figure 61 SSE vertical acceleration: 1D - 2D viscous boundaries 200 - input Ax

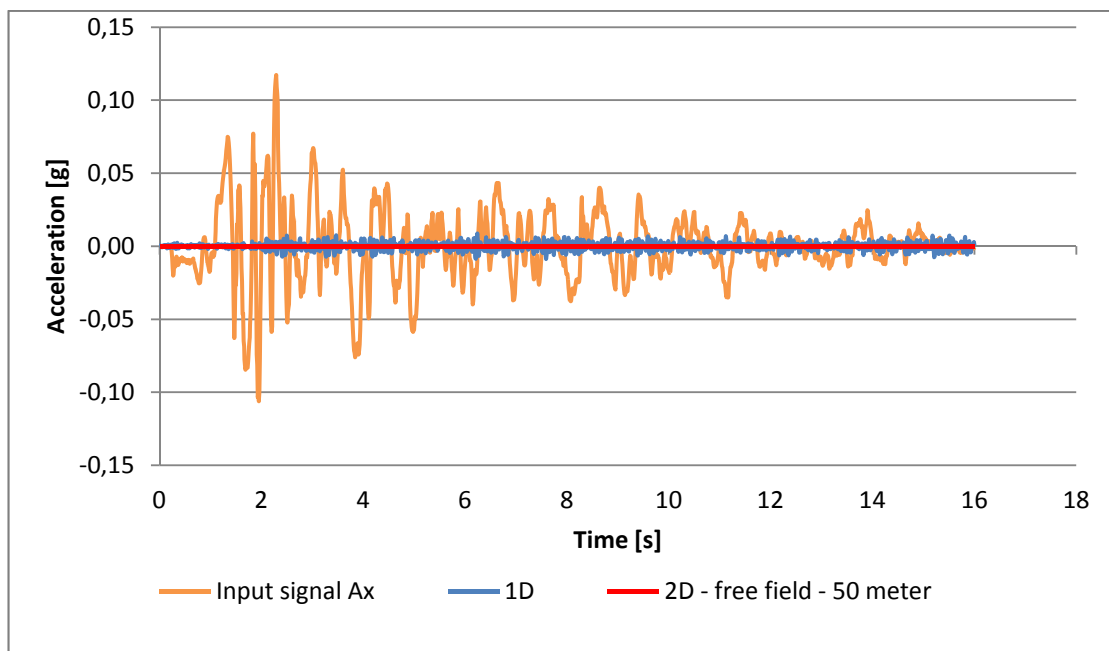


Figure 62 SSE vertical acceleration: 1D - 2D free field boundaries 50 - input Ax

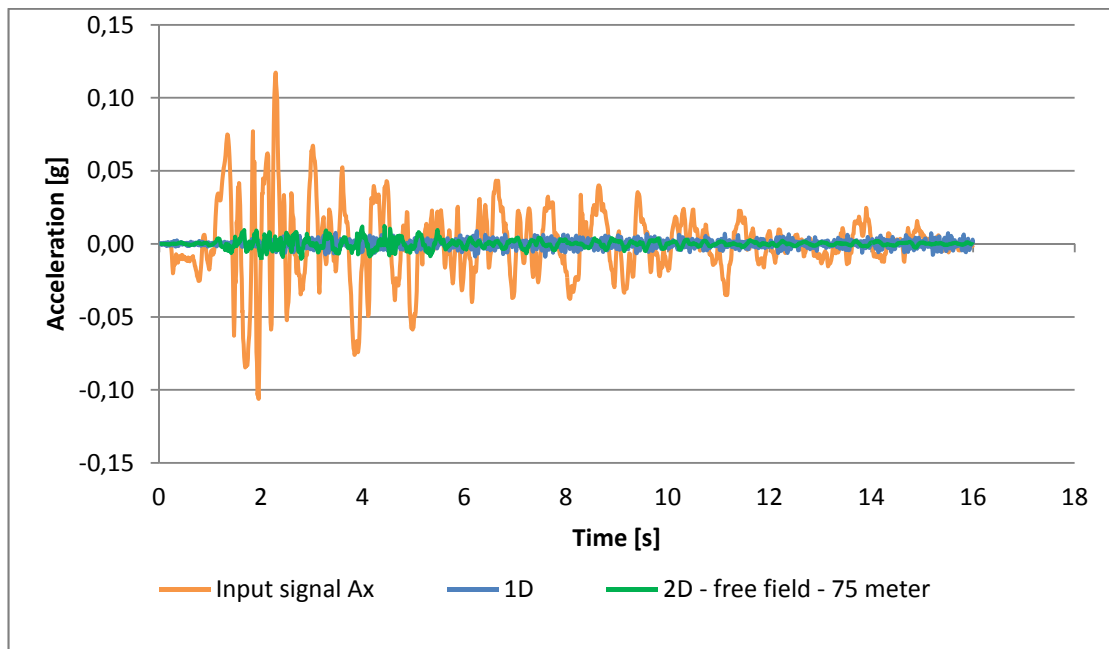


Figure 63 SSE vertical acceleration: 1D - 2D free field boundaries 75 - input Ax

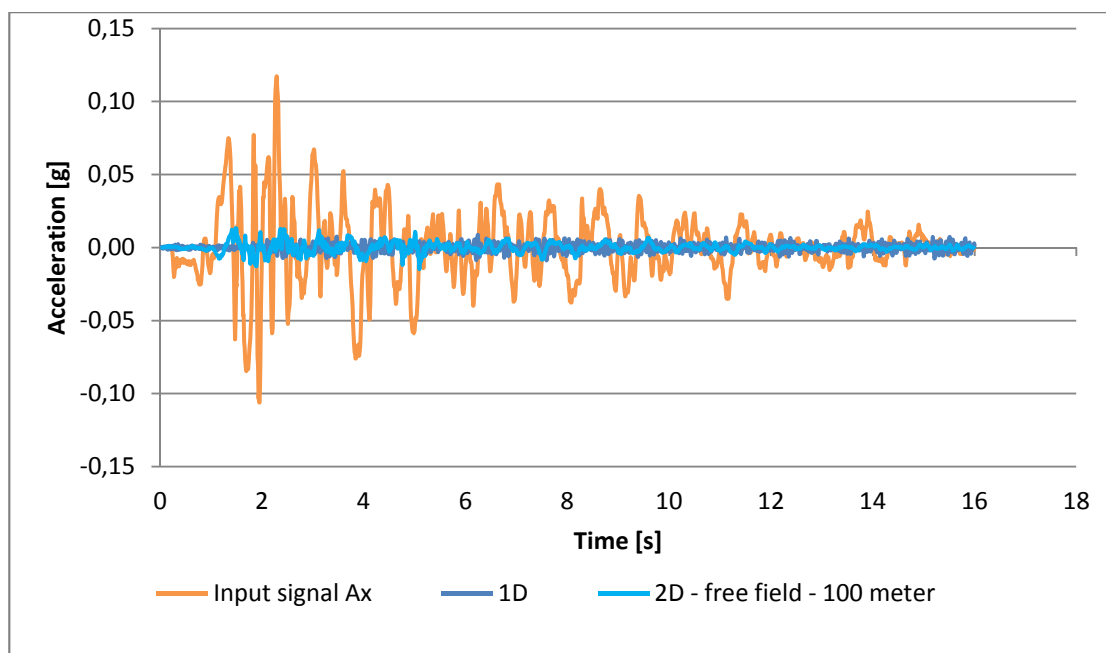


Figure 64 SSE vertical acceleration: 1D - 2D free field boundaries 100 - input Ax

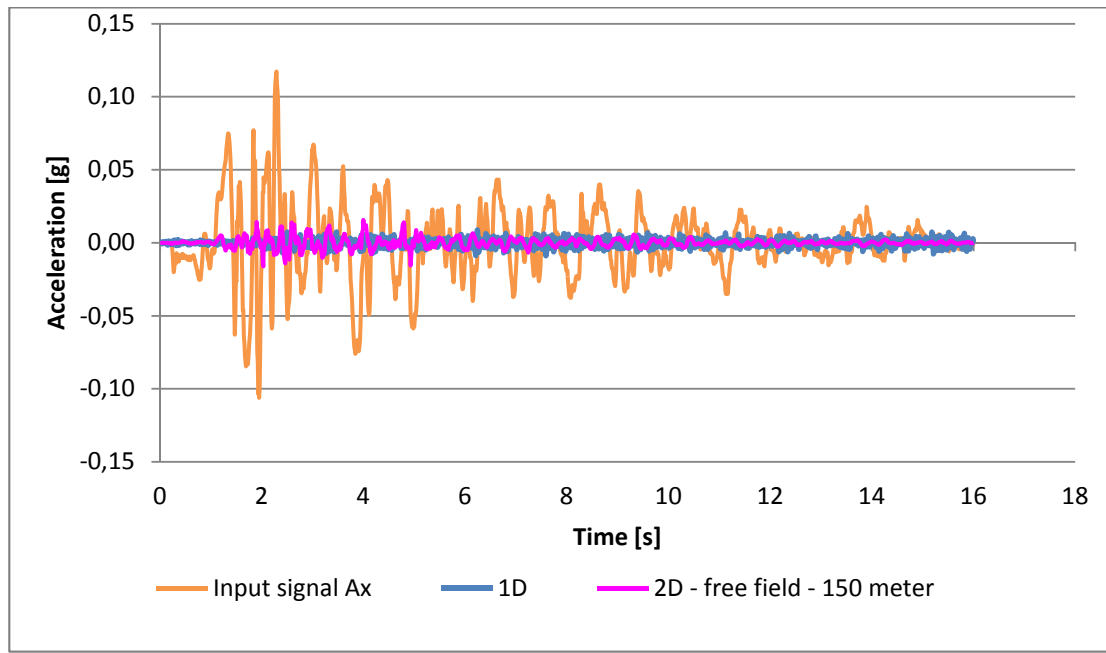
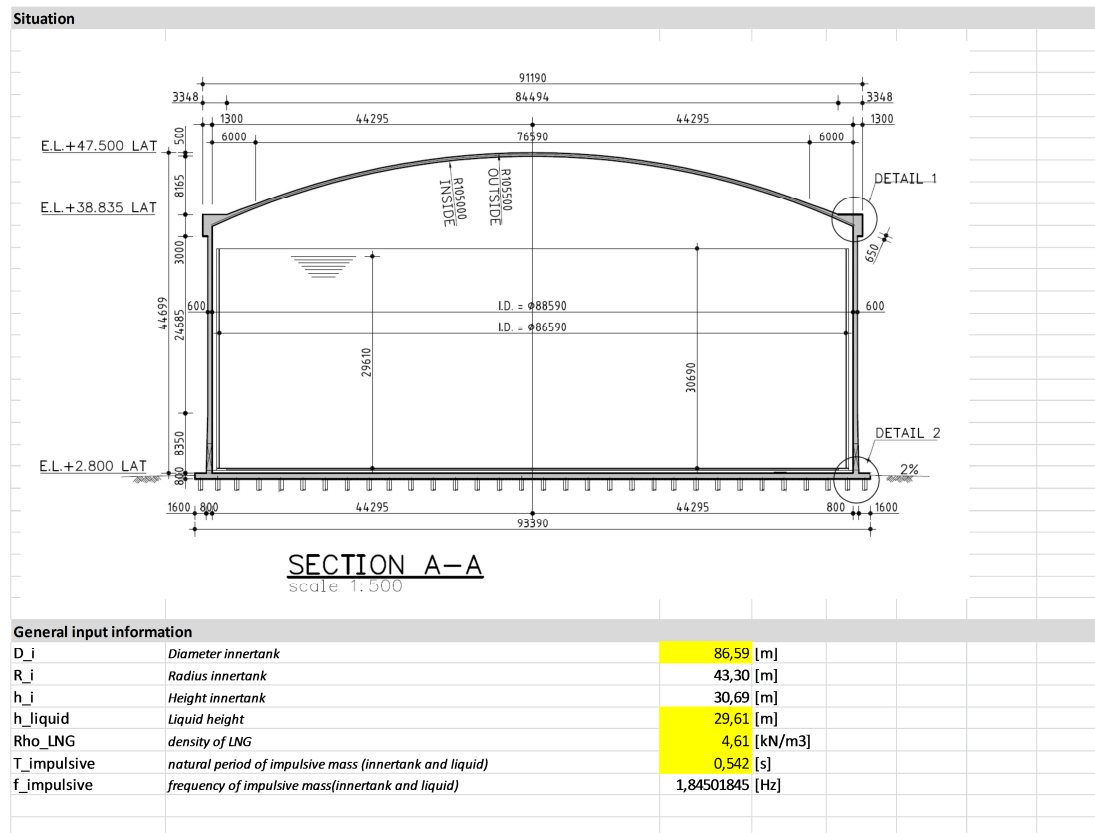


Figure 65 SSE vertical acceleration: 1D - 2D free field boundaries 125 - input Ax

Appendix F

F. CALCULATION INPUT PARAMETERS FOR IMPULSIVE LIQUID MASS



3D situation

V_LNG	Volume of LNG in innertank	174367 [m³]			
W_LNG	Weight LNG in innertank	804363 [kN]			
W_innertank	Weight of innertank (shell, insulation and stiffeners)	10590,00222 [kN]			
M_LNG	Mass LNG in innertank	81952390,46 [kg]			
M_innertank	Mass of innertank (shell, insulation and stiffeners)	1078961 [kg]			

Impulsive mass calculation according to API 620 - Appendix L and NEN-EN 1998-4 Annex A

D	Diameter innertank (=D_i)	86,59 [m]
R	Radius innertank (=R_i)	43,30 [m]
H	Liquid height(=h_liquid)	29,61 [m]
R/H	Ratio radius-liquid height	1,46 [-]
D/H	Ratio diameter-liquid height	2,92 [-]
W_T	Total weight of tank content (=W_LNG)	804363 [kN]
W_S	Total weight of tank shell (=W_innertank)	10590,00222 [kN]

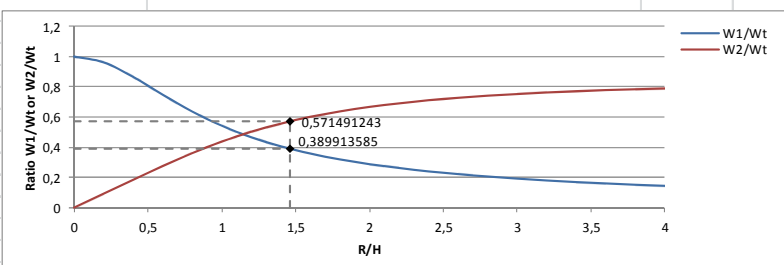


Figure L-2 of API 620 - Appendix L

W_1/W_T	Ratio weight impulsive liquid-total liquid	0,3899 [-]	determined according to figure L-2
W_1	Weight of impulsive liquid (liquid that moves in unison with tank)	313632 [kN]	
W_1_innertank	Weight of impulsive liquid (including innertank)	324222 [kN]	
W_2/W_T	Ratio weight convective liquid-total liquid	0,5715 [-]	determined according to figure L-2
W_2	Weight of convective liquid part (sloshing liquid)	459686 [kN]	

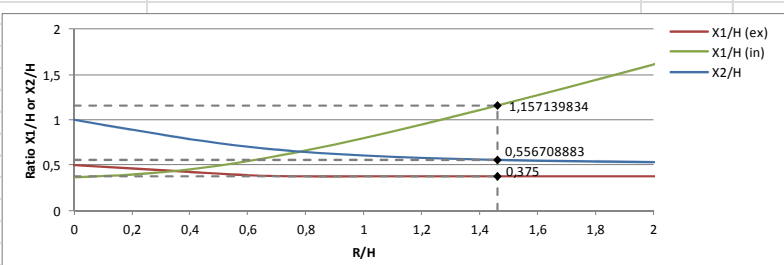


Figure L-3 of API 620 - Appendix L

X_1/H (excluding)	Ratio height impulsive liquid-total liquid (excluding bottom pressure)	0,375 [-]	determined according to figure L-3
X_1 excl. bot. pr.	Height of impulsive liquid (excluding bottom pressure)	11,10 [m]	
X_1/H (including)	Ratio height impulsive liquid-total liquid (including bottom pressure)	1,157 [-]	determined according to figure L-3
X_1 incl. bot. pr.	Height of impulsive liquid (including bottom pressure)	34,26 [m]	
X_2/H	Ratio height convective liquid-total liquid	0,557 [-]	determined according to figure L-3
X_2 excl. bot. pr.	Height of convective liquid (including bottom pressure)	16,48 [m]	

W_impulsive	Weight of impulsive liquid	313632 [kN]
M_impulsive	Mass of impulsive liquid	31954350,38 [kg]
H_impulsive	Modelling height center of gravity of impulsive liquid mass	34,26 [m]

2D situation			
V_LNG_2D	Volume of LNG in 2D cross-section	2564 [m³]	
W_LNG_2D	Weight LNG in 2D cross-section	11828 [kN]	
M_LNG_2D	Mass LNG in 2D cross-section	1205047,053 [kg]	
W_impulsive_2D	Weight of impulsive liquid in 2D cross-section	4612 [kN]	determined with factor W1/WT from figure L-2
M_impulsive_2D	Mass of impulsive liquid in 2D cross-section	469864 [kg]	determined with factor W1/WT from figure L-2
H_impulsive_2D	Modelling height center of gravity of impulsive liquid mass in 2D cross-section	34,26 [m]	determined with factor X1/H from figure L-3
A_innertank	Area of innertank	14237 [m²]	
A_innertank_2D	Area of innertank in 2D cross-section	148 [m²]	
M_innertank	Mass of innertank (shell, insulation and stiffeners)	1078961 [kg]	
M_innertank_2D	Mass of innertank (shell, insulation and stiffeners) in 2D cross-section	11214 [kg]	
W_innertank_2D	Weight of innertank (shell, insulation and stiffeners) in 2D cross-section	110 [kN]	
H_innertank_2D	Modelling height center of gravity of innertank in 2D cross-section	12,86 [m]	determined by center of gravity (from PSE)
<i>Level of innertank masses relative to concrete base slab according to Figure 1 below</i>			
<i>Only the baseslab and foundation piles are modelled in PLAXIS 2D. Therefore all heights of the different masses need to be considered with respect to the base slab, taking into account the overturning moment due to bottom pressure and the depth of insulation. See figure 1 below</i>			
<i>Figure 1 Geometry of tank base-wall connection</i>			
H_impulsive_2D_eff	Effective modelling height center of gravity of impulsive liquid in 2D cross-section	35,12 [m]	
H_innertank_2D_eff	Effectmodelling height center of gravity of innertank in 2D cross-section	13,72 [m]	
<i>Combining steel innertank and impulsive liquid according to Figure 2</i>			
<i>The steel innertank and impulsive liquid are moving simultaneously and as a whole. Mass and heights can therefore be combined according to Figure 2 below</i>			
<i>Figure 2 Combining tank shell mass and impulsive liquid mass</i>			
M_impulsive_2D_eq	Equivalent impulsive mass (combination of impulsive liquid and innertank)	4655 [kN]	
W_impulsive_2D_eq	Equivalent impulsive weight (combination of impulsive liquid and innertank)	474486 [kg]	
H_impulsive_2D_eq	Equivalent height of combined impulsive mass	35,12 [m]	
<i>input parameters for beam system based on frequency of combined impulsive mass</i>			
<i>The PLAXIS input parameters for the vibrating beam are based on the theory described in chapter 7 (formula 7.4 and 7.8) and the masses and heights calculated before</i>			
m	Mass of system = W_impulsive_2D_eq	474486 [kg]	
L_beam	Length of vibrating beam = H_impulsive_2D_eq	35,12 [m]	
d_beam_2D	2D: Side of rectangle	3 [m]	r/l = 0,085414 < 0,1
length_mass_2D	Length of mass on top of beam	0,5 [m]	
f	Frequency of the system	1,845 [Hz]	
w_n	Natural frequency of system	11,59 [m⁻¹]	
m	Mass of system	474486 [kg]	
L_beam	Length of beam	35,12 [m]	
d_beam	Sides of beam	3,00 [m]	
A_beam	Area, based on a rectangular cross-section	3,00 [m²]	
I_beam	Moment of inertia, based on rectangular cross-section	2,25E+00 [m⁴]	
I_massa	Length of mass on top of beam	0,5 [m]	
E_beam	Elasticity modulus beam in formula	4,111E+11 [N/m²]	
E_beam	Elasticity modulus in PLAXIS	4,111E+08 [kN/m²]	
EA_beam	Axial stiffness beam PLAXIS 2D	1,233E+09 [kN]	
El_beam	Bending stiffness beam PLAXIS 2D	9,250E+08 [kNm²]	
rho_massa	Unit weight of mass on top of beam	9,309E+03 [kN/m³]	
E_massa	Elasticity modulus of mass in PLAXIS	4,111E+11 [kN/m²]	
EA_mass	Axial stiffness mass PLAXIS 2D	1,233E+12 [kN]	
El_mass	Bending stiffness mass PLAXIS 2D	9,250E+11 [kNm²]	

Check deflection at top of beam		
F	Force at top of the beam	750 [kN]
L	Length of beam	35,12 [m]
Ebeam	Elasticity modulus in PLAXIS	4,111E+08 [kN/m ²]
Ibeam	Moment of Inertia, based on square cross-section	2,25E+00 [m ⁴]
Abeam	Area, based on a square cross-section	3,00 [m ²]
Ux,1;hand	Bending due to force F	1,17E-02 [m]
Ux,2;hand	Bending due to shear	5,13E-05 [m]
Ux,total;hand	Total bending from hand calculation	1,18E-02 [m]
Ux,total;PLAXIS	Total bending from PLAXIS	1,18E-02 [m]
Error	difference between hand and PLAXIS	0,02%
Check frequency of system		
f _{input}	Input frequency of the system	1,85 [Hz]
f _{PLAXIS}	frequency found in PLAXIS	1,83 [Hz]
Error	difference between hand and PLAXIS	0,65%
Auxiliary structure		
Figure 3 Stiffness relation auxiliary structure		
EA _{horizontal support}	Axial stiffness of horizontal support in PLAXIS 2D	2,500E+16 [kN/m]
El _{horizontal support}	Bending stiffness of horizontal support in PLAXIS 2D	2,500E+16 [kNm ² /m]
EA _{vertical support}	Axial stiffness of vertical support in PLAXIS 2D	2,500E+11 [kN/m]
El _{vertical support}	Bending stiffness of vertical support in PLAXIS 2D	2,500E+13 [kNm ² /m]

Appendix G

G. VERIFICATION OF FLUID BEHAVIOUR (BEAM ON AUXILIARY STRUCTURE)

G.1 Considered models

In this verification of the modelling of the fluid behaviour three differed models are considered:

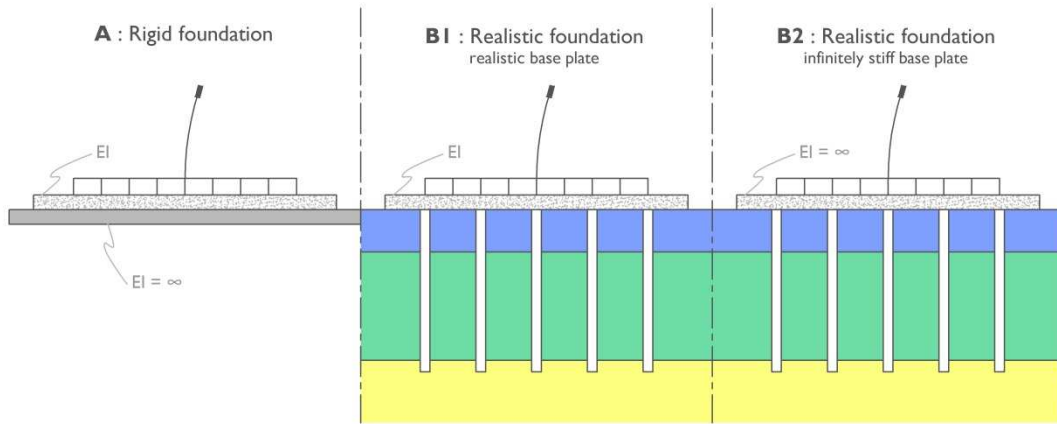


Figure 66 Different calculation models for verification of fluid behaviour

- Model A : Rigid foundation, consisting of an elastic concrete layer with high stiffness. The model is depicted in Figure 67;
- Model B1 : Realistic foundation with base plate with realistic stiffness. The model is depicted in Figure 68;
- Model B2 : Realistic foundation with infinitely stiff base plate. Model is equal to the one depicted in Figure 68.

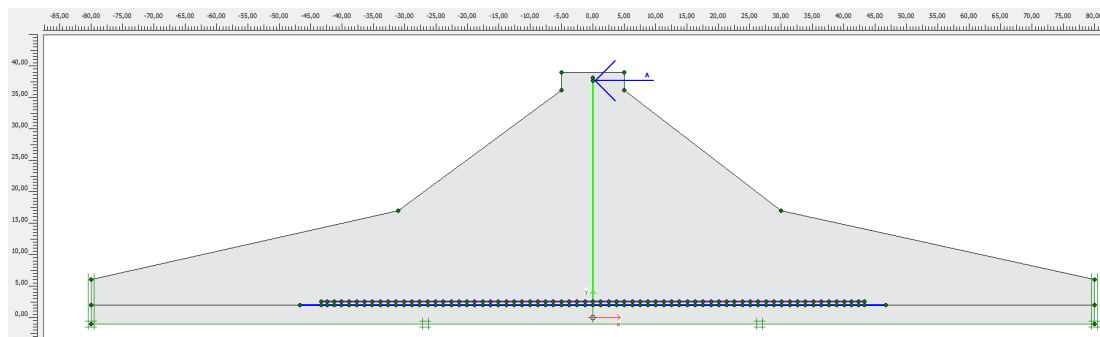


Figure 67 model with rigid foundation

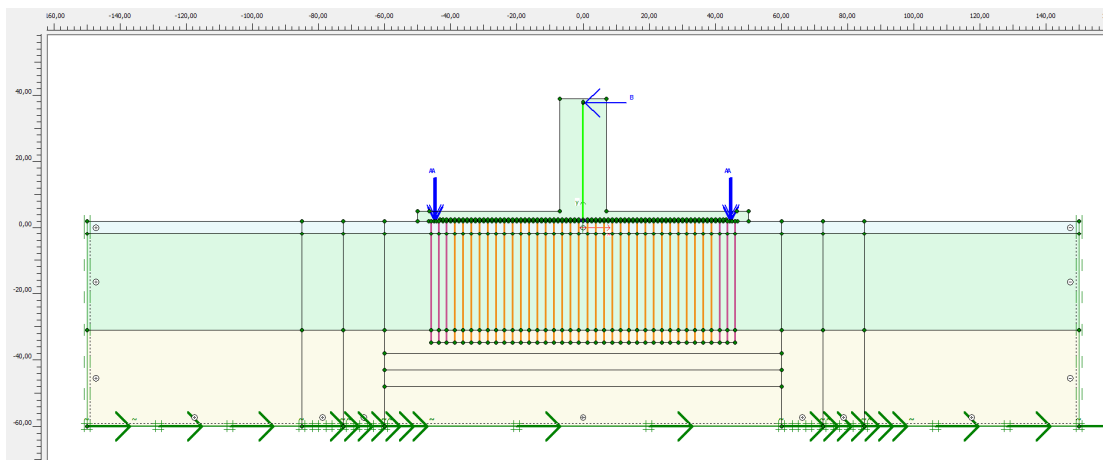


Figure 68 model with realistic foundation, base plate stiffness is varying

G.2 Static behaviour after building phase

In this situation all forces in the auxiliary structure are generated by the weight on top of the beam. No further loads are applied.

G.2.1 Axial forces in vertical supports

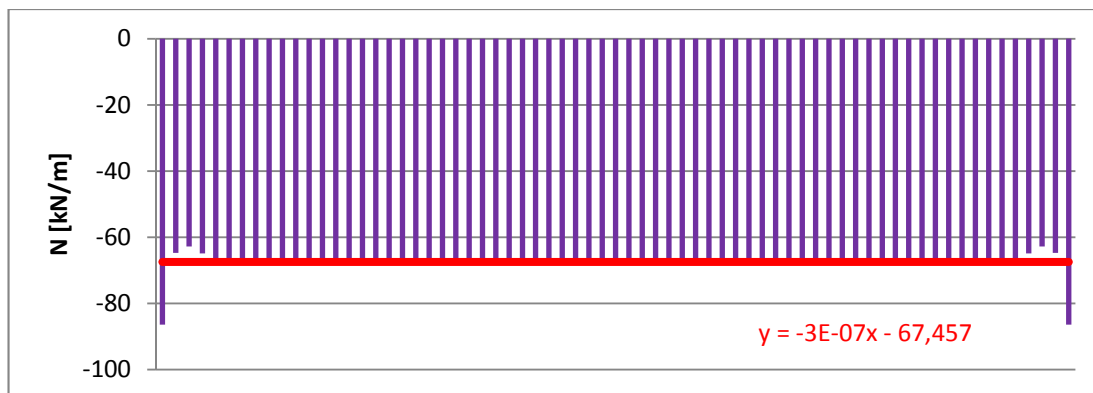


Figure 69 Axial forces in vertical supports – Model A

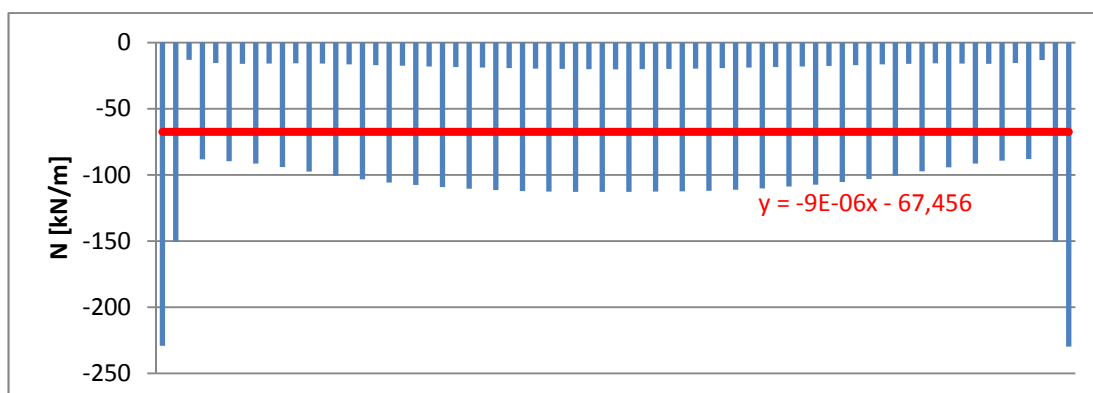


Figure 70 Axial forces in vertical supports – Model B1

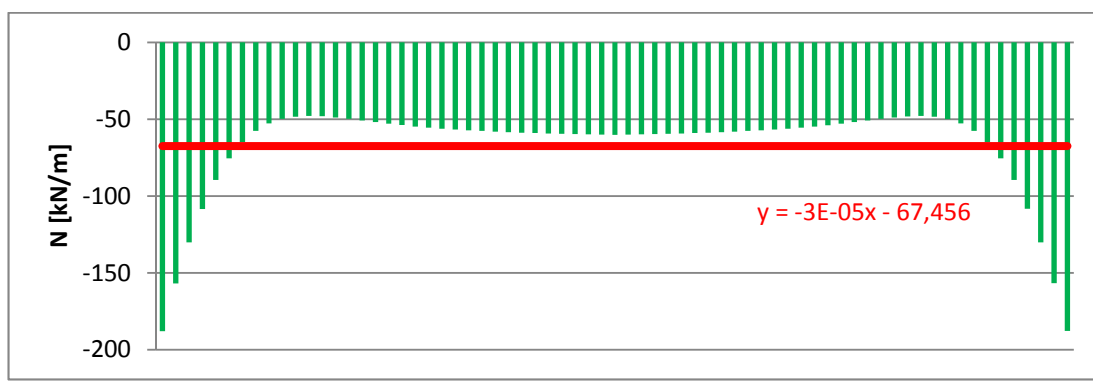


Figure 71 Axial forces in vertical supports – Model B2

G.2.2 Base plate displacements (in case of realistic foundations)

Base plate displacements are only considered for models B1 and B2 with a realistic foundation.

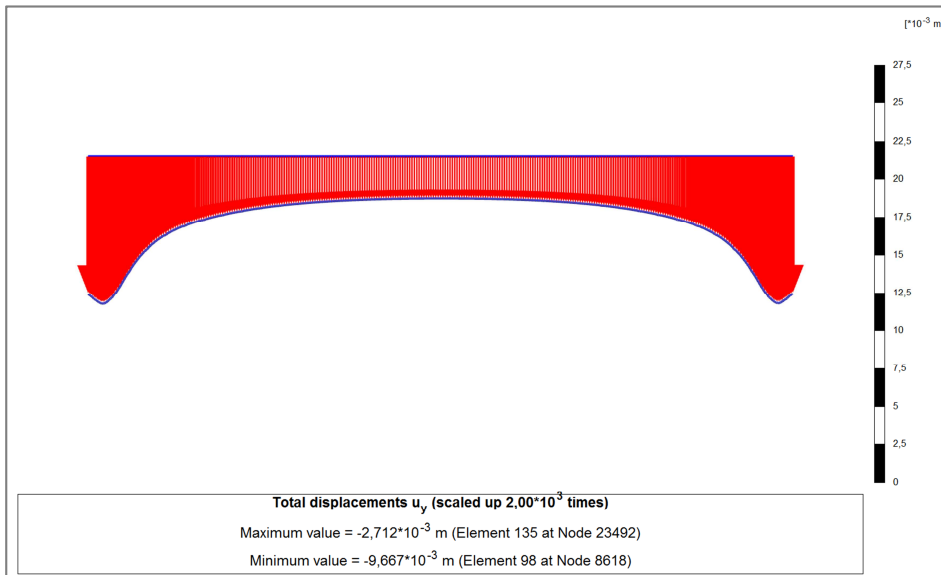


Figure 72 base plate displacements after building phase for base plate with realistic stiffness

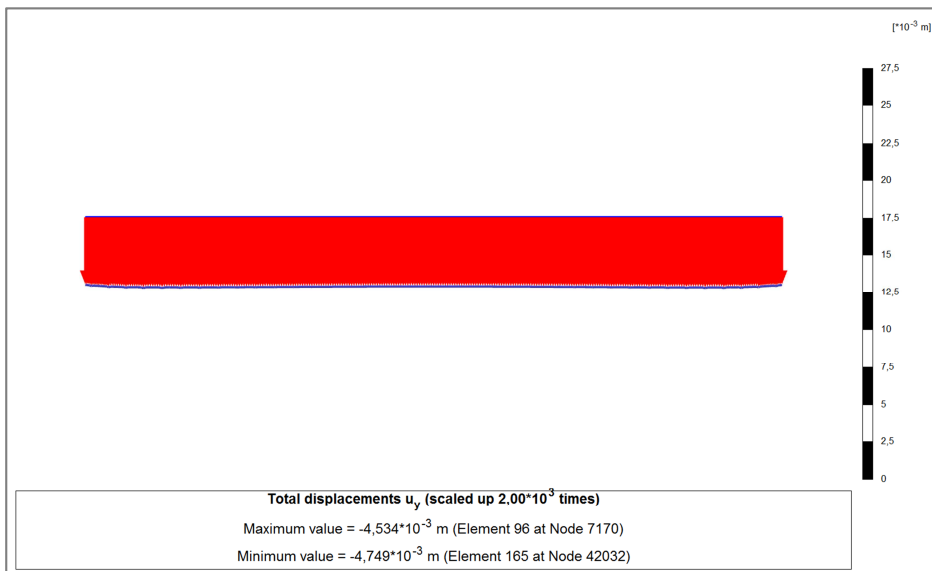


Figure 73 base plate displacements after building phase for infinitely stiff base plate

G.3 Static behaviour after loading phase

In this phase the structure is loaded by the weight on top of the beam and a horizontal force of -750 KN, applied at the top of the vibrating beam. The situation is depicted in Figure 74

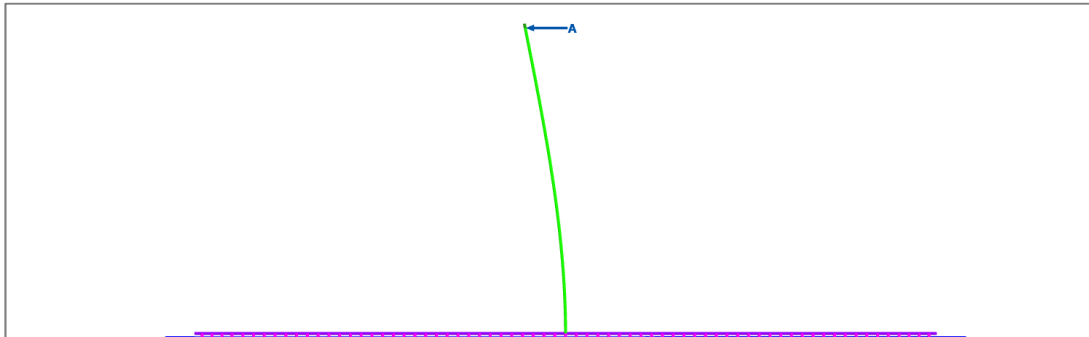


Figure 74 Situation static loading

G.3.1 Axial forces in vertical supports

In the figures below the axial forces in the vertical supports of the auxiliary structure are presented for the models A, B and B1 with respectively: a rigid foundation, a realistic foundation with realistic base plate stiffness and a realistic foundation with infinitely stiff base plate.

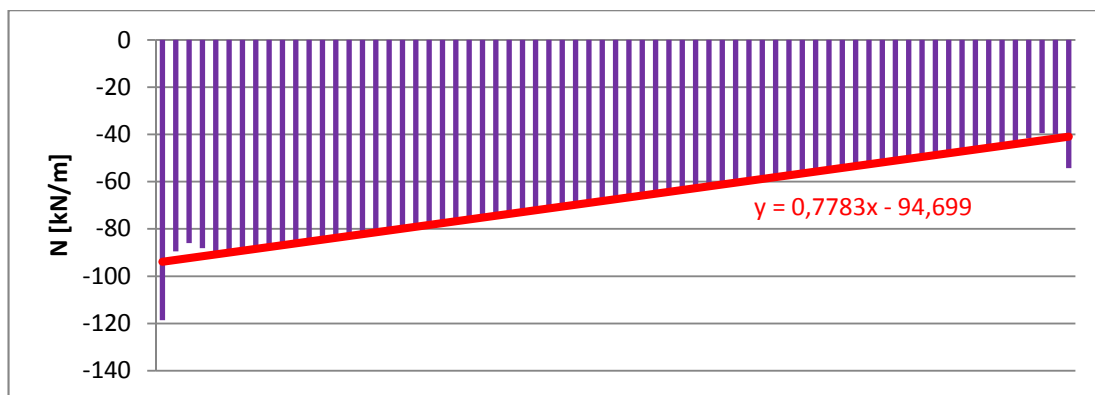


Figure 75 Axial forces [kN/m] in vertical supports - rigid foundation

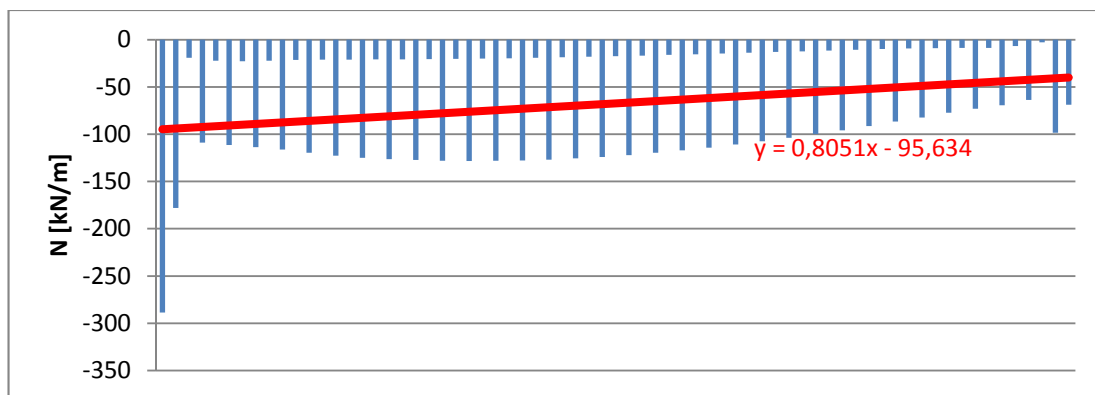


Figure 76 Axial forces [kN/m] in vertical supports - realistic foundation - realistic base plate stiffness



Figure 77 Axial forces [kN/m] in vertical supports - realistic foundation - infinitely stiff base plate

G.3.2 Shear forces in vertical supports

In the figures below the shear forces in the vertical supports of the auxiliary structure are presented for the models A, B and B1 with respectively: a rigid foundation, a realistic foundation with realistic base plate stiffness and a realistic foundation with infinitely stiff base plate.

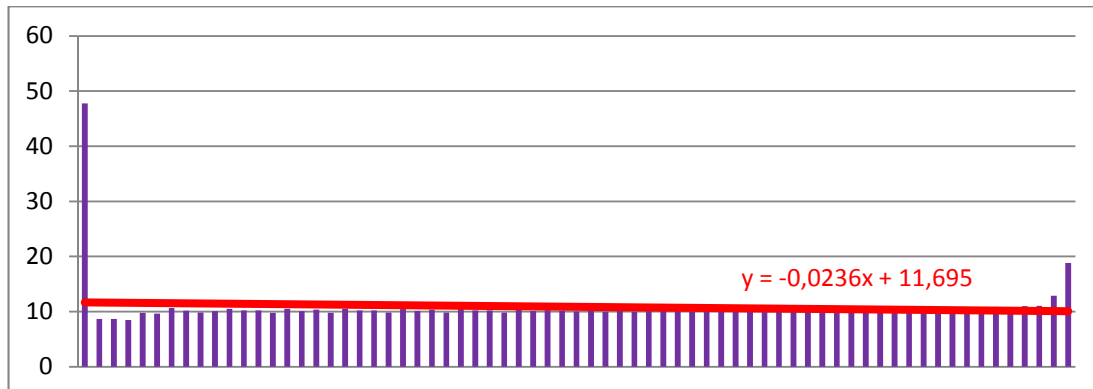


Figure 78 Shear forces [kN/m] in vertical supports - rigid foundation

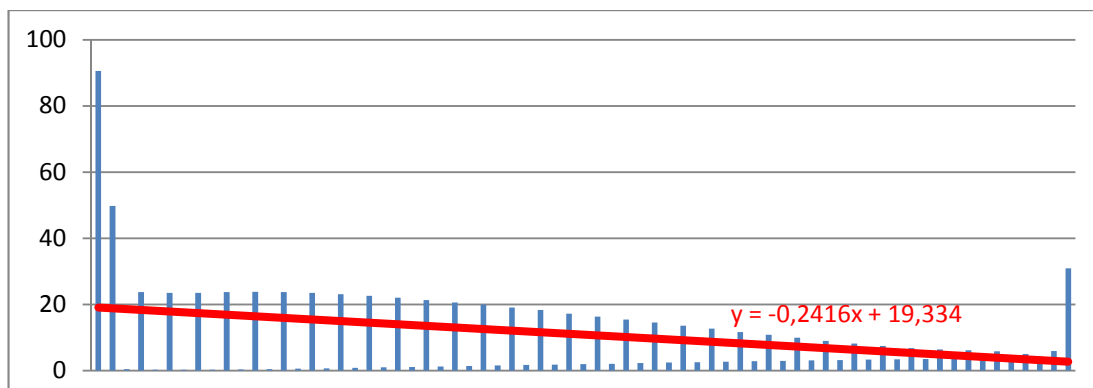


Figure 79 Shear forces [kN/m] in vertical supports - realistic foundation - realistic base plate stiffness

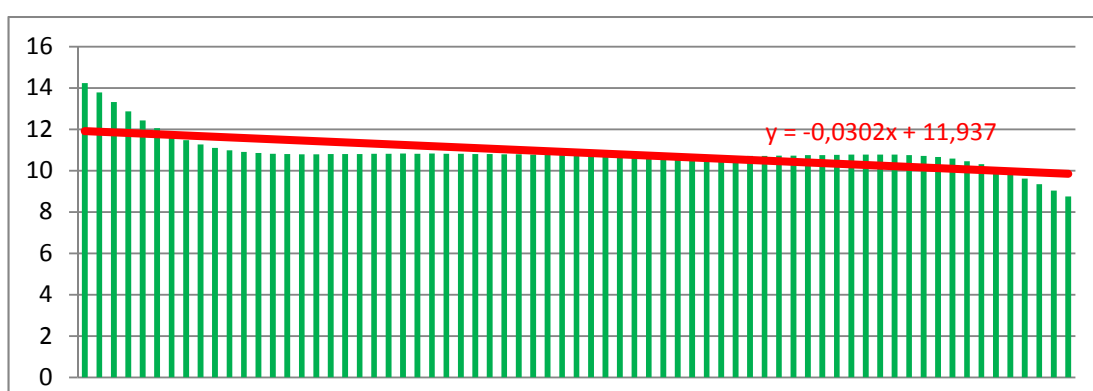


Figure 80 Shear forces in vertical supports - realistic foundation - infinitely stiff base plate

G.3.3 Base plate displacements (in case of realistic foundation)

Base plate displacements are only considered for models B1 and B2 with a realistic foundation.

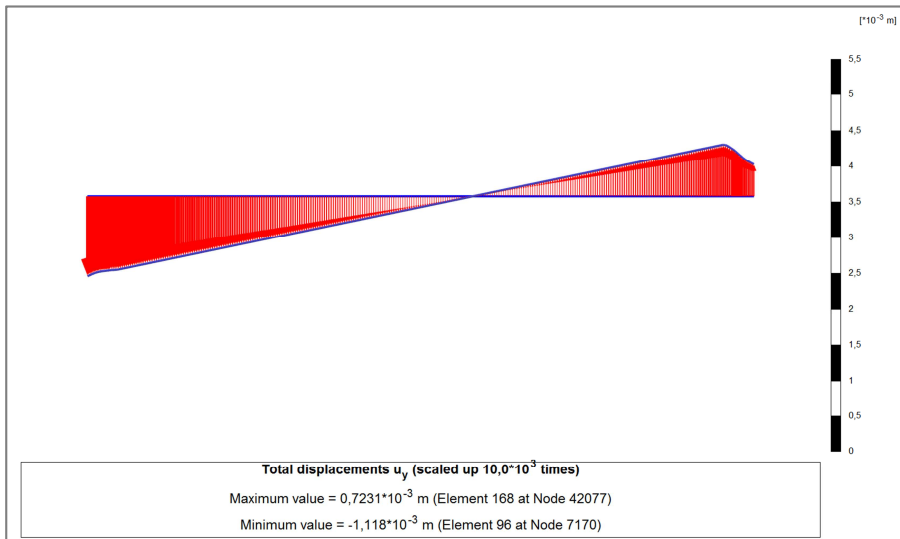


Figure 81 base plate displacements after loading phase for base plate with realistic stiffness

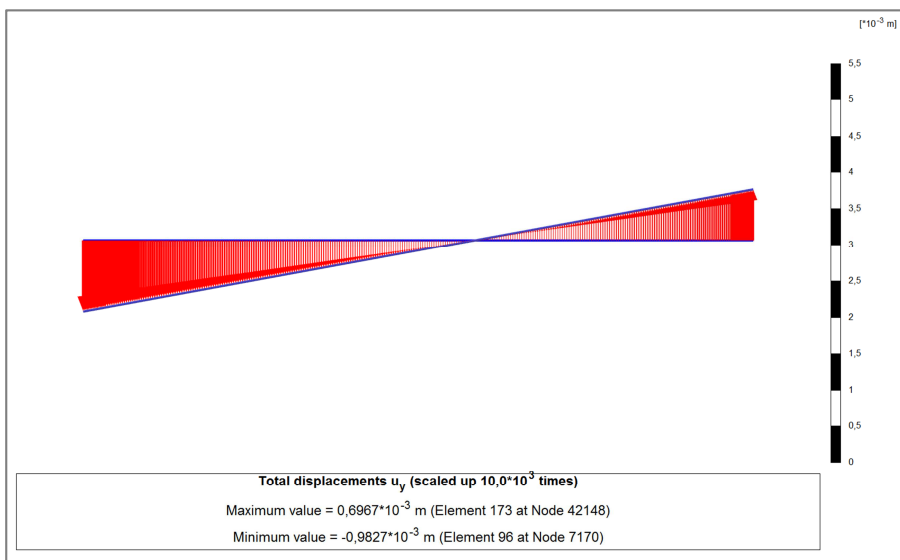


Figure 82 base plate displacements after loading phase for infinitely stiff base plate

G.3.4 Axial forces in embedded piles (in case of realistic foundation)

In the figures below the axial forces in the embedded pile rows are presented for the models A, B and B1 with respectively: a realistic foundation with realistic base plate stiffness and a realistic foundation with infinitely stiff base plate.

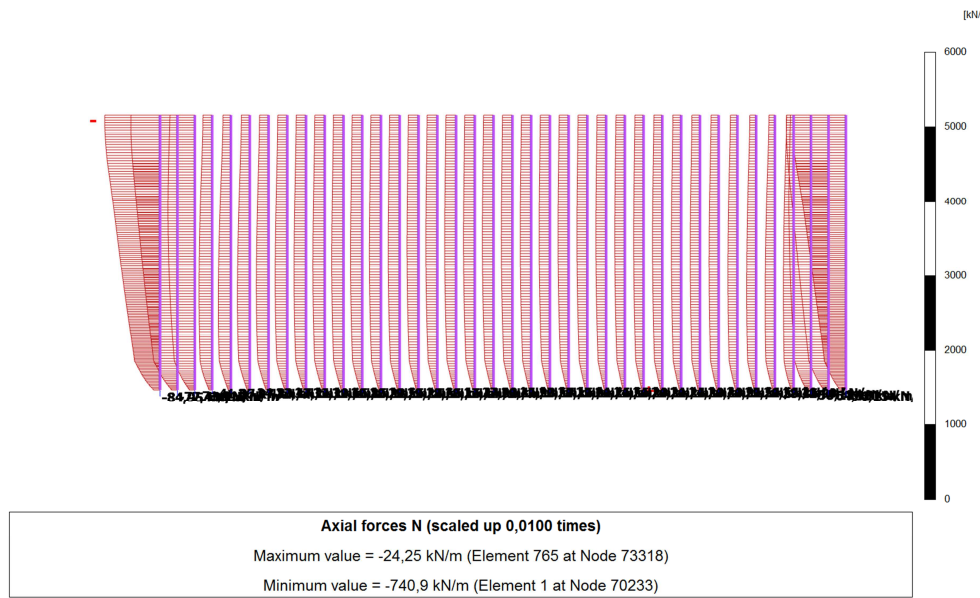


Figure 83 Axial forces in embedded piles after loading - realistic foundation with realistic base plate stiffness

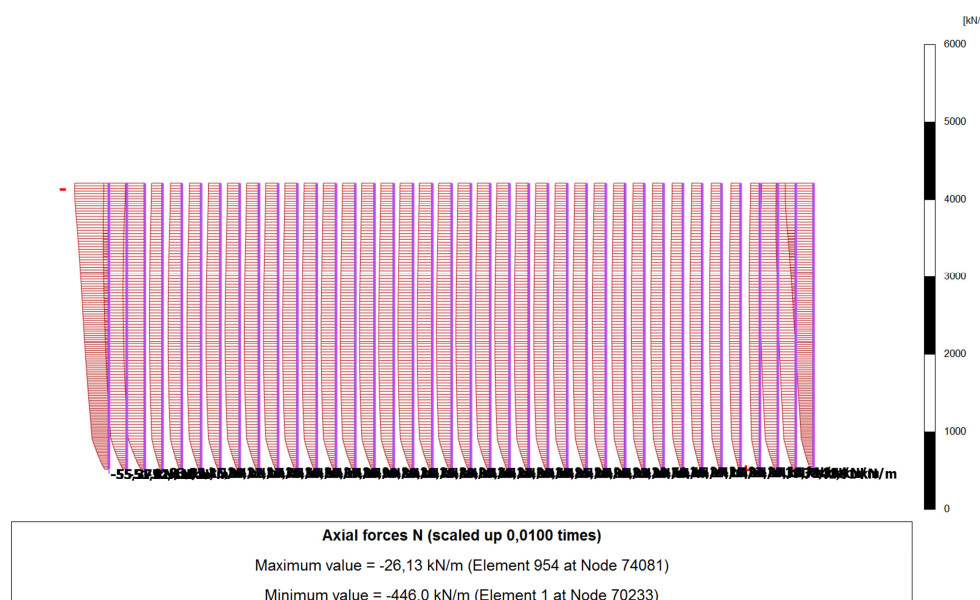


Figure 84 Axial forces in embedded piles after loading - realistic foundation with infinitely stiff base plate

G.3.5

Pile moments in embedded piles (in case of realistic foundation)

In the figures below the moments in the embedded pile rows are presented for the models A, B and B1 with respectively: a realistic foundation with realistic base plate stiffness and a realistic foundation with infinitely stiff base plate.

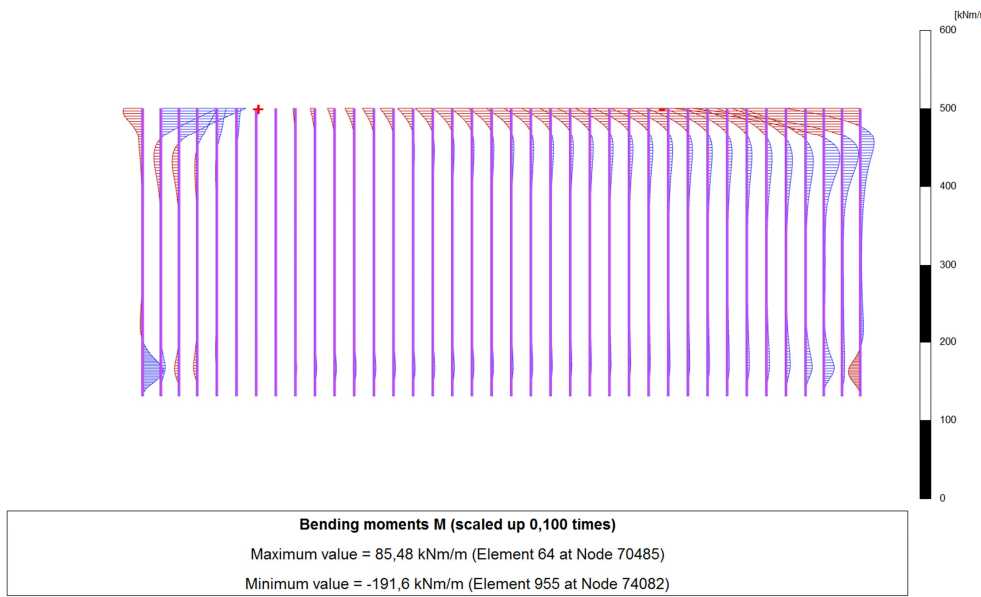


Figure 85 moments in embedded piles after loading - realistic foundation with realistic base plate stiffness

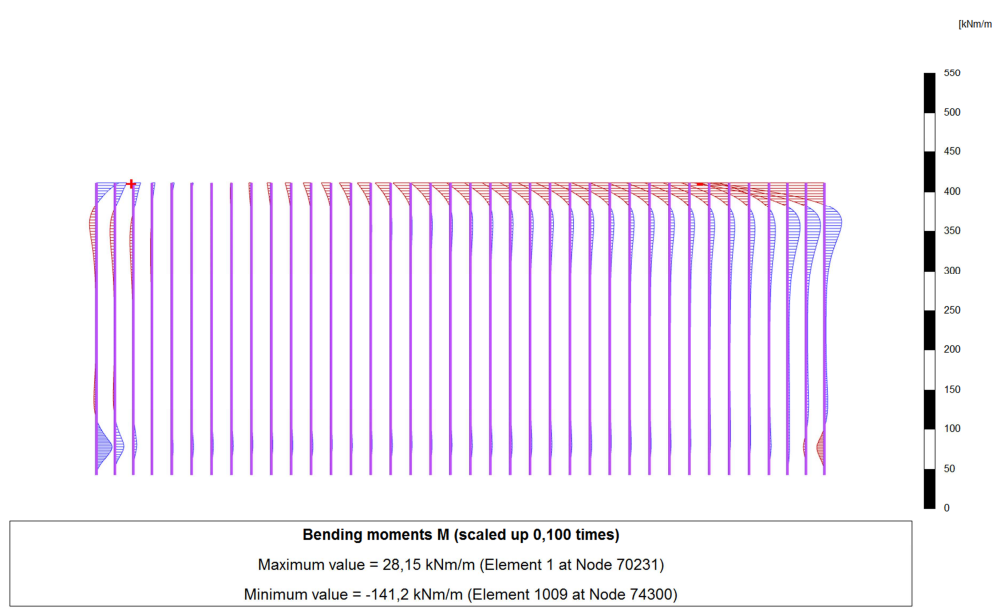


Figure 86 moments in embedded piles after loading - realistic foundation with infinitely stiff base plat

G.4 Dynamic behaviour after

In this phase the structure is only loaded by the weight on top of the beam. The horizontal force applied in the loading phase (see Figure 74) is released and the system is allowed to vibrate for 5 seconds.

G.4.1 Horizontal displacements and frequencies

In the figures below the horizontal displacements of different construction elements (together with the related frequencies) are presented for the models A, B and B1 with respectively: a stiff foundation, a realistic foundation with realistic base plate stiffness and a realistic foundation with infinitely stiff base plate. The frequencies are directly related to the horizontal displacements.

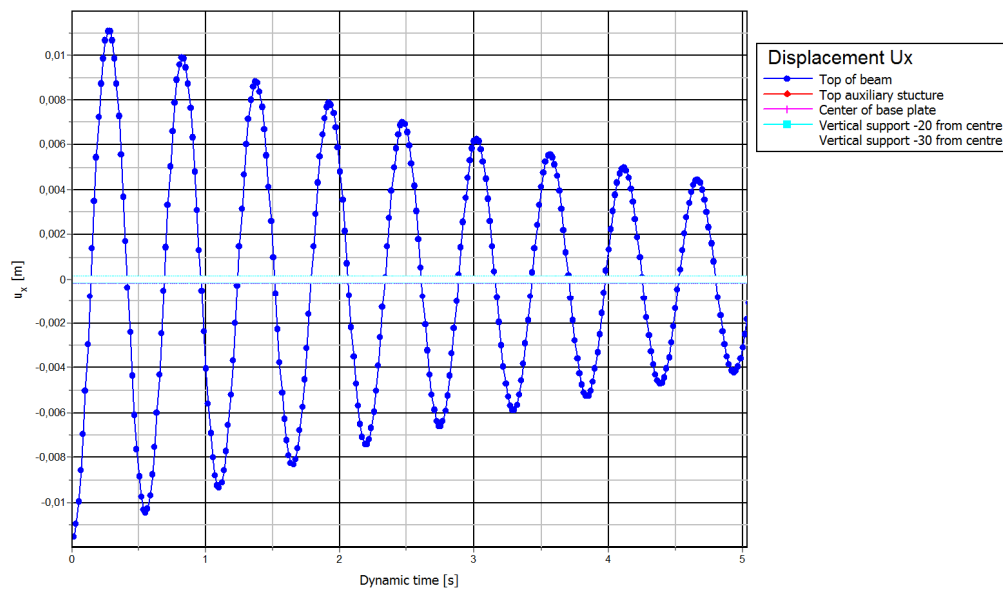


Figure 87 Horizontal displacements in model A

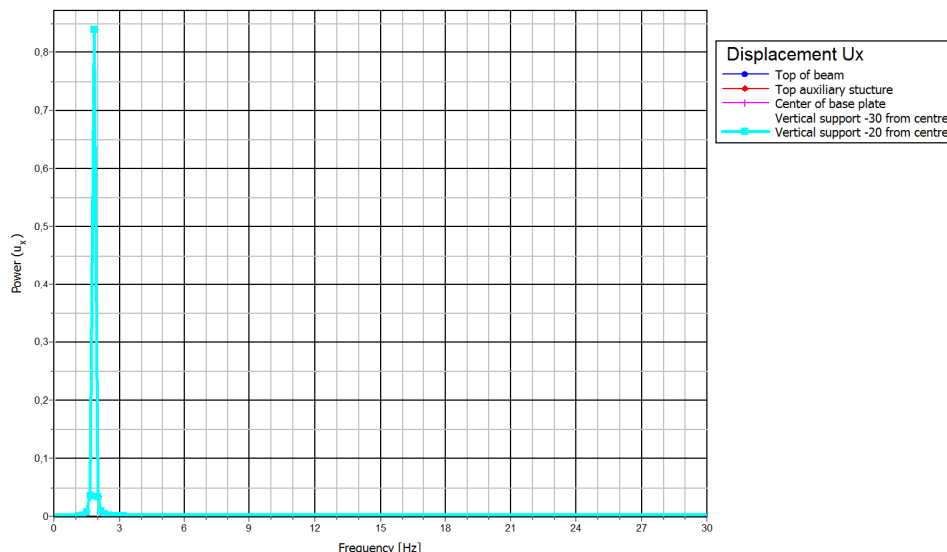


Figure 88 Frequencies related to horizontal displacements in model A

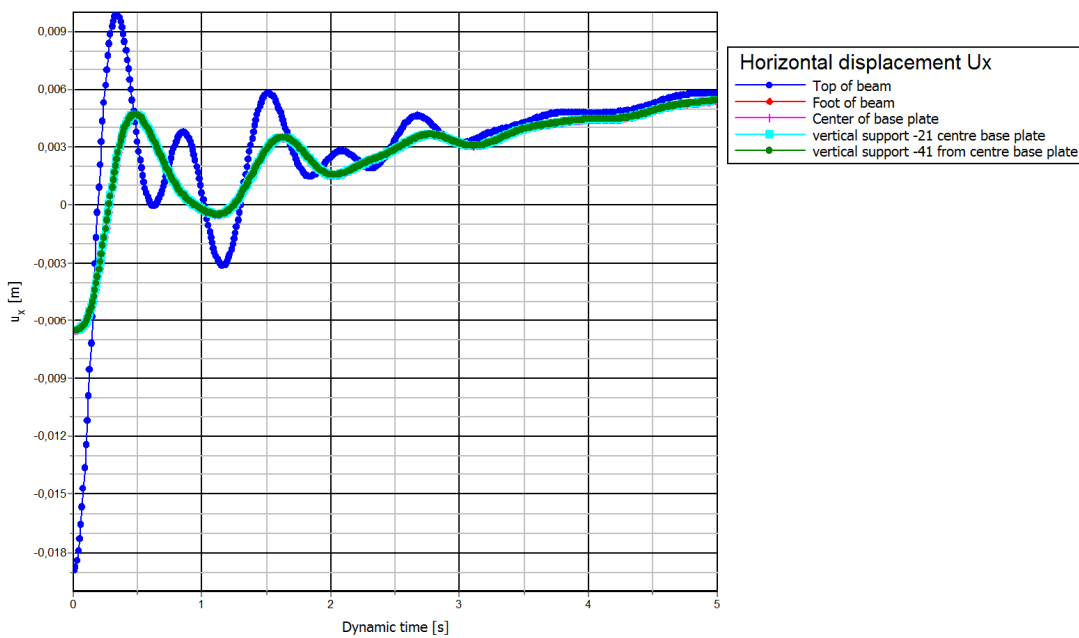


Figure 89 Horizontal displacements in model B1

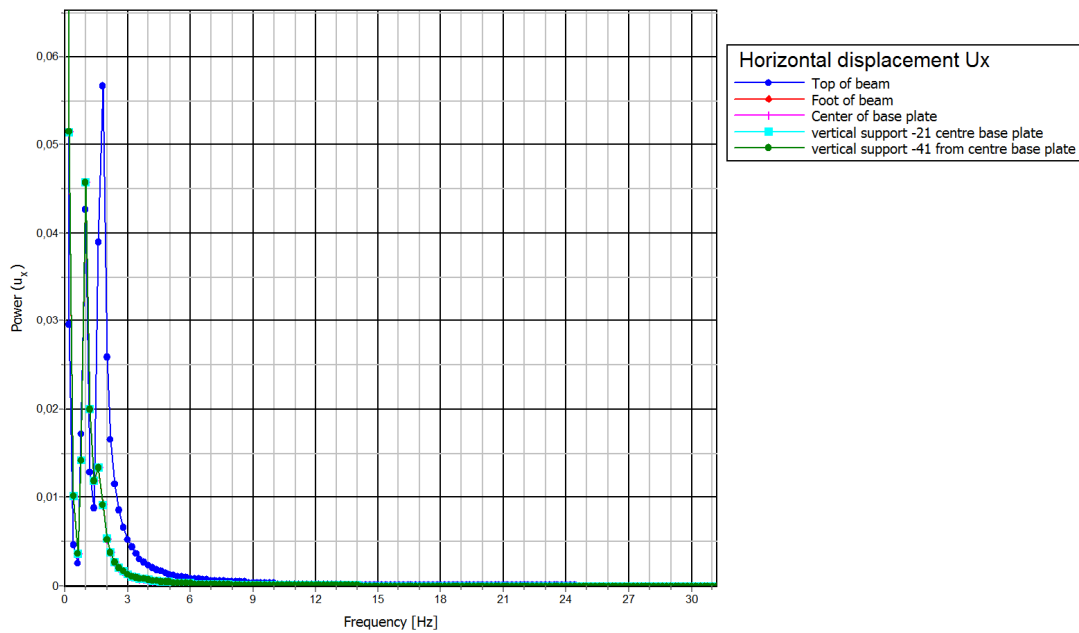


Figure 90 Frequencies related to horizontal displacements in model B1

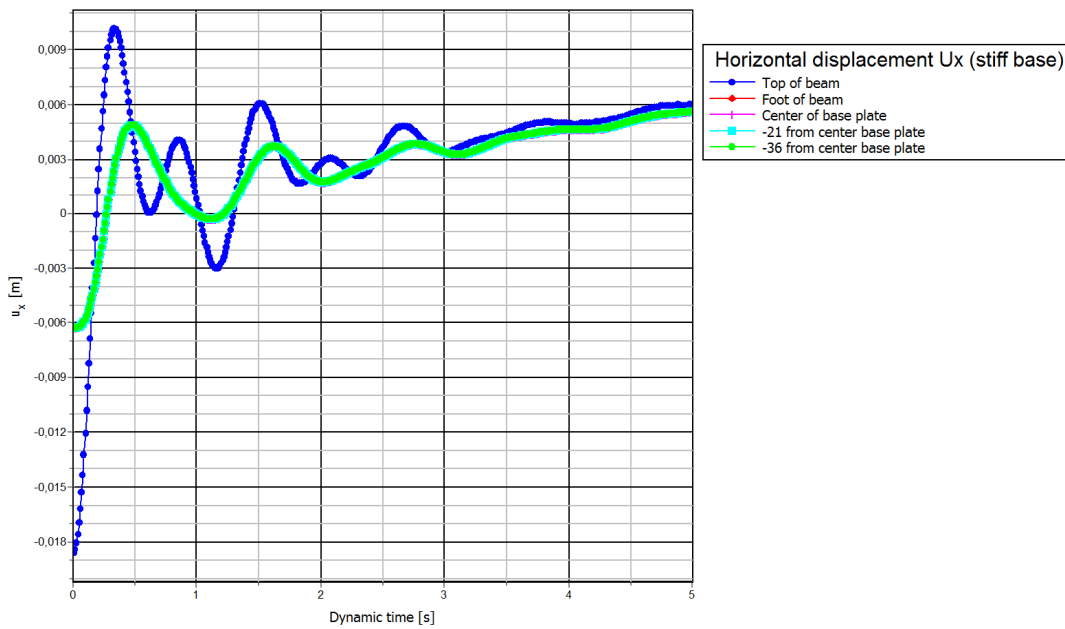


Figure 91 Horizontal displacements in model B2

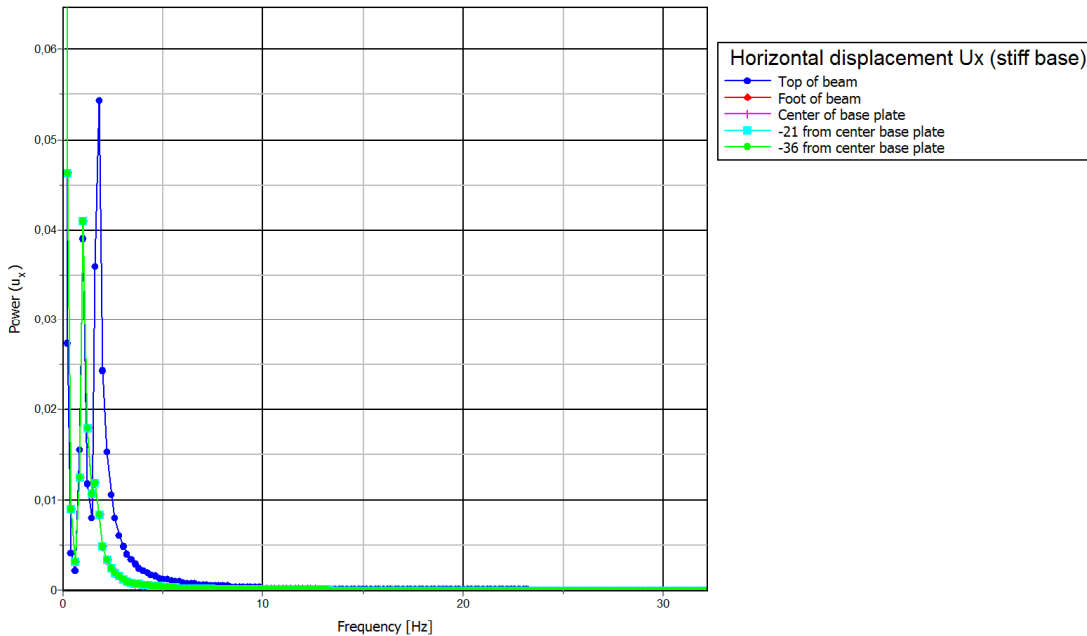


Figure 92 Frequencies related to horizontal displacements in model B2

Model A shows a different response than model B1 and B2. The displacement of the base plate and the auxiliary structure is negligible small compared to the displacement of the vibrating beam due to the stiff foundation. Only one natural frequency is found. This frequency is 1.83 Hz and is directly related to the beam on top of the auxiliary structure. The frequency shows a deviation of only 2% compared the input frequency (1.85 Hz) based on stiffness properties of the beam.

Model B1 and B2 show an identical response but very different than model A. Due to the soil and pile foundation the base plate shows an additional displacement. Displacement of the vibrating beam relative to the auxiliary structure is equal to model A. This can be seen in Figure

89 and/or by subtracting the displacement of the base plate from the displacement of the top of the beam. Two dominant frequencies are found in the movement of the vibrating beam: 1 Hz and 1.83 Hz. The first frequency is related to the movement of the base plate/soil/piles and the second is related to the input frequency related to the stiffness properties of the vibrating beam. The frequency of 1.83 Hz is dominant over the frequency of 1 Hz, especially for the force distribution in the vertical supports of the auxiliary structure. This is shown in the figures in the next paragraph.

G.4.2 Axial forces in vertical supports of auxiliary structure and frequencies

In the figures below the axial forces in vertical supports of the auxiliary structure (together with the related frequencies) are presented for the models A, B and B1 with respectively: a stiff foundation, a realistic foundation with realistic base plate stiffness and a realistic foundation with infinitely stiff base plate. The frequencies are directly related to the horizontal displacements.

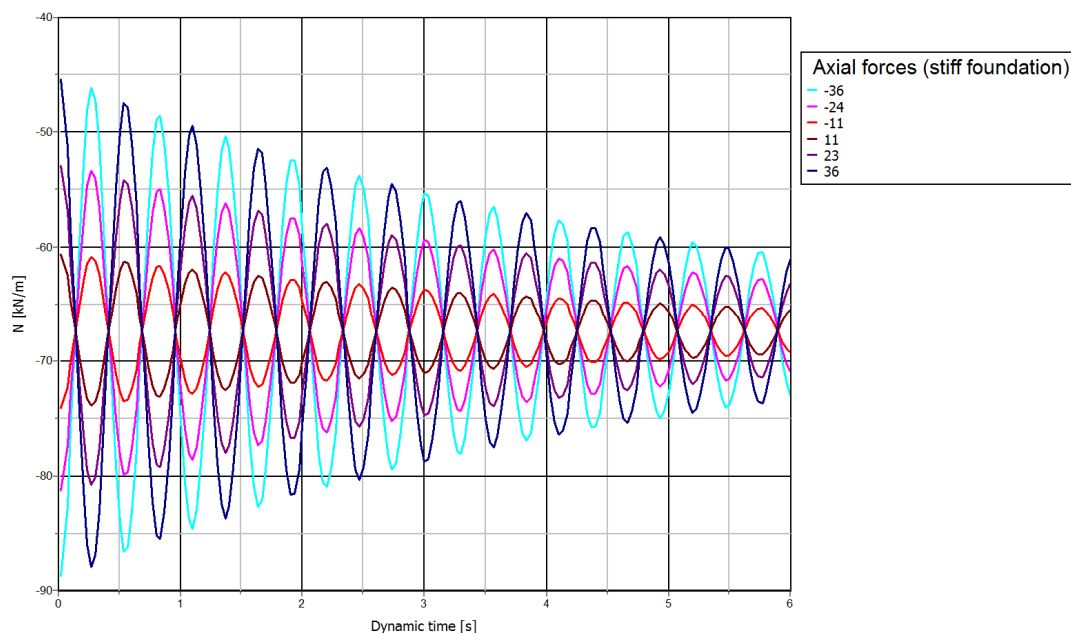


Figure 93 Axial forces in vertical supports - model A

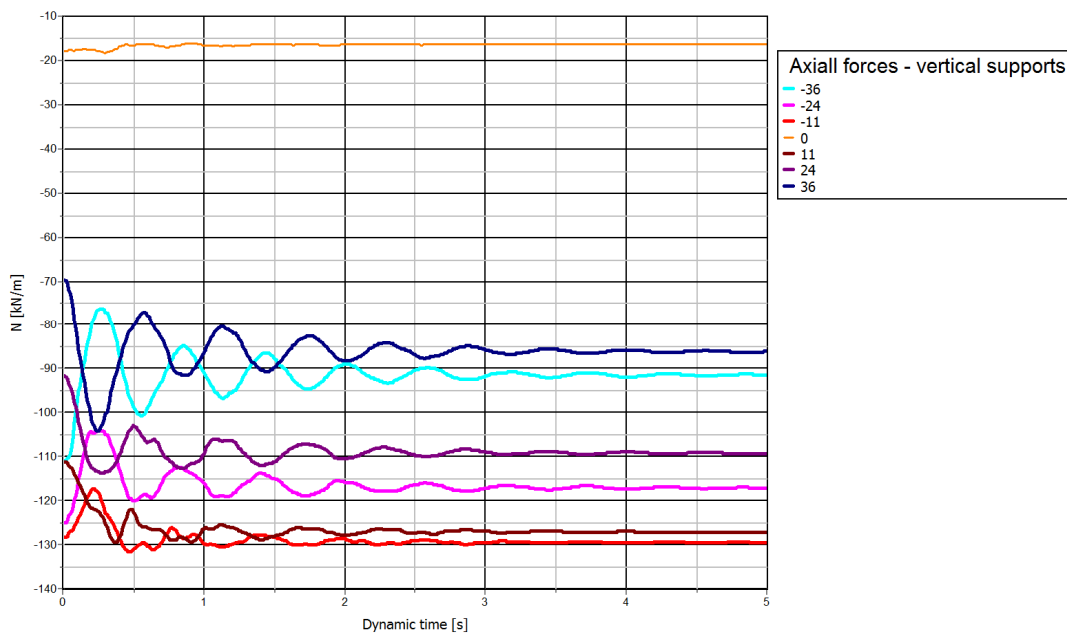


Figure 94 Axial forces in vertical supports - model B1

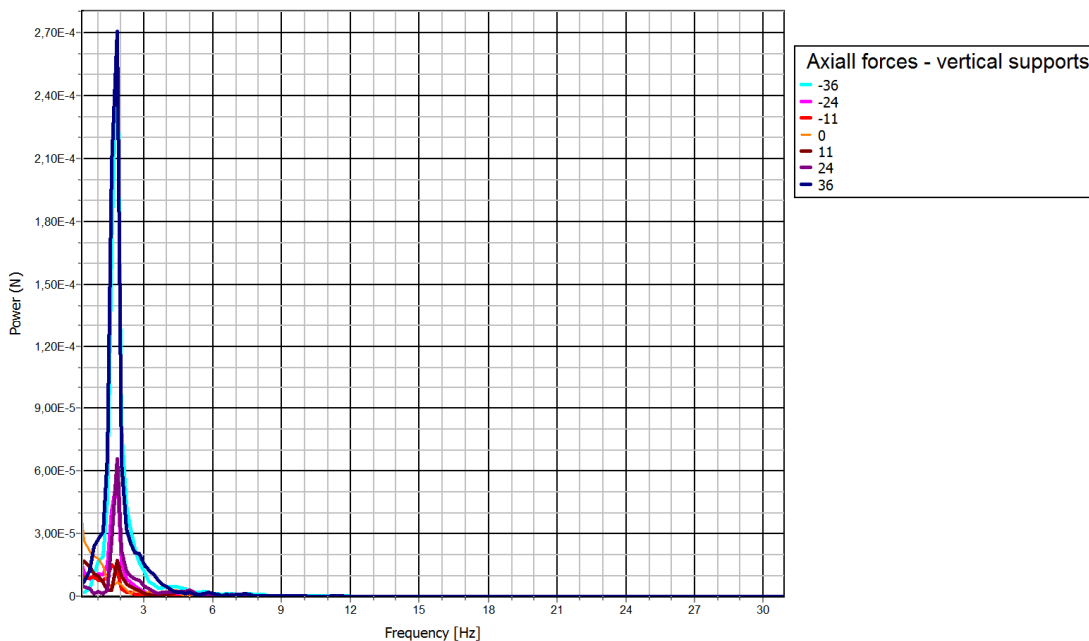


Figure 95 Frequency related to axial forces in vertical supports - model B1

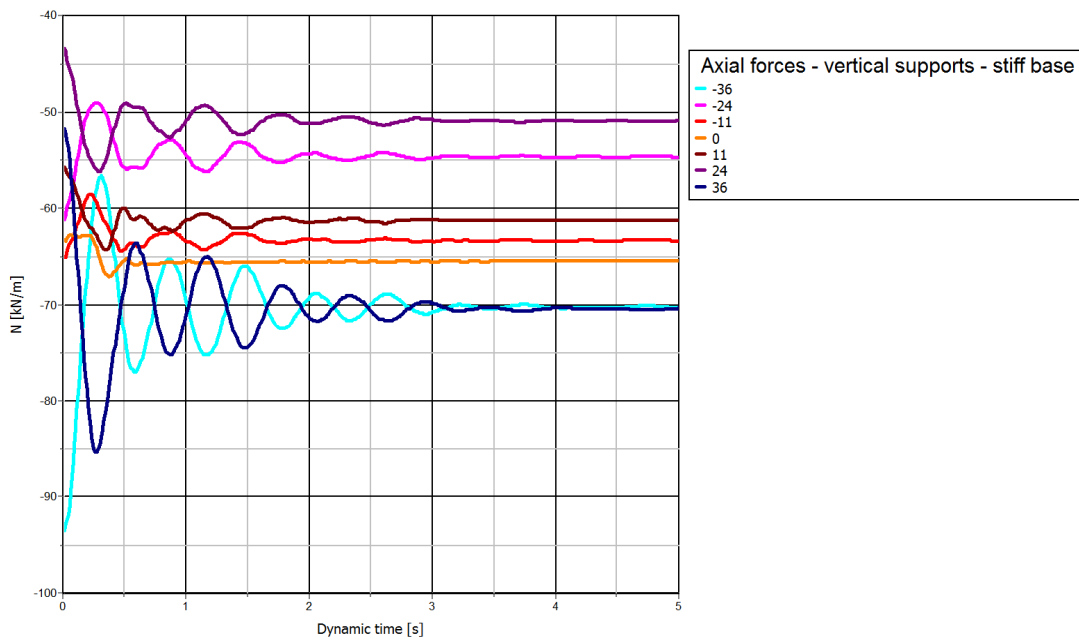


Figure 96 Axial forces in vertical supports - model B2

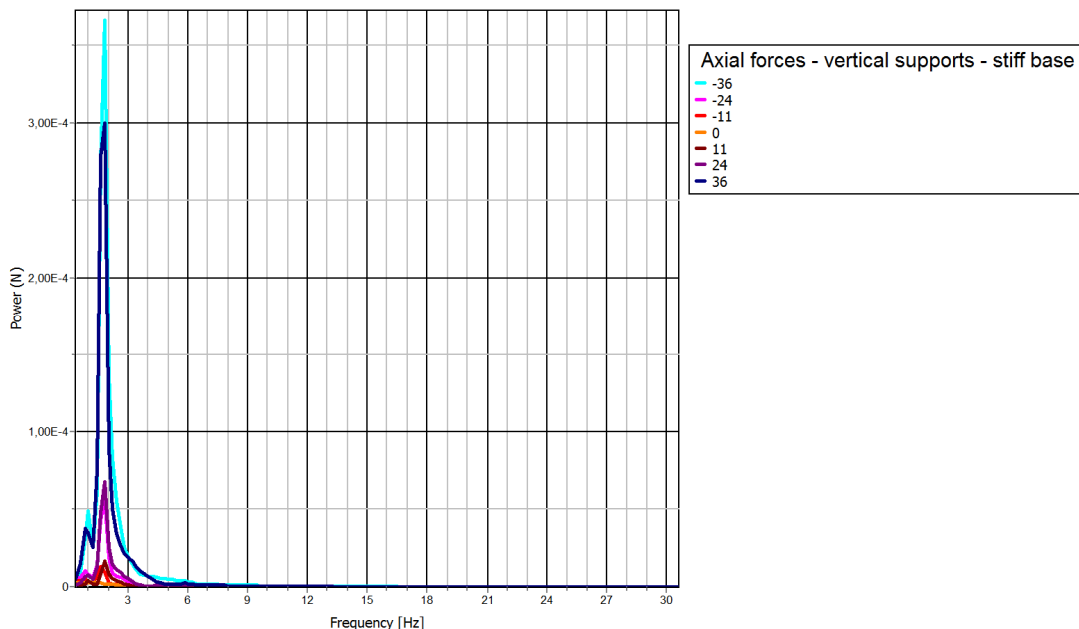


Figure 97 Frequency related to axial forces in vertical supports - model B2

The distribution of vertical forces over the width of the base plate (directly related to the axial forces in the vertical supports) is related to the frequency of the vibrating beam on top of the auxiliary structure. In model B1 and B2 there is only a small influence of the frequency related to the soil/piles/base plate.

Appendix H

H. RESULTS EARTHQUAKE CALCULATIONS

In this appendix the results of the SSE earthquake calculations are presented for two different situations:

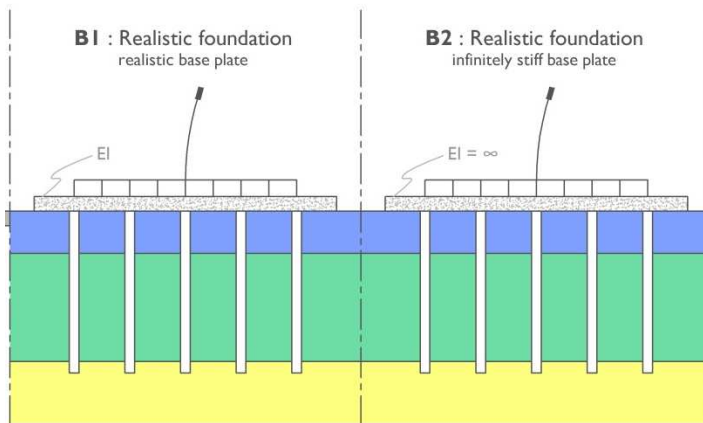


Figure 98 different calculation models

- Model B1 : Realistic foundation with base plate with realistic stiffness.
- Model B2 : Realistic foundation with infinitely stiff base plate.

The further properties of the models and earthquake signals that are used in the calculations are discussed in chapter 9 of the report. This chapter provides an overview of the most important results:

- Horizontal displacements of construction and soil during earthquake;
- Axial forces in vertical supports to judge normative situations for overturning moments;
- Shear forces in vertical supports;
- Comparison between dynamic and pseudo static pile forces.

H.1

Horizontal displacements

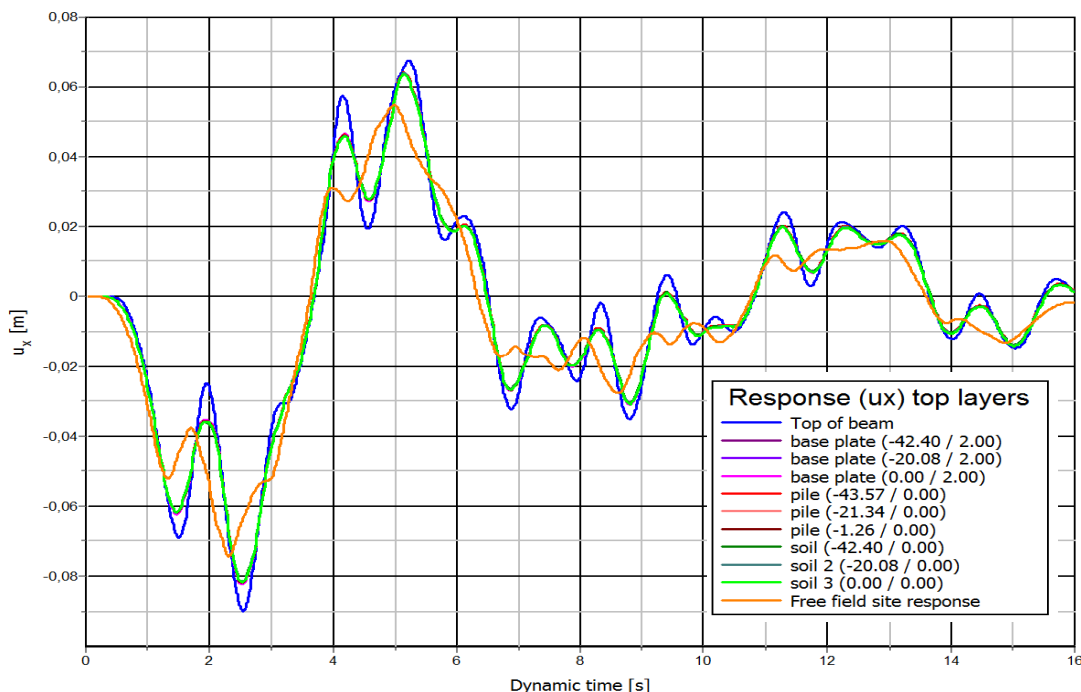


Figure 99 Horizontal displacement of over width of base plate – Model B1

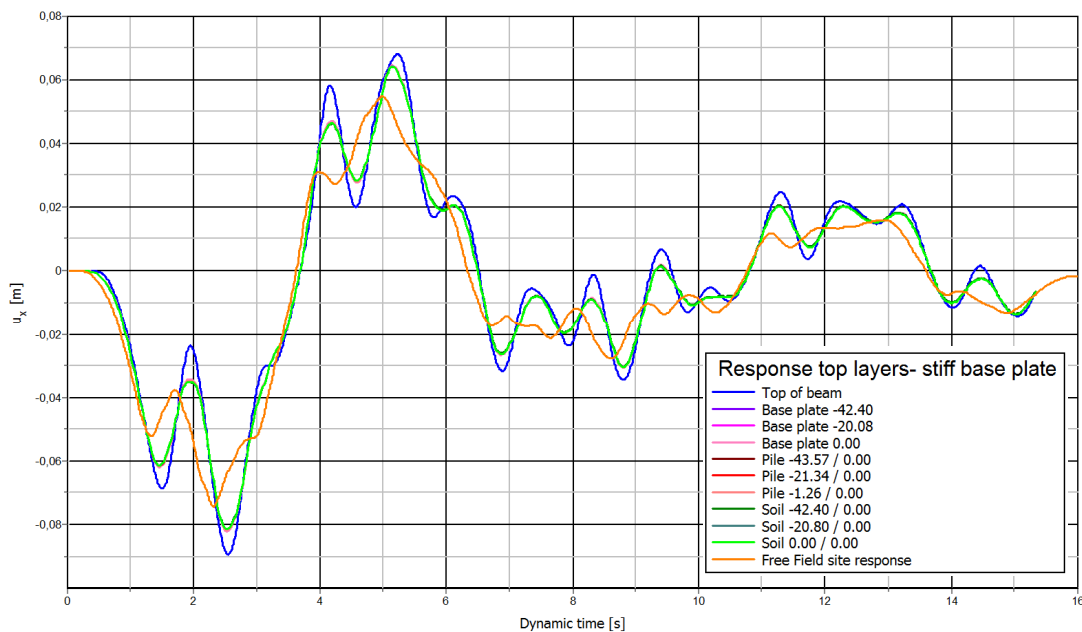


Figure 100 Horizontal displacement of over width of base plate – Model B2

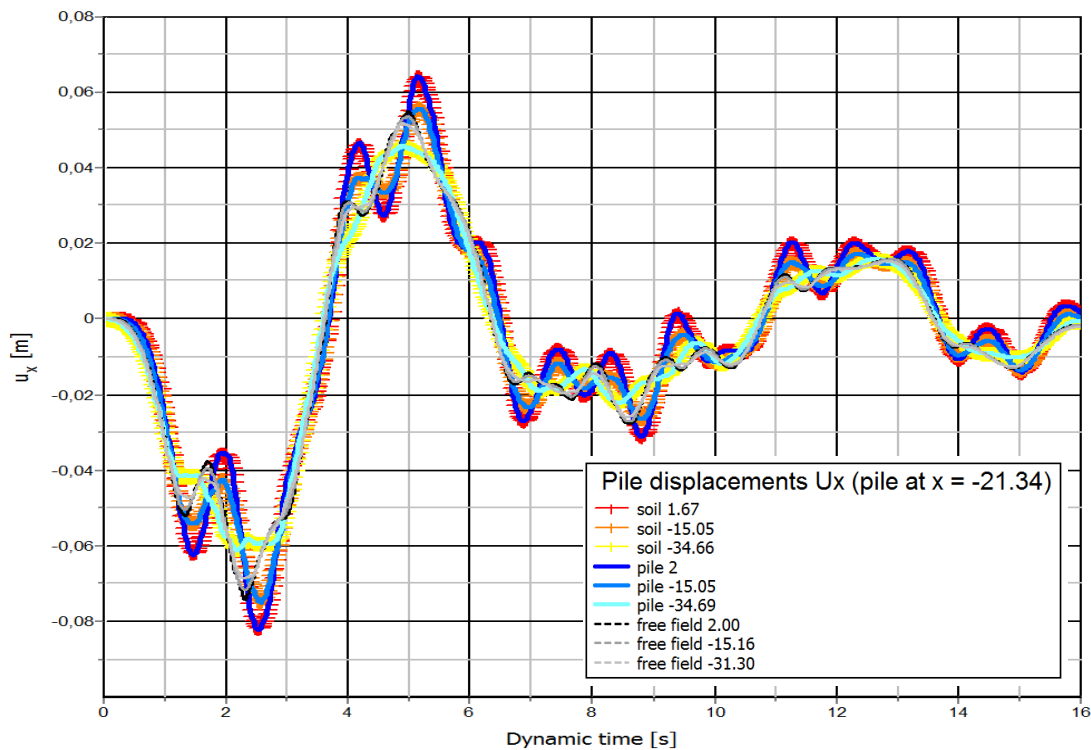


Figure 101 Horizontal displacement over length of pile(s) – Model B1

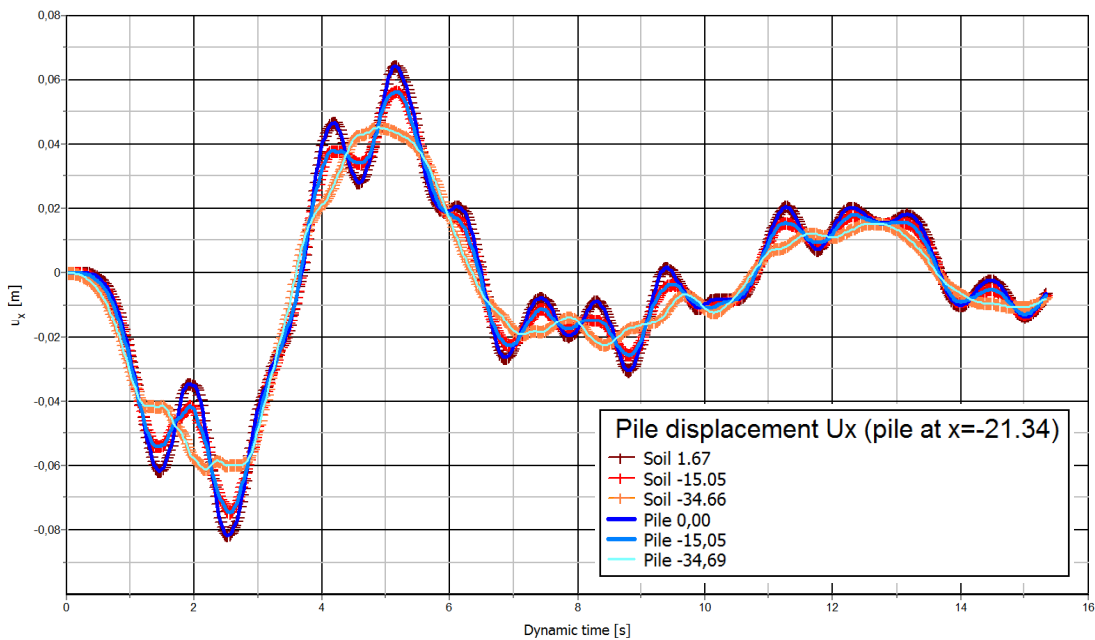


Figure 102 Horizontal displacement over length of pile(s) – Model B2

H.2 Axial forces in vertical supports of auxiliary structure during SSE earthquake

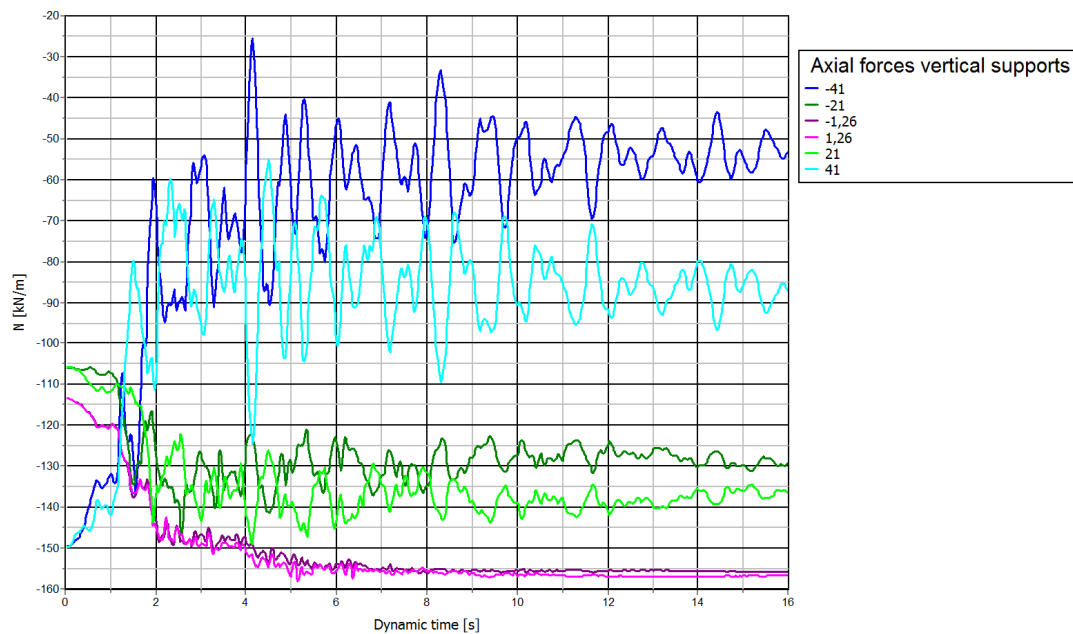


Figure 103 Axial forces in vertical supports of auxiliary structure - model B1

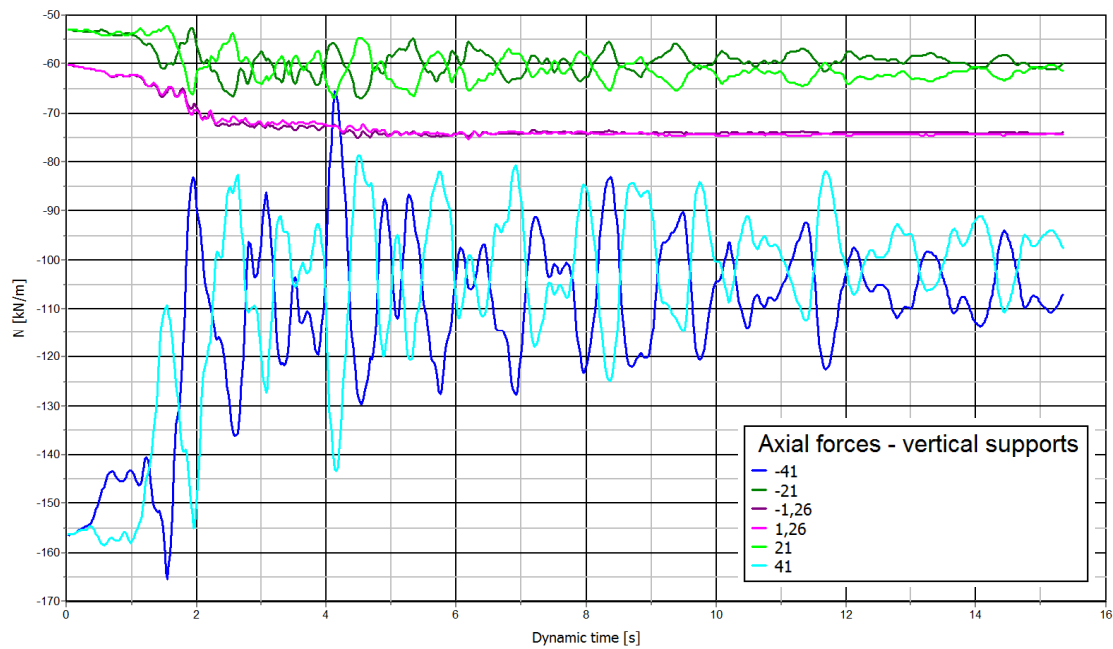


Figure 104 Axial forces in vertical supports of auxiliary structure - model B2

H.3

Shear forces in vertical supports of auxiliary structure during SSE earthquake

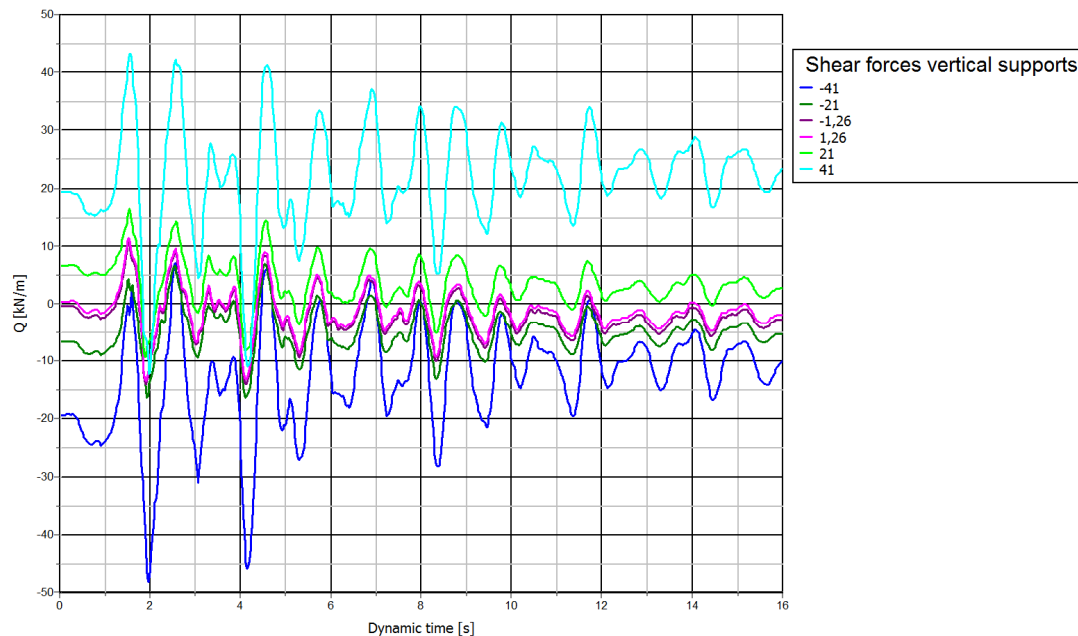


Figure 105 Shear forces in vertical supports of auxiliary structure - model B1

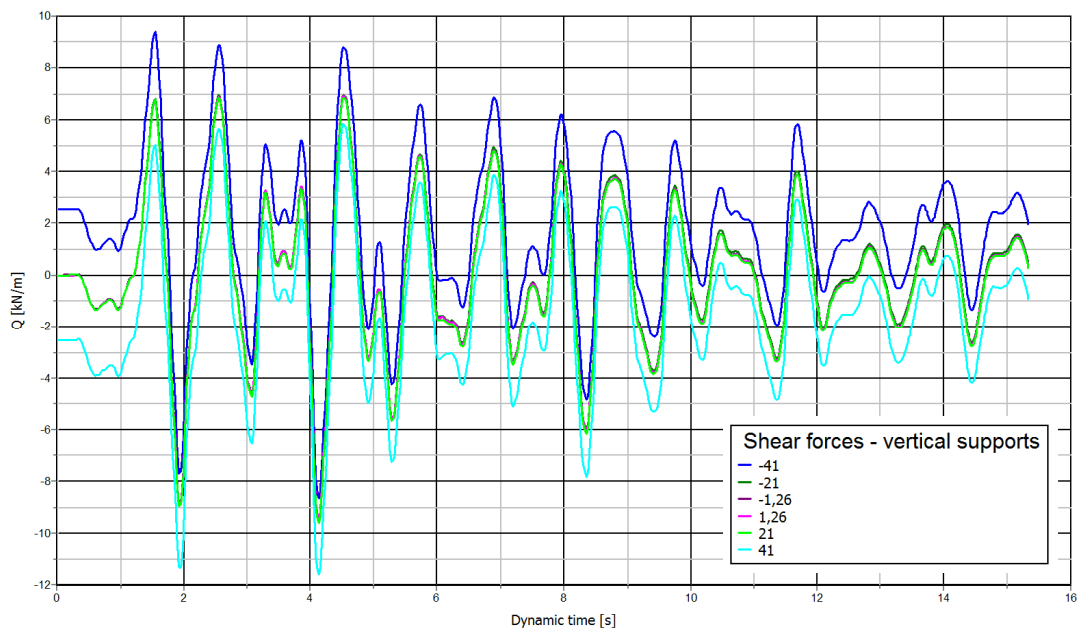
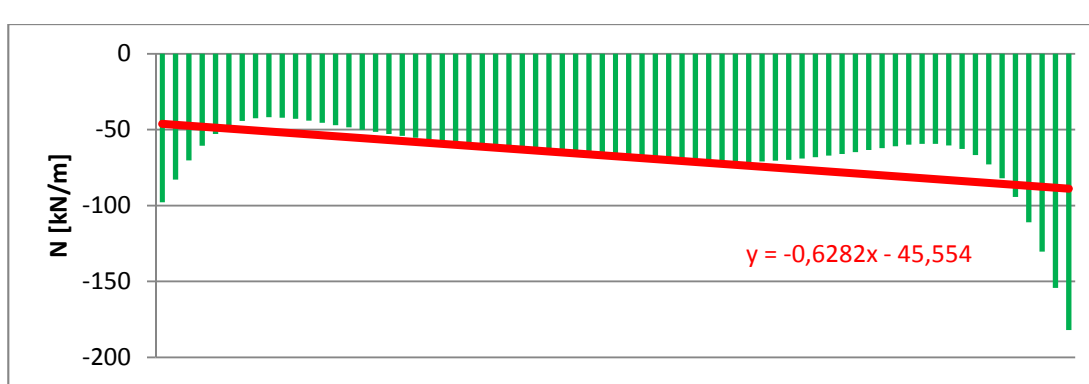
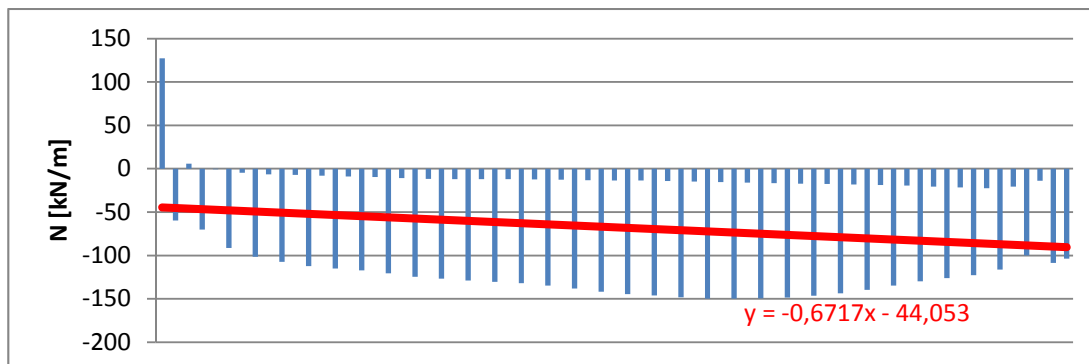


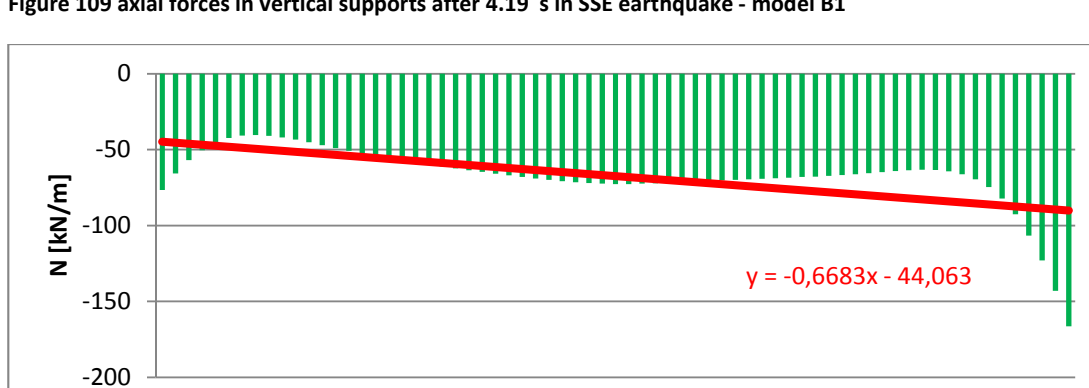
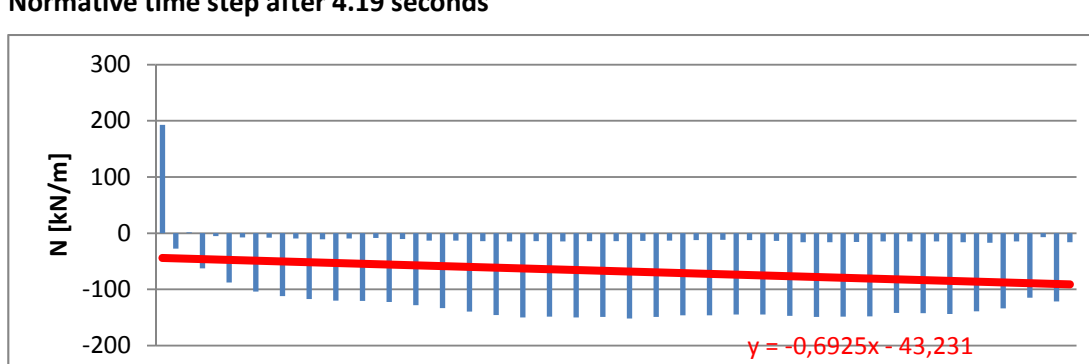
Figure 106 Shear forces in vertical supports of auxiliary structure - model B2

H.4 Axial forces in vertical supports of auxiliary structure during normative time steps

H.4.1 Normative time step after 1.92 seconds

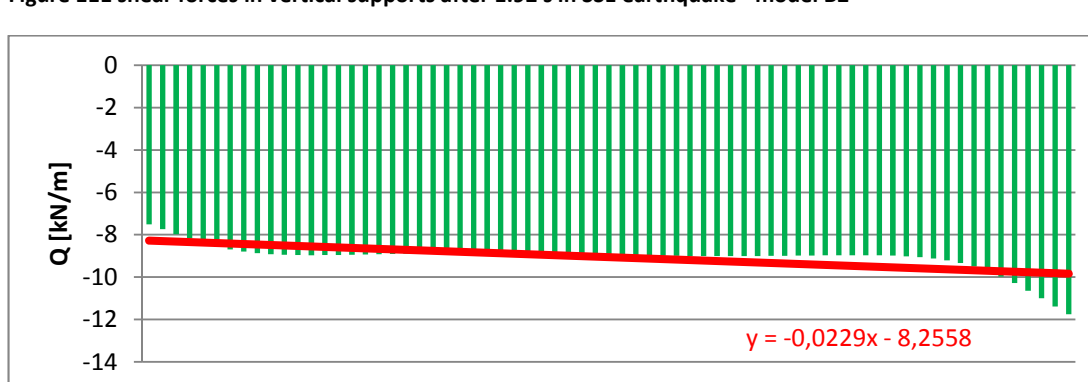
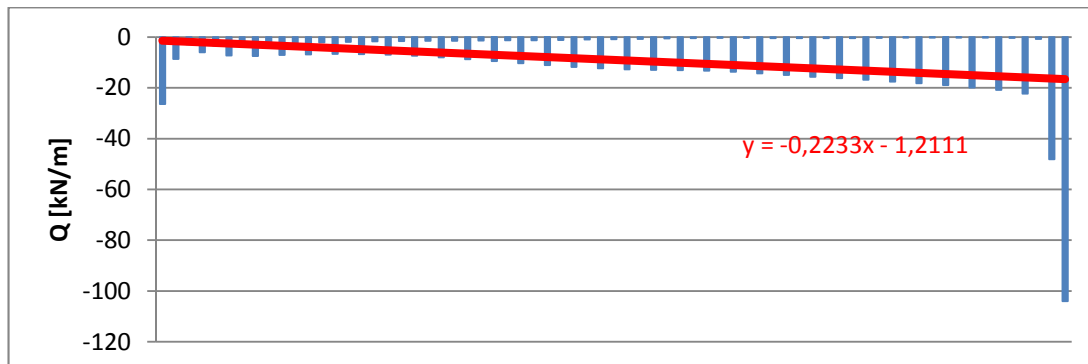


H.4.2 Normative time step after 4.19 seconds

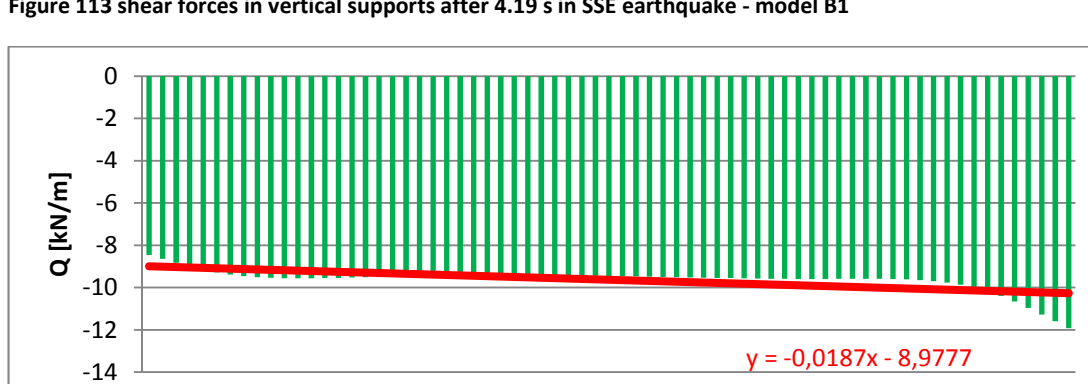
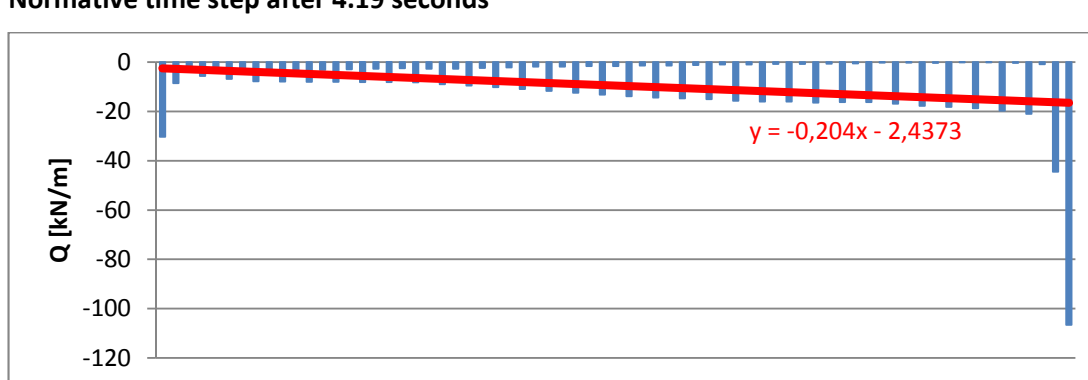


H.5 Shear forces in vertical supports of auxiliary structure during normative time steps

H.5.1 Normative time step after 1.92 seconds



H.5.2 Normative time step after 4.19 seconds



H.6

Dynamic and Pseudo static pile forces

The uncoupled calculation method used in the MDOF is compared to a full dynamic method using PLAXIS 2D. The normative situations during the earthquake calculations are considered. Reaction forces from the superstructure (auxiliary structure) are read out from the dynamic model and used as input for a (pseudo) static model with exactly the same geometry and properties. In total 5 different models are considered:

- **Model B1** Full dynamic model with realistic base plate stiffness;
- **Model B2** Full dynamic model with infinitely stiff base plate.
- **Model B1.1** Pseudo static model with realistic base plate stiffness. All forces from auxiliary are read out from the dynamic calculation and applied as static force at their original location;
- **Model B2.1** Pseudo static model with infinitely stiff base plate. All forces from auxiliary are read out from the dynamic calculation and applied as static force at their original location;
- **Model B2.2** Pseudo static model with infinitely stiff base plate. All forces from the auxiliary structure are summarized and applied as vertical force, shear force and overturning moment at the base slab centre.

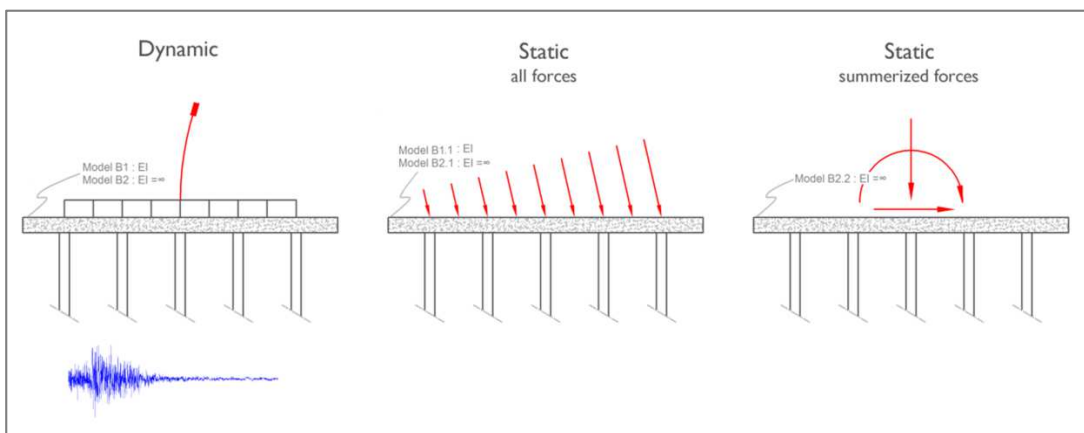


Figure 115 Considered models for comparison of uncoupled- and full dynamic method

Colours used in the enumeration above Figure 115 are corresponding to the results on the next 15 pages.

In chapter 9.3.2 of the report three comparisons are made between the different full dynamic and pseudo static models:

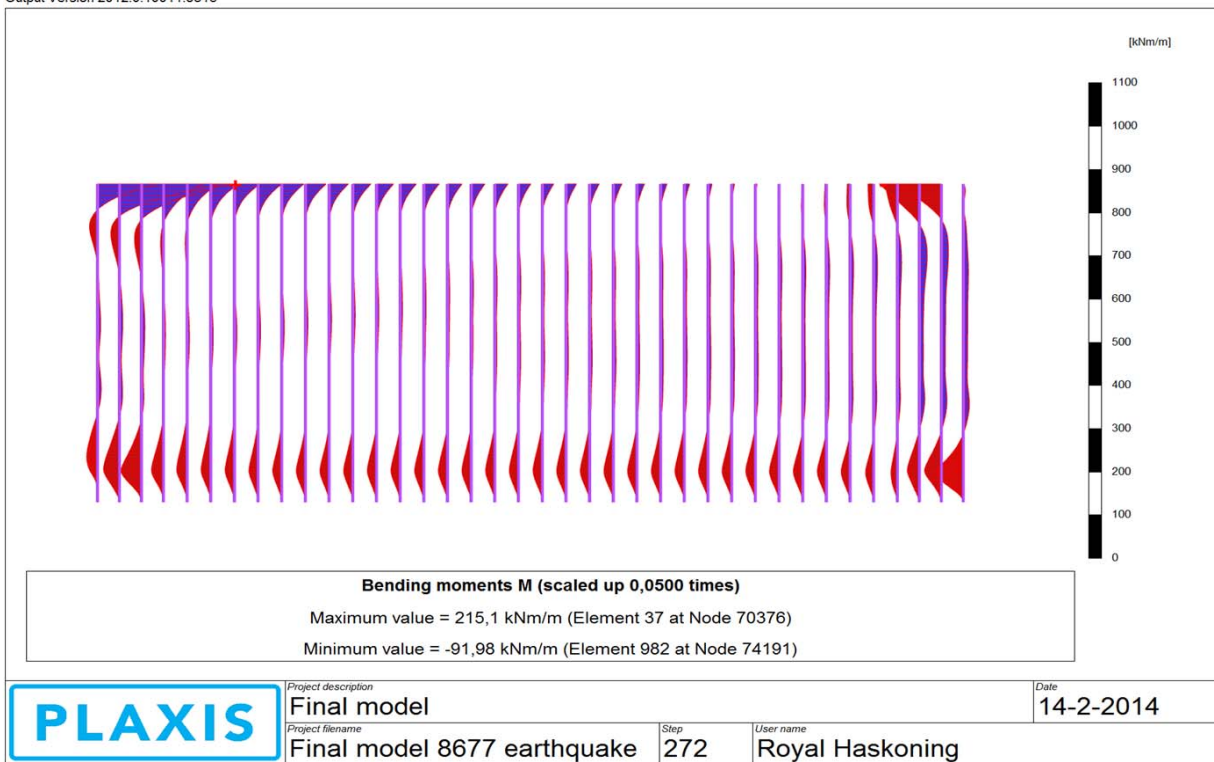
- **Model B1 versus B1.1**: Full dynamic model with realistic base plate stiffness compared to (pseudo) static model with realistic base plate stiffness. All forces from auxiliary are read out from the dynamic calculation and applied as static force at their original location;
- **Model B2 versus B2.1**: Full dynamic model with infinitely stiff base plate compared to (pseudo) static model with infinitely stiff base plate.
- **Model B versus B2.1**: Full dynamic model with infinitely stiff base plate compared to (pseudo) static model with infinitely stiff base plate. All forces from the auxiliary structure are summarized and applied as vertical force, shear force and overturning moment at the base slab centre.

◦

Earthquake : MOMENTS

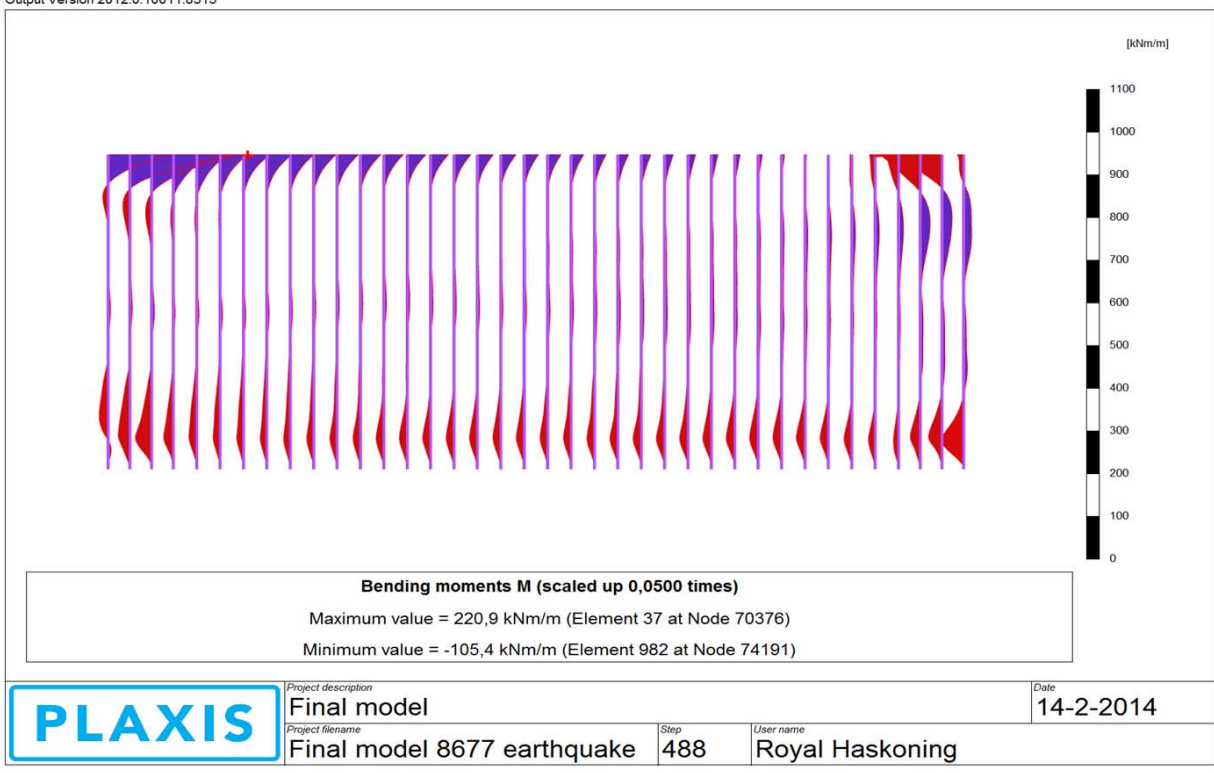
1,93 seconds
step 272

Output Version 2012.0.10011.8315



4,13 seconds
step 488

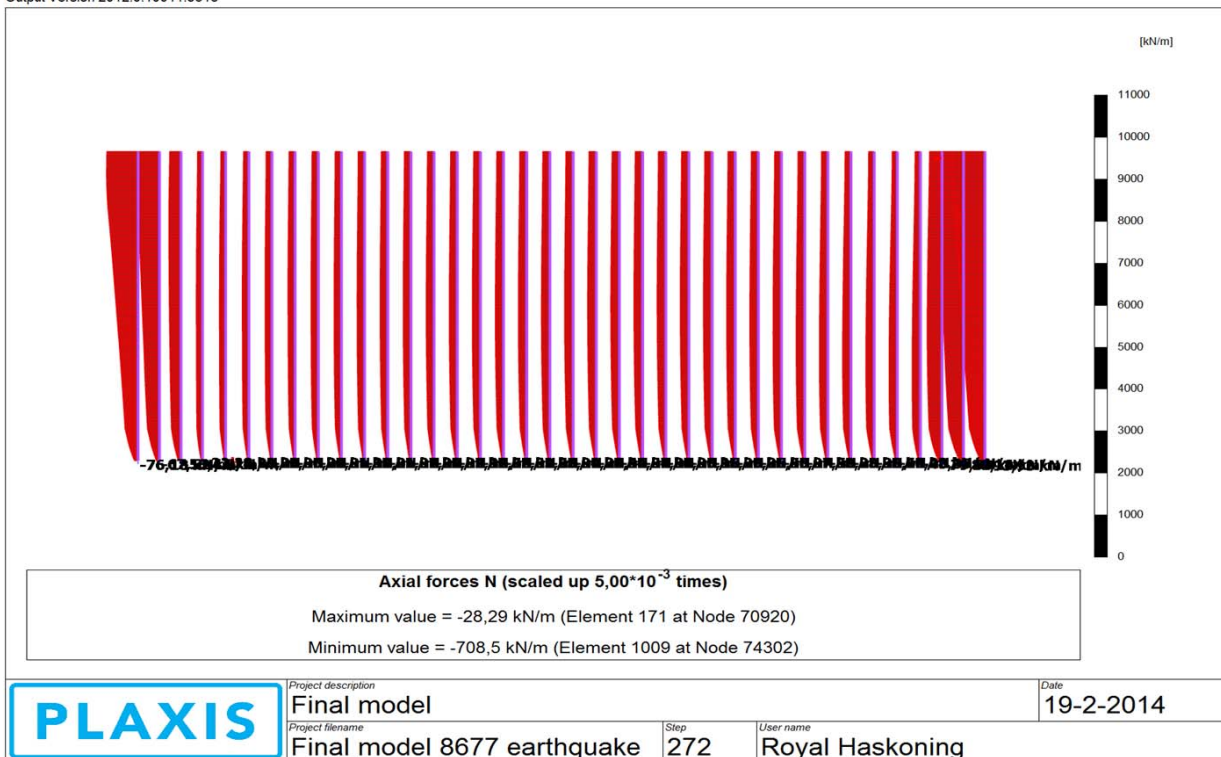
Output Version 2012.0.10011.8315



Earthquake : AXIAL FORCES

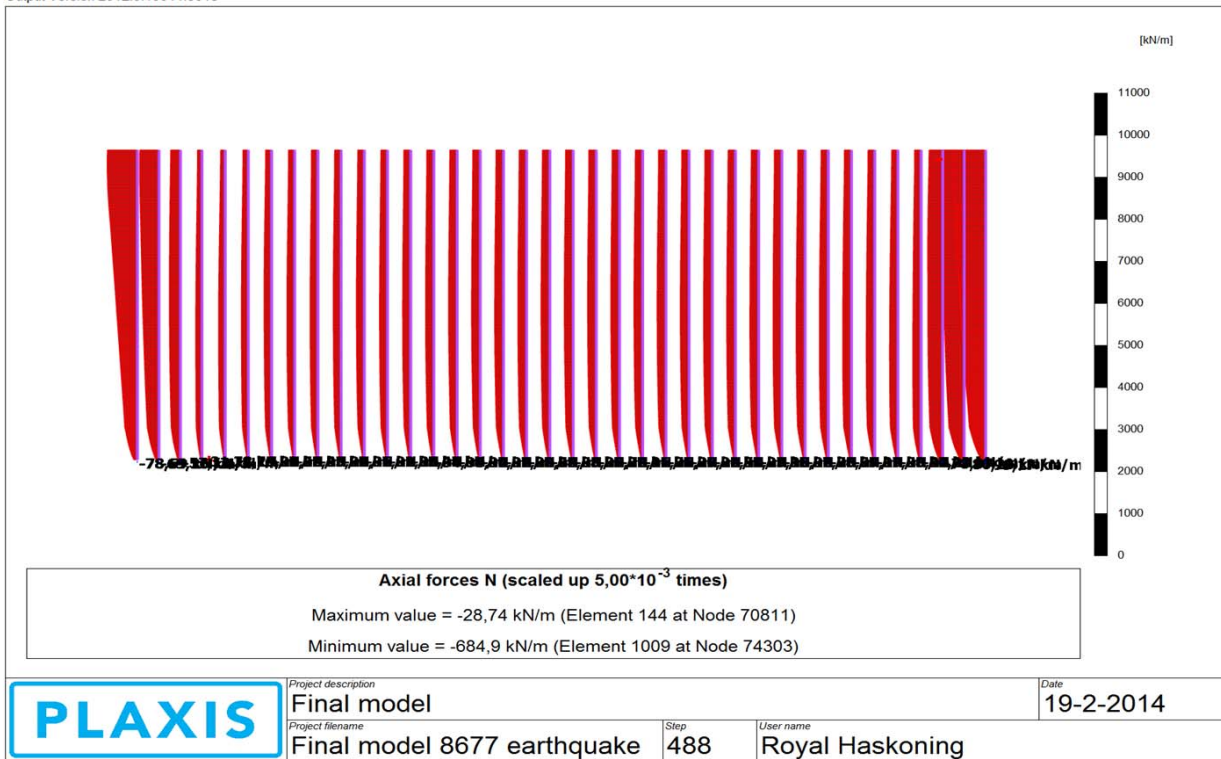
1,93 seconds
step 272

Output Version 2012.0.10011.8315



4,13 seconds
step 488

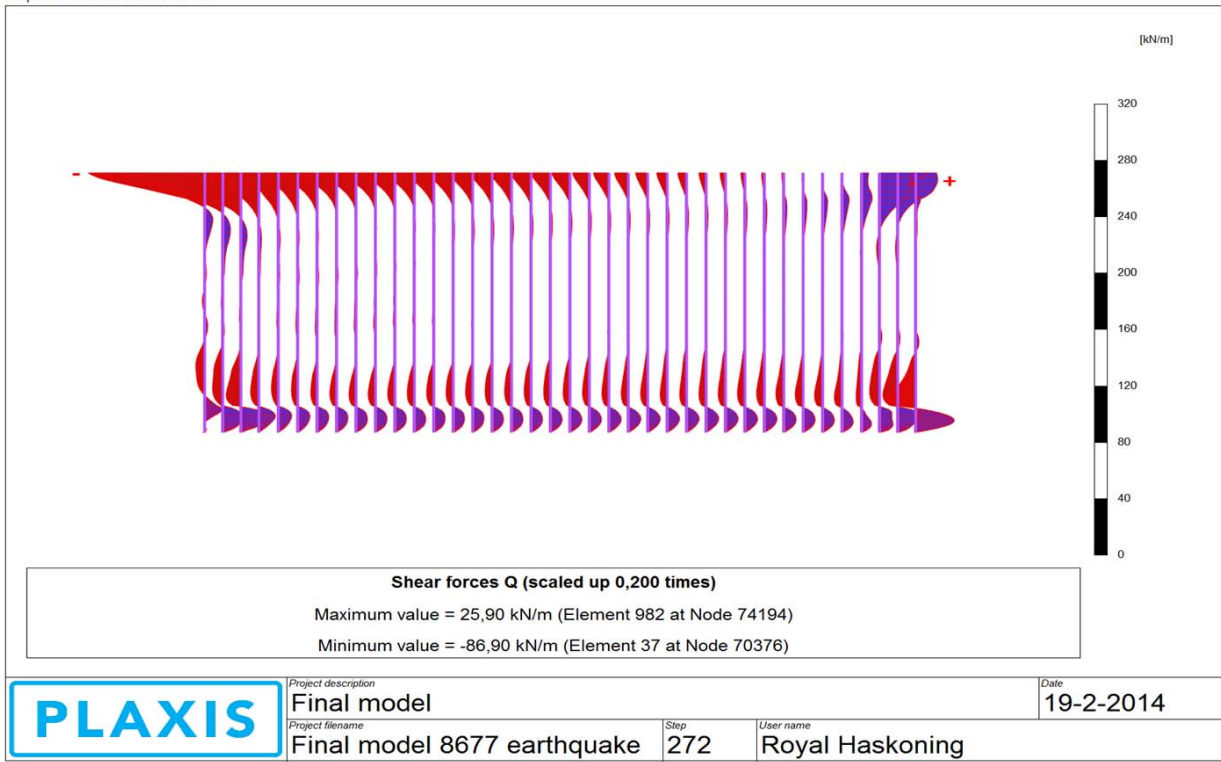
Output Version 2012.0.10011.8315



Earthquake : LATERAL FORCES

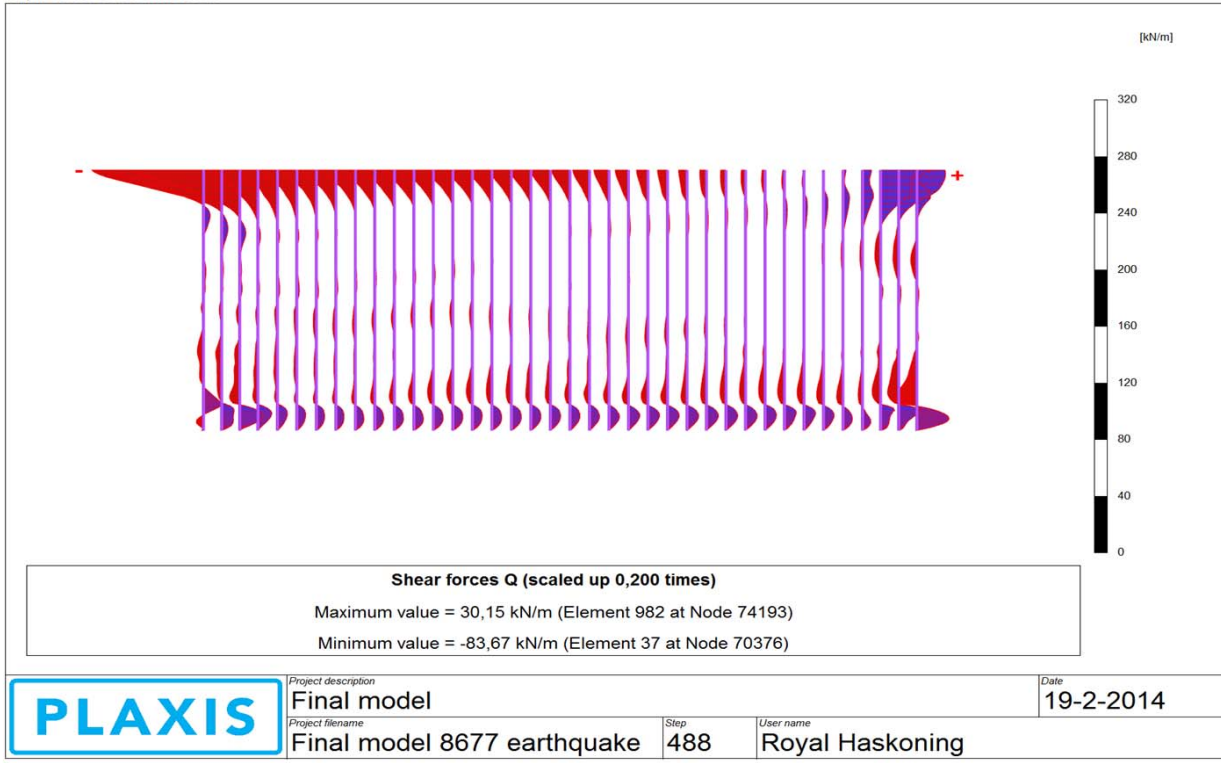
1,93 seconds
step 272

Output Version 2012.0.10011.8315



4,13 seconds
step 488

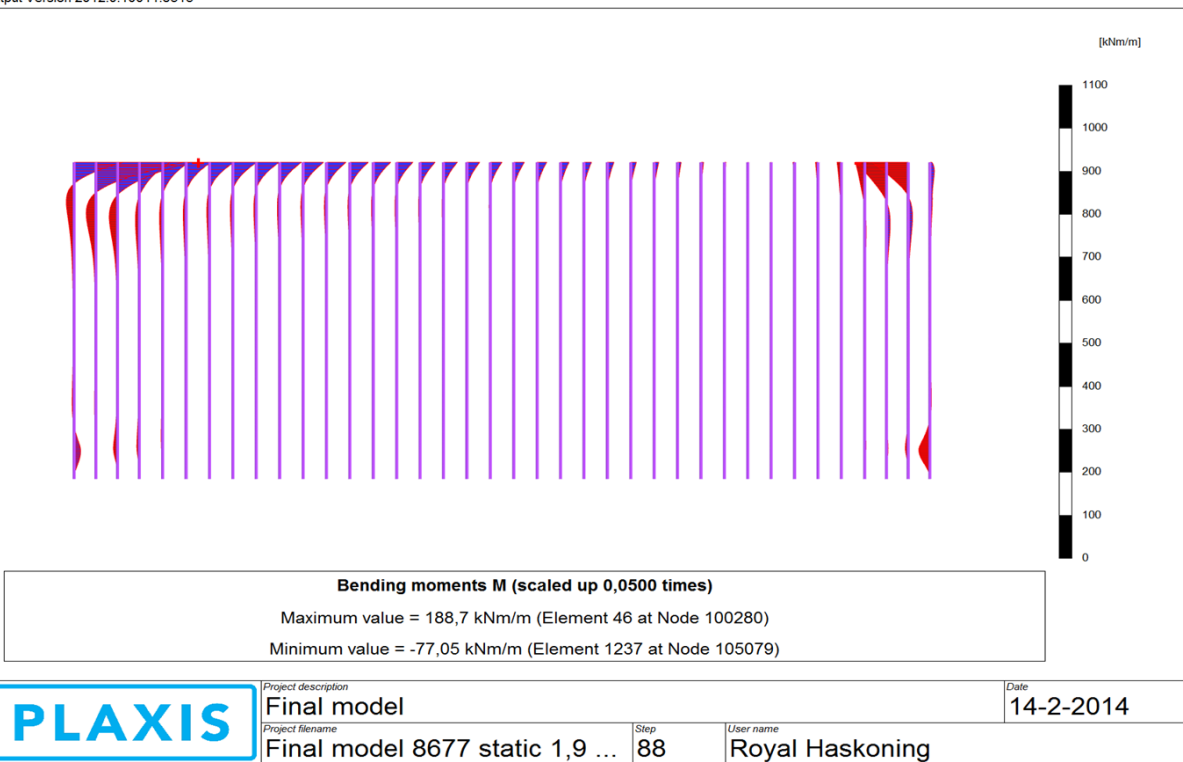
Output Version 2012.0.10011.8315



Static - Normal bas eplate stiffness : MOMENTS

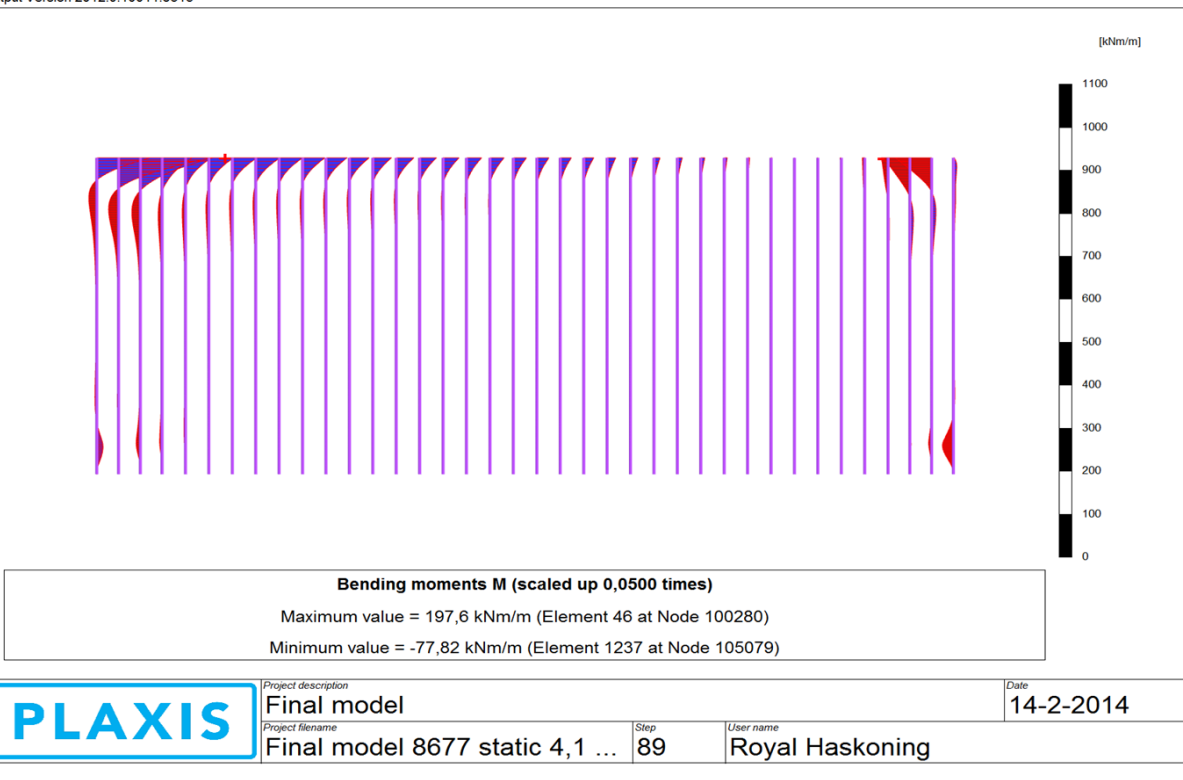
1,93 seconds
step 272

Output Version 2012.0.10011.8315



4,13 seconds
step 488

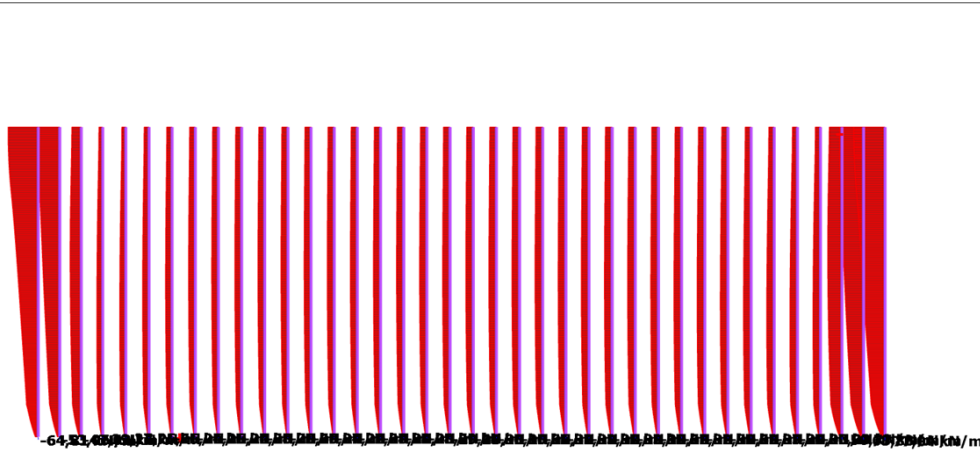
Output Version 2012.0.10011.8315



Static - Normal base plate stiffness : AXIAL FORCES

1,93 seconds
step 272

Output Version 2012.0.10011.8315



PLAXIS

Project description
Final model

Project filename
Final model 8677 static 1,9 ...

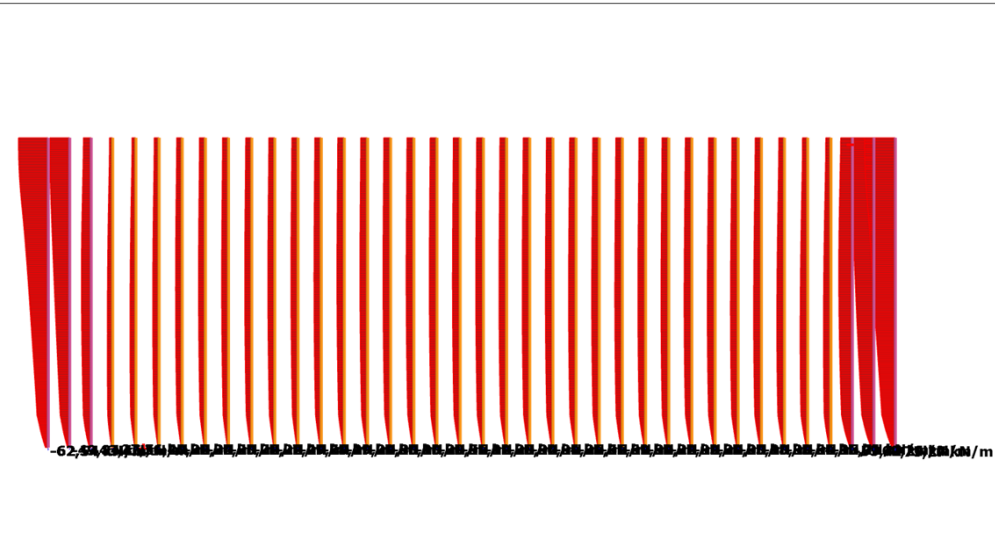
Step
88

User name
Royal Haskoning

Date
19-2-2014

4,13 seconds
step 488

Output Version 2012.0.10011.8315



PLAXIS

Project description
Final model

Project filename
Final model 8677 static 4,1 ...

Step
89

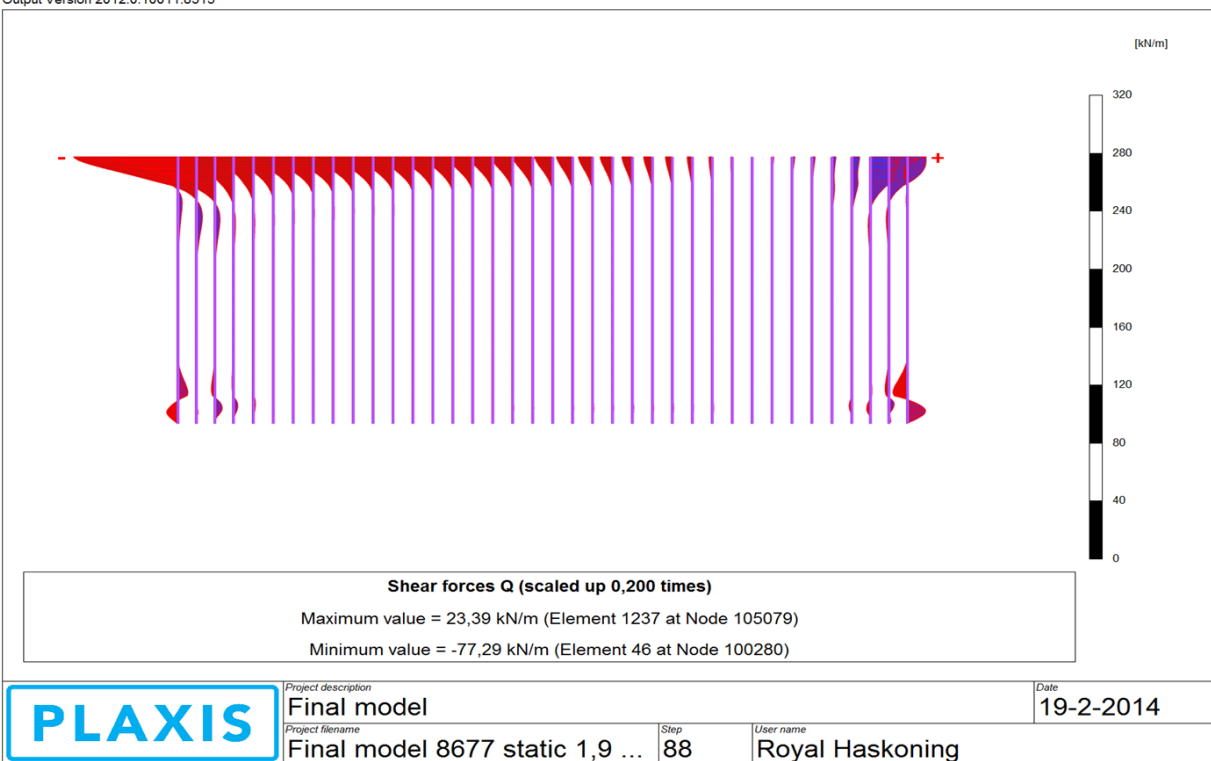
User name
Royal Haskoning

Date
19-2-2014

Static - Normal base plate stiffness : LATERAL FORCES

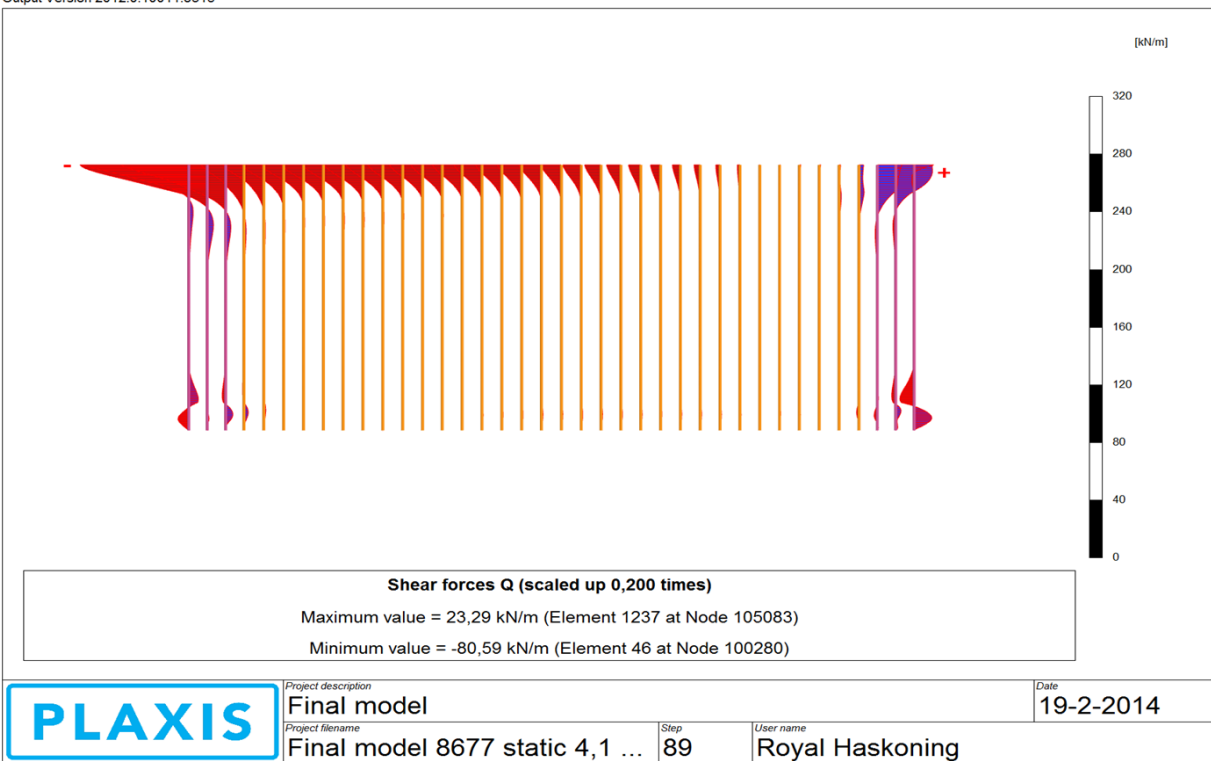
1,93 seconds
step 272

Output Version 2012.0.10011.8315



4,13 seconds
step 488

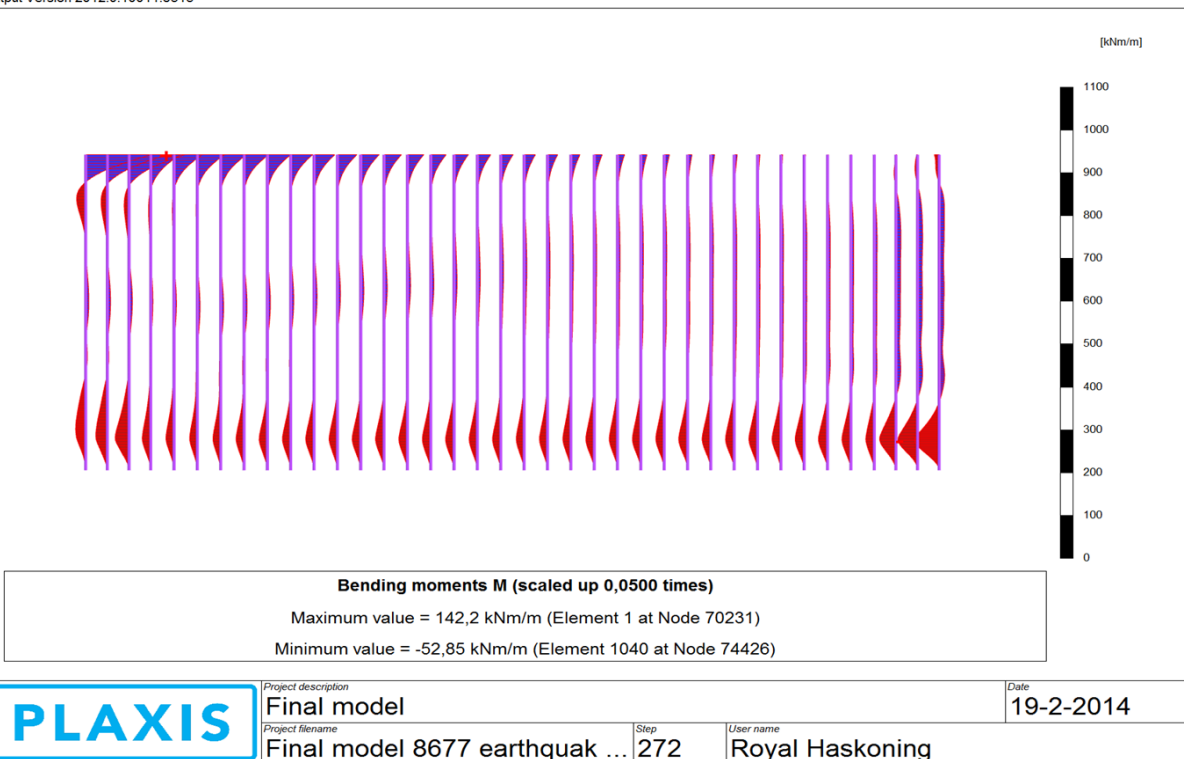
Output Version 2012.0.10011.8315



Earthquake - Infinitely stiff base plate : MOMENTS

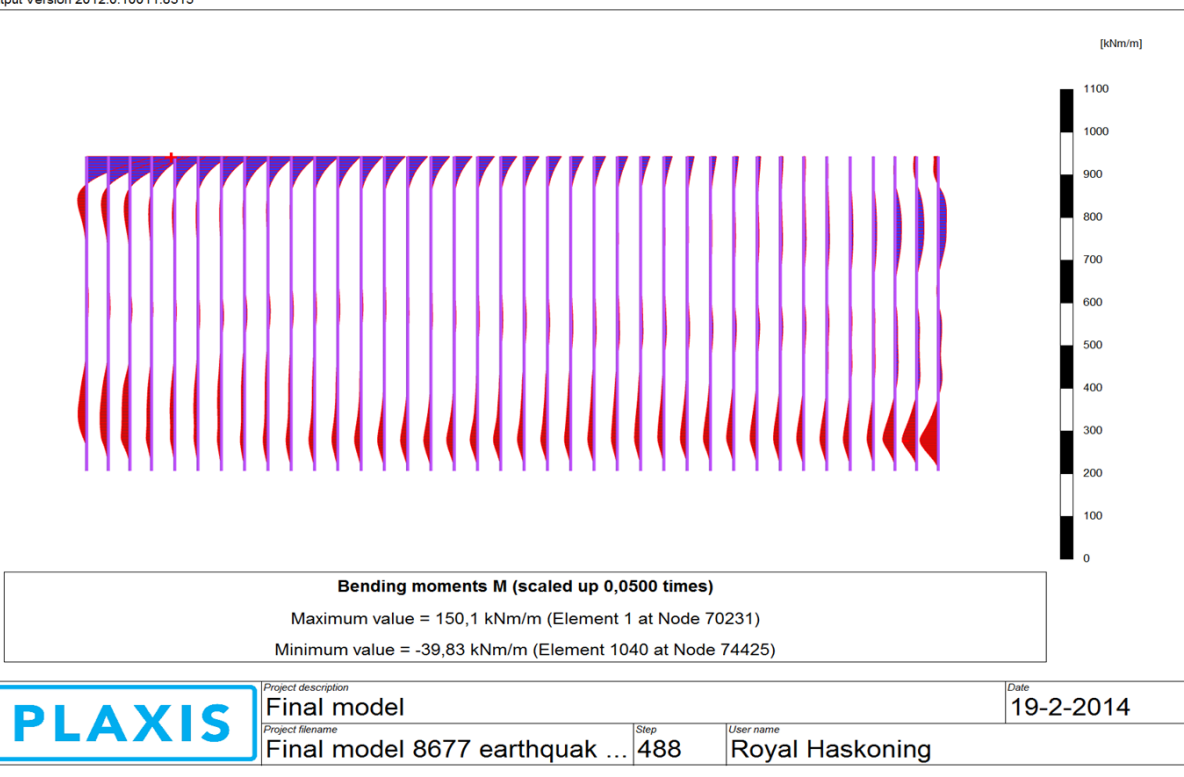
1,93 seconds
step 272

Output Version 2012.0.10011.8315



4,13 seconds
step 488

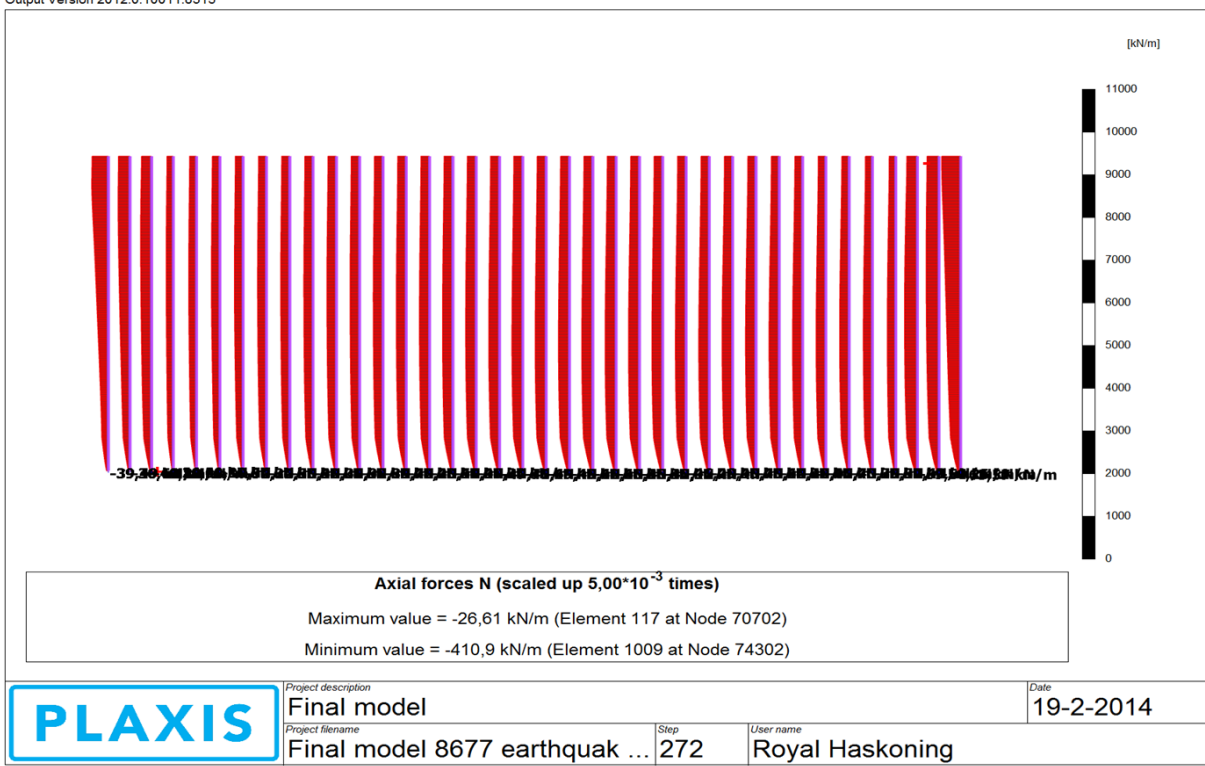
Output Version 2012.0.10011.8315



Earthquake - Infinitely stiff base plate : AXIAL FORCES

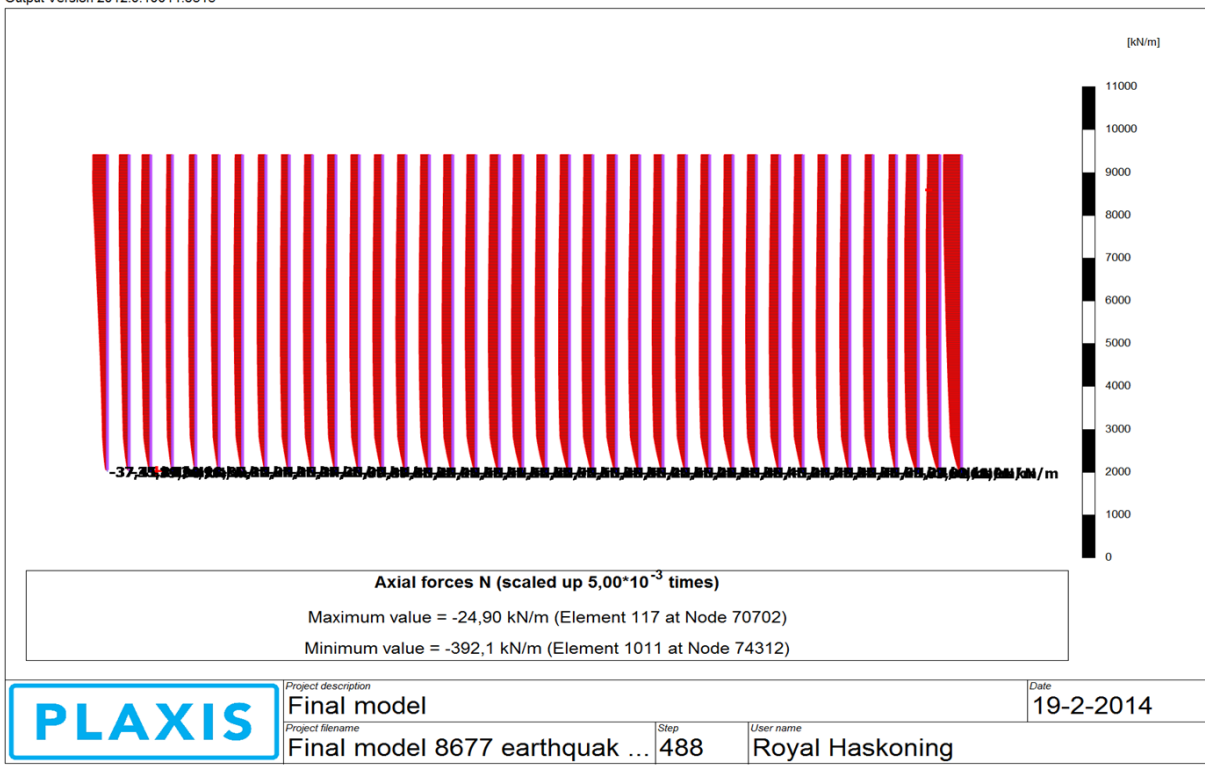
1,93 seconds
step 272

Output Version 2012.0.10011.8315



4,13 seconds
step 488

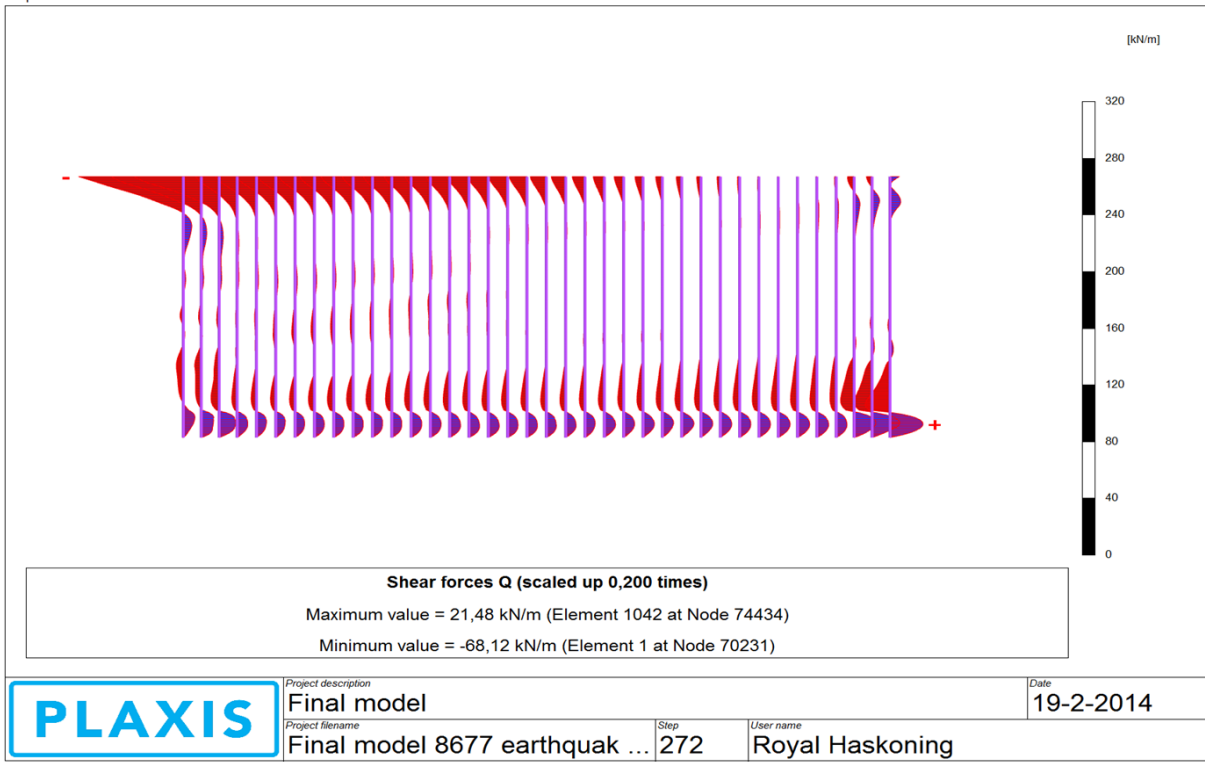
Output Version 2012.0.10011.8315



Earthquake - Infinitely stiff base plate : LATERAL FORCES

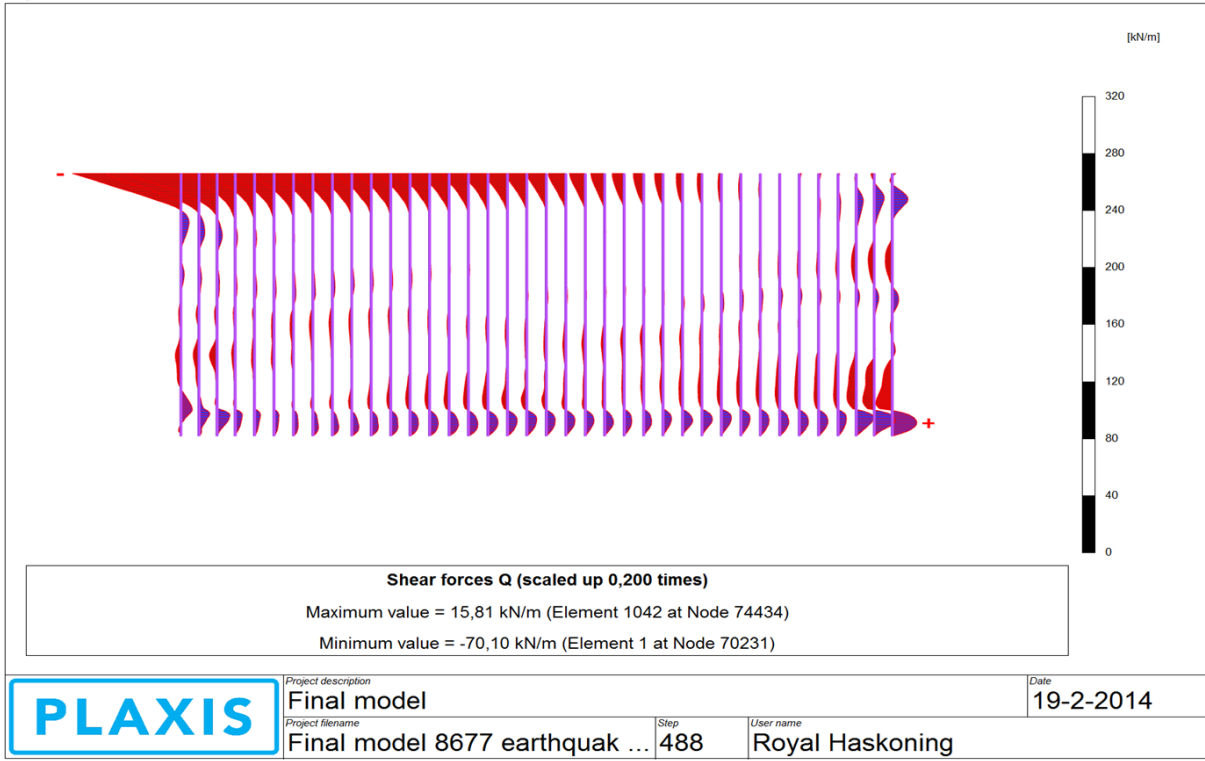
1,93 seconds
step 272

Output Version 2012.0.10011.8315



4,13 seconds
step 488

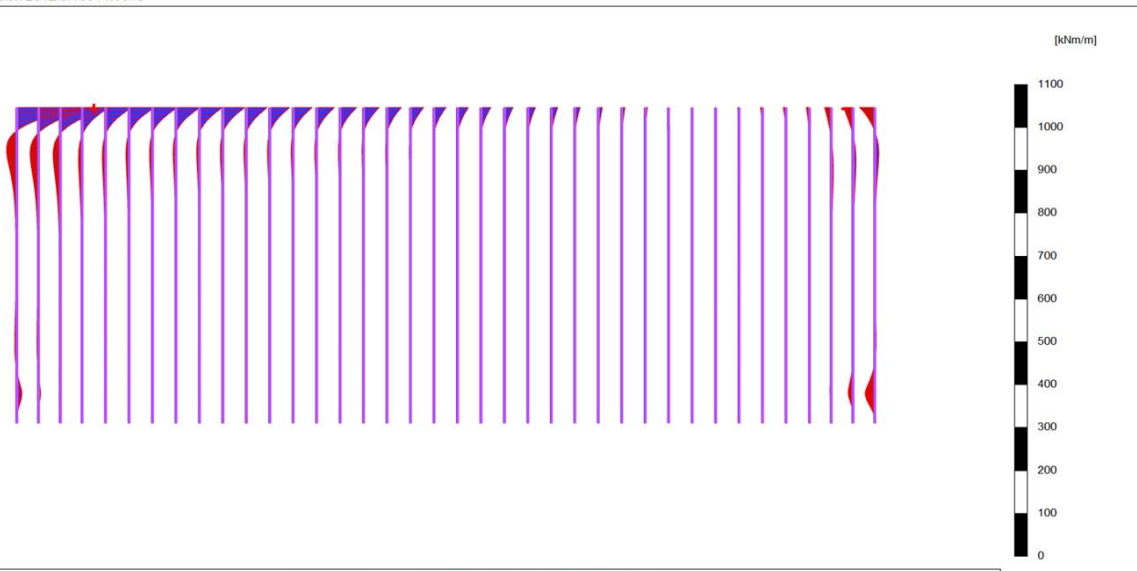
Output Version 2012.0.10011.8315



Static - Infinitely stiff base plate - all forces : MOMENTS

1,93 seconds
step 272

Output Version 2012.0.10011.8315



Bending moments M (scaled up 0,0500 times)

Maximum value = 133,7 kNm/m (Element 1 at Node 100355)

Minimum value = -33,19 kNm/m (Element 1272 at Node 105464)



Project description

Final model

Project filename

Final model 8677 static stif ...

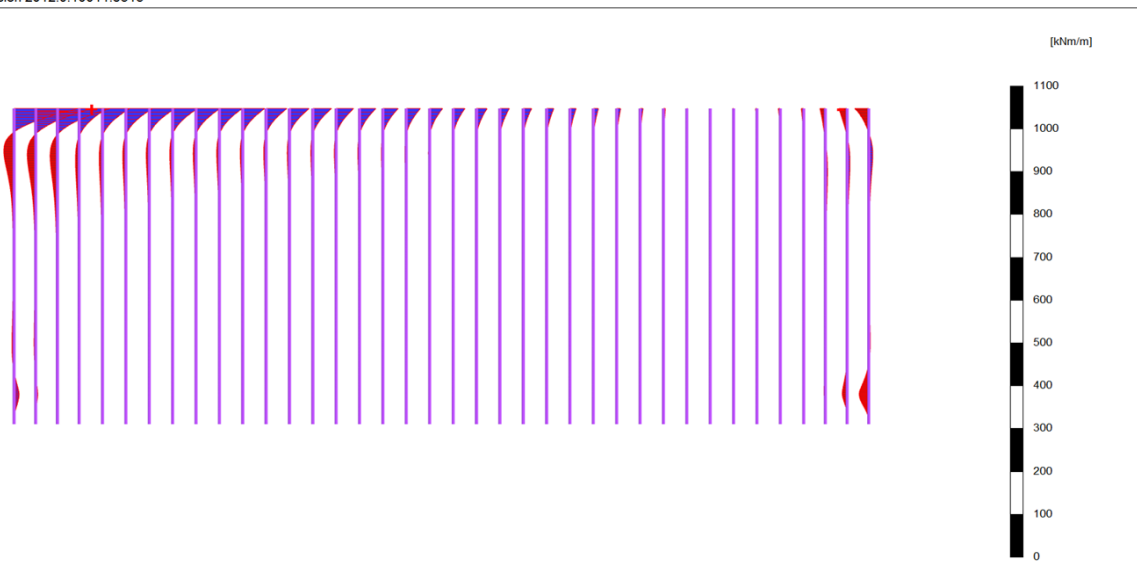
Step
49

User name
Royal Haskoning

Date
14-2-2014

4,13 seconds
step 488

Output Version 2012.0.10011.8315



Bending moments M (scaled up 0,0500 times)

Maximum value = 136,8 kNm/m (Element 1 at Node 100409)

Minimum value = -30,22 kNm/m (Element 1272 at Node 105530)



Project description

Final model

Project filename

Final model 8677 static stif ...

Step
49

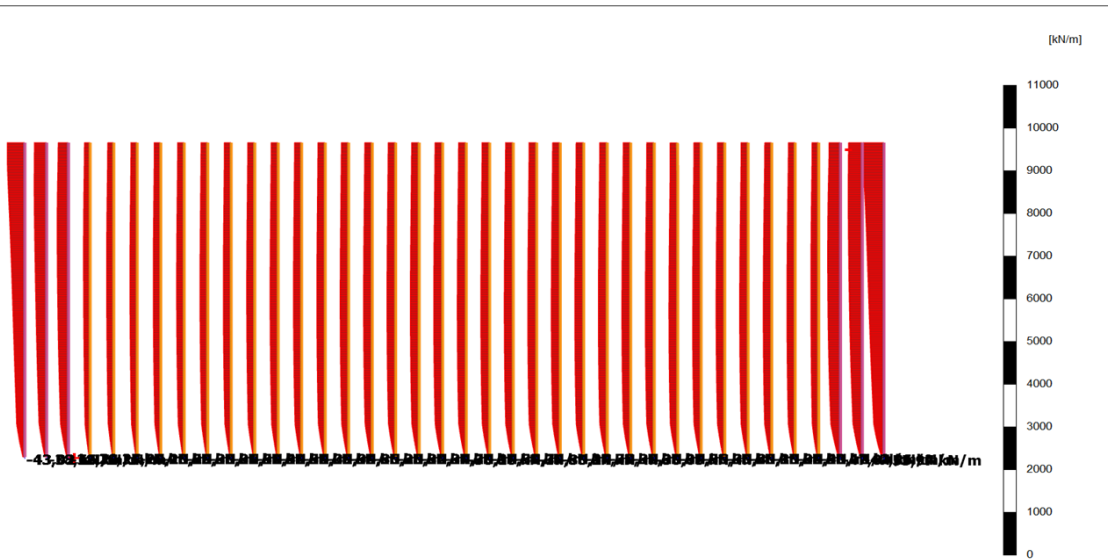
User name
Royal Haskoning

Date
14-2-2014

Static - Infinitely stiff base plate - all forces : AXIAL FORCES

1,93 seconds
step 272

Output Version 2012.0.10011.8315



PLAXIS

Project description
Final model

Project filename
Final model 8677 static stif ...

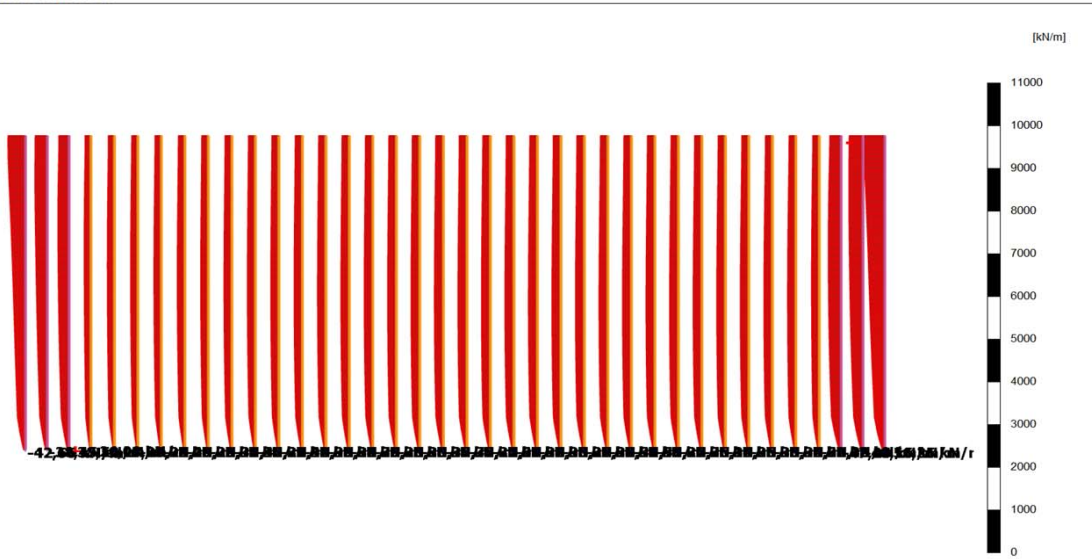
Step
49

User name
Royal Haskoning

Date
19-2-2014

4,13 seconds
step 488

Output Version 2012.0.10011.8315



PLAXIS

Project description
Final model

Project filename
Final model 8677 static stif ...

Step
49

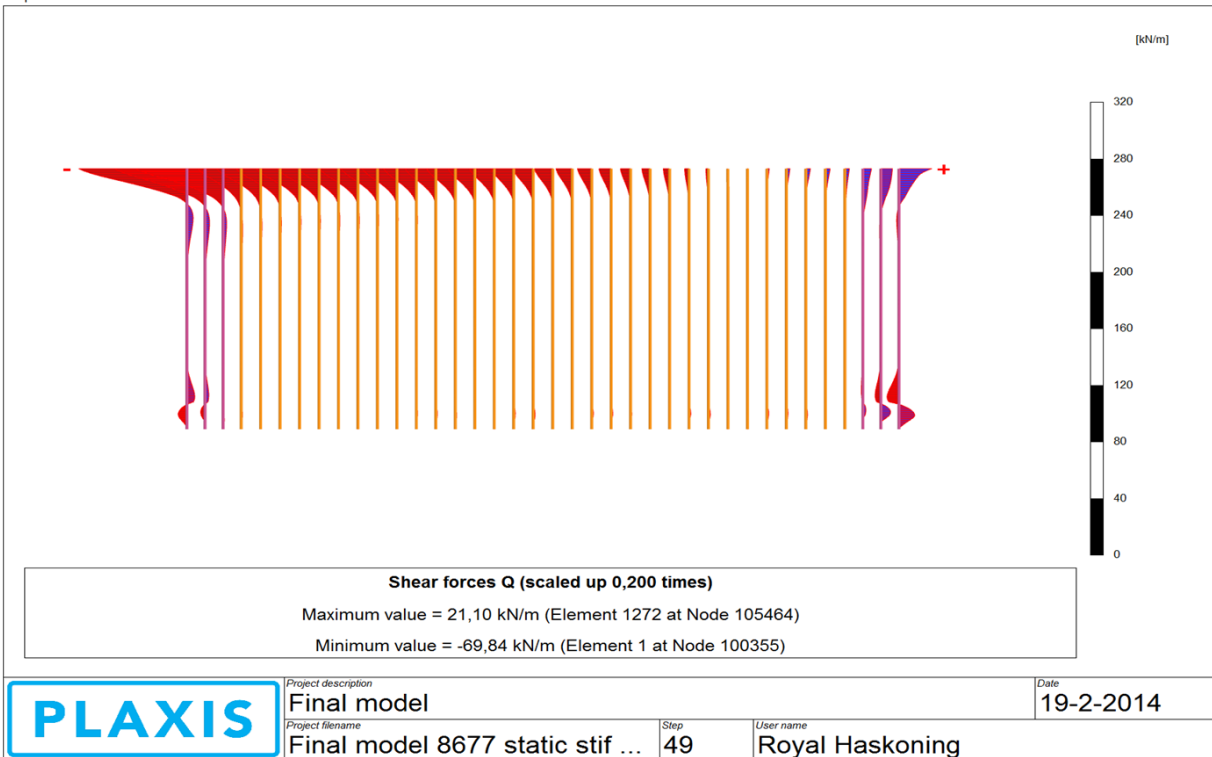
User name
Royal Haskoning

Date
19-2-2014

Static - Infinitely stiff base plate - all forces : LATERAL FORCES

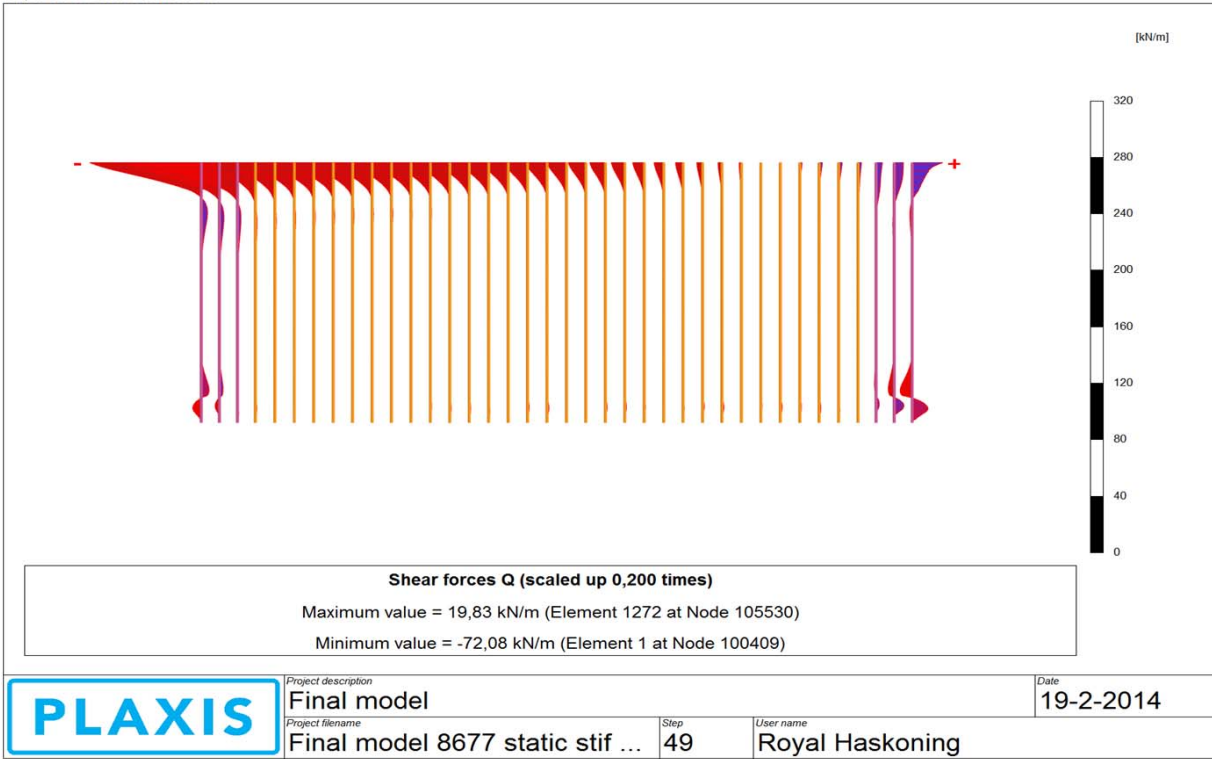
1,93 seconds
step 272

Output Version 2012.0.10011.8315



4,13 seconds
step 488

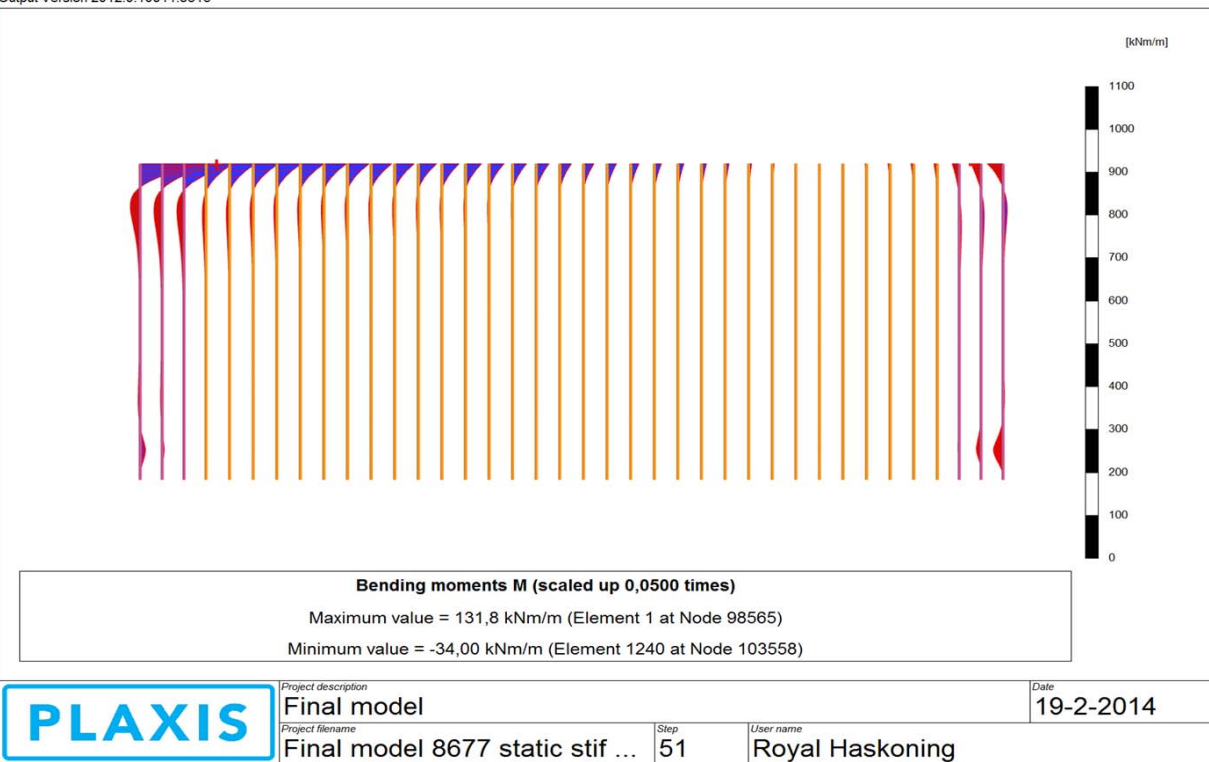
Output Version 2012.0.10011.8315



Static - Infinitely stiff base plate - summerized forces : MOMENTS

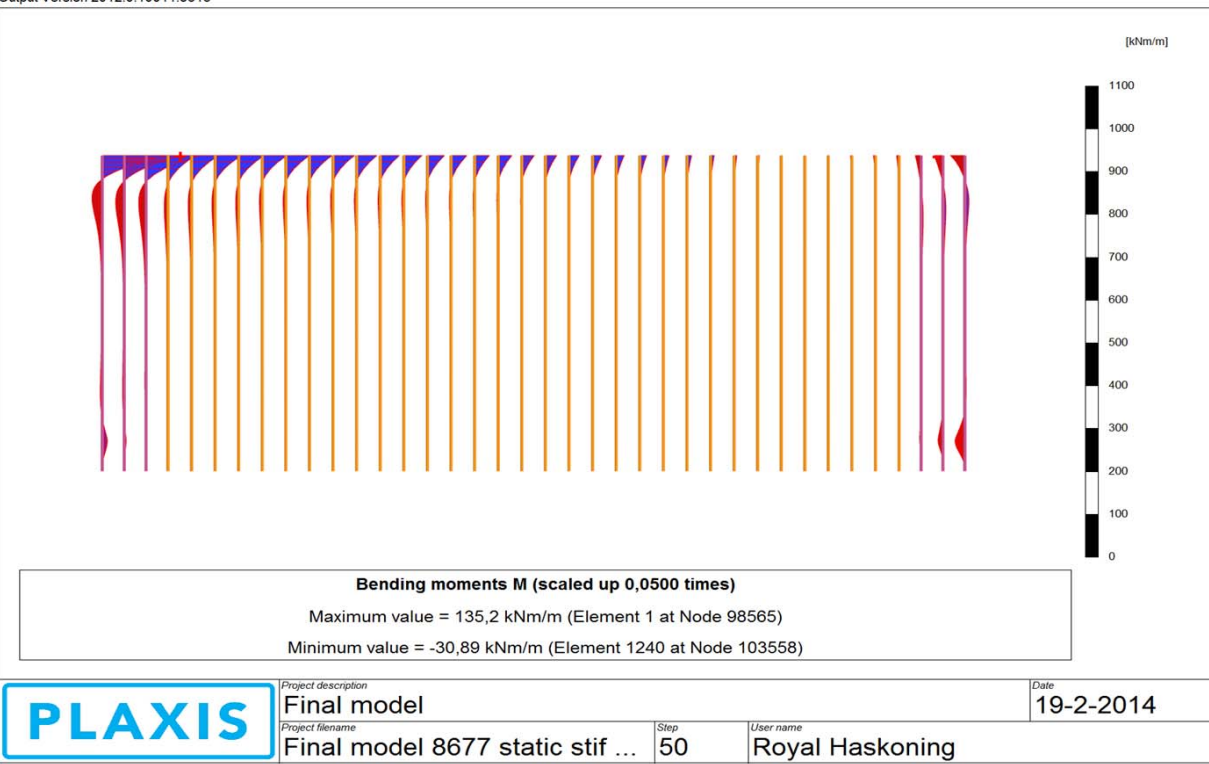
1,93 seconds
step 272

Output Version 2012.0.10011.8315



4,13 seconds
step 488

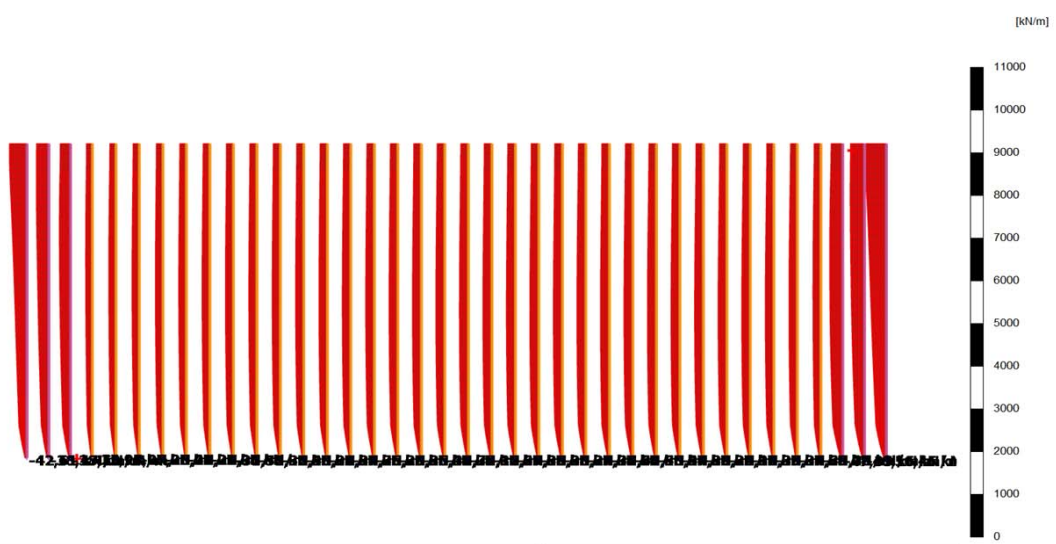
Output Version 2012.0.10011.8315



Static - Infinitely stiff base plate - summerized forces : AXIAL FORCES

1,93 seconds
step 272

Output Version 2012.0.10011.8315



PLAXIS

Project description

Final model

Project filename

Final model 8677 static stif ...

Step

51

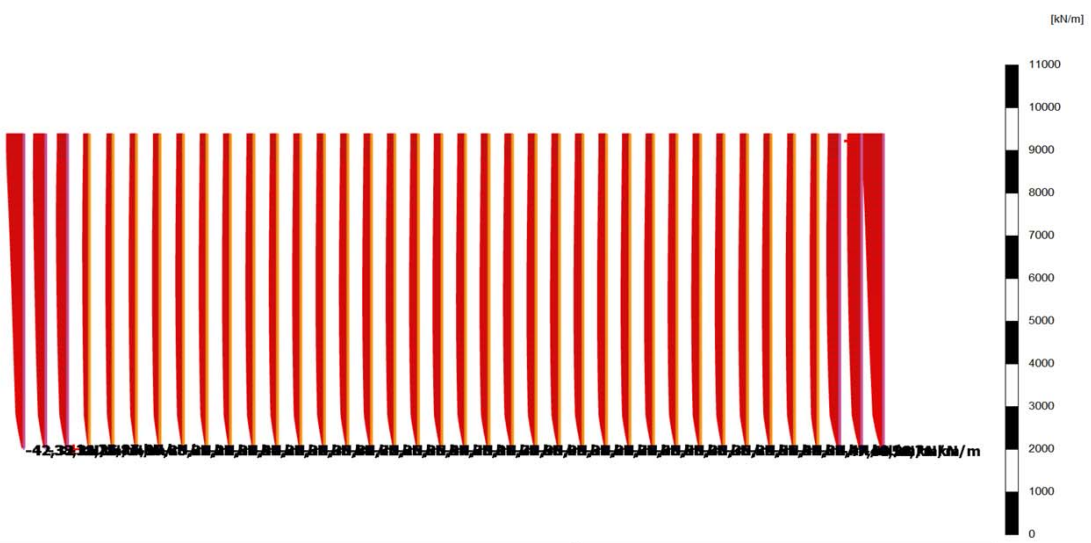
User name

Royal Haskoning

Date
19-2-2014

4,13 seconds
step 488

Output Version 2012.0.10011.8315



PLAXIS

Project description

Final model

Project filename

Final model 8677 static stif ...

Step

50

User name

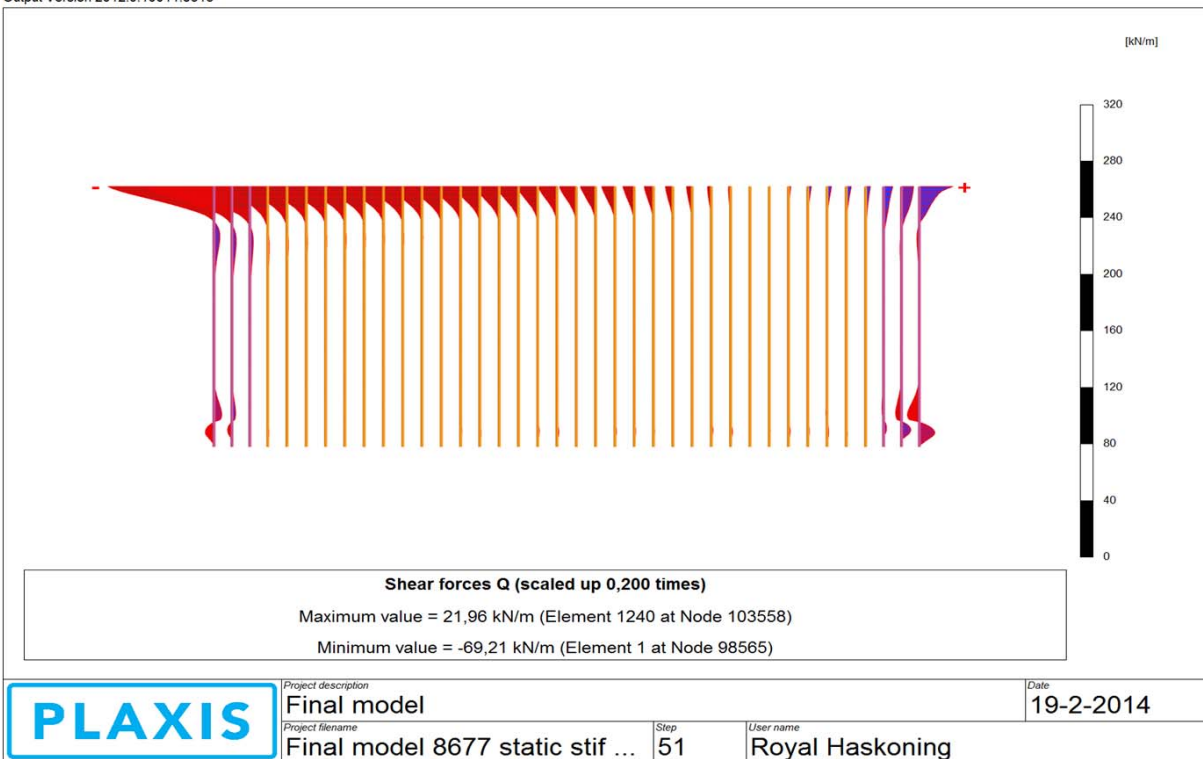
Royal Haskoning

Date
19-2-2014

Static - Infinitely stiff base plate - summerized forces : LATERAL FORCES

1,93 seconds
step 272

Output Version 2012.0.10011.8315



4,13 seconds
step 488

Output Version 2012.0.10011.8315

